VILNIUS UNIVERSITY
FACULTY OF CHEMISTRY AND GEOSCIENCES
INSTITUTE OF CHEMISTRY
DEPARTMENT OF ANALYTICAL AND ENVIRONMENTAL CHEMISTRY

Dmitrij Gritsok
Pharmaceutical Chemistry
Master's thesis

INVESTIGATION OF DEEP EUTECTIC SOLVENTS FOR THE DETERMINATION OF β-CARYOPHYLLENE BY SOLID PHASE MICROEXTRACTION TECHNIQUE

Scientific advisor
assist. dr. Vilius Poškus

Vilnius 2022

LIST OF ABBREVIATIONS

L. – Linnaeus
EO – essential oil
ssp. – several species
desf. – Desfontaines
PPi – inorganic pyrophosphate
CB_1 – type 1 cannabinoid receptor
CB_2 – type 2 cannabinoid receptor
2-AG – 2-arachidonoylglycerol
ANA – anandamide
THC – tetrahydrocannabinol
CNS – central nervous system
IL-1β – interleukin 1 beta
TNF-α – tumour necrosis factor-alfa
IL-6 – interleukin 6
CRP – C-reactive protein
iNOS – inducible nitric oxide synthase
COX-1 – cyclooxygenase 1
COX-2 – cyclooxygenase 2
NF-kB – nuclear factor kappa-light-chain-enhancer of activated B cells
PGE-2 – prostaglandin E_2
ROS – reactive oxygen species
DPPH – 2,2-diphenyl-1-picrylhydrazyl
FRAP – ferric reducing ability of plasma
ORAC – oxygen radical absorbance capacity
ABTS – 2,2'-azinobis[3-ethylbenzothiazoline-6-sulfonic acid]
PPAR-α – peroxisome proliferator-activated receptor alpha
PPAR-γ – peroxisome proliferator-activated receptor gamma
MAPK – mitogen-activated protein kinase
PI3K – phosphoinositide 3-kinase
Akt – protein kinase B
mTOR – the mammalian target of rapamycin
STAT3 – signal transducer and activator of transcription 3
NAFLD – non-alcoholic fatty liver disease
NASH – non-alcoholic steatohepatitis
var. – variety
FDA – Food and Drug Administration
EFSA – European Food Safety Authority
WHO – World Health Organisation
COVID-19 – coronavirus disease 2019
SARS-COV-2 – severe acute respiratory syndrome coronavirus 2

UAE – ultrasound-assisted extraction
MAE – microwave-assisted extraction
SFE – supercritical fluid extraction
IL – ionic liquid
[DMIM][DMP] –1,3-dimethylimidazolium dimethyl phosphate
[BMIM][BF4] – 1-butyl-3-methylimidazolium tetrafluoroborate
DES – deep eutectic solvent
HPLC – high-performance liquid chromatography
HPTLC – high-performance thin-layer chromatography
GC – gas chromatography
HS – headspace
P&T-HS – purge and trap headspace
FED-HS – full evaporation dynamic headspace
SPME – solid phase microextraction
SBSE – stir-bar sorptive extraction
SDME – single-drop microextraction
LDME – liquid phase microextraction
DI-SPME – direct immersion solid phase microextraction
MS – mass spectrometry
FID – flame ionisation detector
SIR – single ion recording
ACS – American Chemical Society
RSC – Royal Society of Chemistry
HBA – hydrogen bond acceptor
HBD – hydrogen bond donor
T_f – freezing point
cP – centipoise
$(n\text{-}Bu)_4NCl$ – tetrabutylammonium chloride
THEDES – therapeutic deep eutectic solvents
NADES – natural deep eutectic solvents
mS – millisiemens
mN – millinewton
FTIR – Fourier-transform infrared spectroscopy
NMR – nuclear magnetic resonance
EG – ethylene glycol
SDF – spatial distribution function
API – active pharmaceutical ingridient
DNA – dezoxyribonucleic acid
RNA – ribonucleic acid
NIST – National Institute of Standards and Technology

CONTENTS

INTRODUCTION

In recent years, a growing emphasis on innovations in extraction techniques has been stirred up by green chemistry. Such contemporary methods use microwave radiation, ultrasound, supercritical fluids, or sorbents. In the meantime, it encourages conducting scientific investigations aimed to simplify the detection, and quantification of natural compounds such as terpenes, flavonoids, phenolic acids, alkaloids, etc.

Within the scope of this thesis, attention was paid to a natural bicyclic sesquiterpene β-caryophyllene, which is found in many essential oils, including *Cannabis sativa* L. Due to its unique ability to selectively bind to the CB_2 receptor, β-caryophyllene has been identified as an anti-inflammatory, antimicrobial, antitumor, and antioxidant agent. Moreover, β-caryophyllene is known to exhibit analgesic properties and relieve anxiety and pain. It is a valuable candidate for the treatment of neurodegenerative disorders, cancer, and osteoporosis.

The determination of β-caryophyllene from essential oil requires time-consuming and laborious extraction from plant material. Solid phase microextraction allows the determination of β-caryophyllene directly in the solid or liquid sample. Nevertheless, selecting appropriate calibration media is crucial in this technique. Deep eutectic solvents were chosen for this role, as they exhibit unique properties of well-known ionic liquids, but at the same time are biodegradable, easily synthesised, and non-toxic

The **aim of the research work** is to investigate the application of deep eutectic solvents as a calibration media for the determination of β-caryophyllene by solid phase microextraction. In order to achieve the aim of this work, the following **tasks** have arisen:

1. To provide a theoretical basis for an in-depth understanding of ongoing research by preparing a systematised literature review about the following subjects: β-caryophyllene, solid phase microextraction and deep eutectic solvents.
2. To perform time-saving microwave-assisted synthesis of deep eutectic solvents.
3. To investigate the performance of deep eutectic solvents as medium in headspace solid phase microextraction by comparison of GC-MS peak areas of β-caryophyllene.
4. To select an appropriate deep eutectic solvent for further adjustment of solid phase microextraction parameters (equilibration time, sorption time)
5. To quantify the concentration of β-caryophyllene in a fat-rich matrix (hemp seed oil) by gas chromatographic – mass spectrometric analysis using optimised conditions of solid phase microextraction.

1. CARYOPHYLLENES

1.1 Definition

Terpenes represent a large class of natural products with numerous biological functions (Chizzola, 2013). Terpenes are classified based on organisation and the number of isoprene units they contain (**Table 1**) (Mabou & Yossa, 2021; Cox-Georgian, Ramadoss, Dona, & Basu, 2019).

Table 1. Classification of terpenes.

Number of carbon atoms	Number of isoprene units	Class	Formula
5	1	Hemiterpenes	C_5H_8
10	2	Monoterpenes	$C_{10}H_{16}$
15	3	Sesquiterpenes	$C_{15}H_{24}$
20	4	Diterpenes	$C_{20}H_{32}$
25	5	Sesterpenes	$C_{25}H_{40}$
30	6	Triterpenes	$C_{30}H_{48}$
40	7	Tetraterpenes	$C_{40}H_{64}$

Caryophyllenes belong to the class of primary sesquiterpenes and consist of three isoprene units. β-Caryophyllene is the main representative of caryophyllenes (Fidyt, Fiedorowicz, Strządała, & Szumny, 2016). It is notable for having a cyclobutane ring and a trans-double bond in a 9-membered ring. Both γ-caryophyllene and α-caryophyllene are its isomers, where the former has a cis-double bond in a 9-membered ring and the latter has the cyclobutane-opened ring and hence 11 carbons in the cycle (**Fig. 1**).

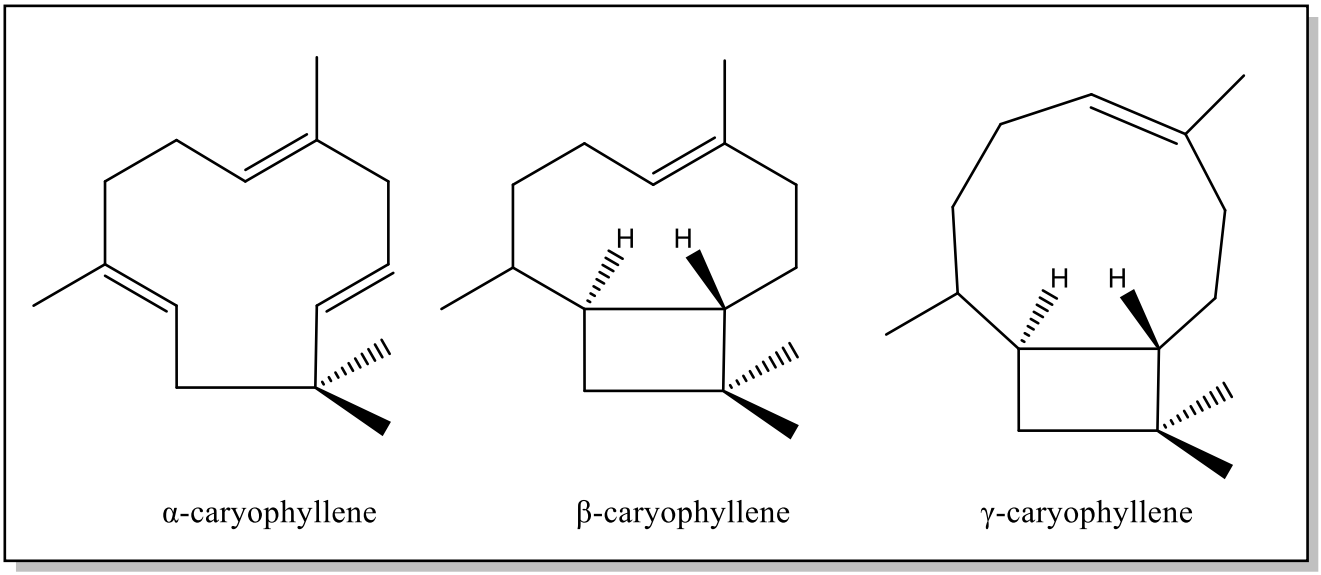

Fig. 1. Structures of caryophyllenes

The derivatives of α-, β-, and γ-caryophyllene can also be related to the term ‘caryophyllenes’. The most known compound is a β-caryophyllene oxide (Sain, et al., 2014), where a double bond is oxidised to the epoxide group (**Fig. 2)**.

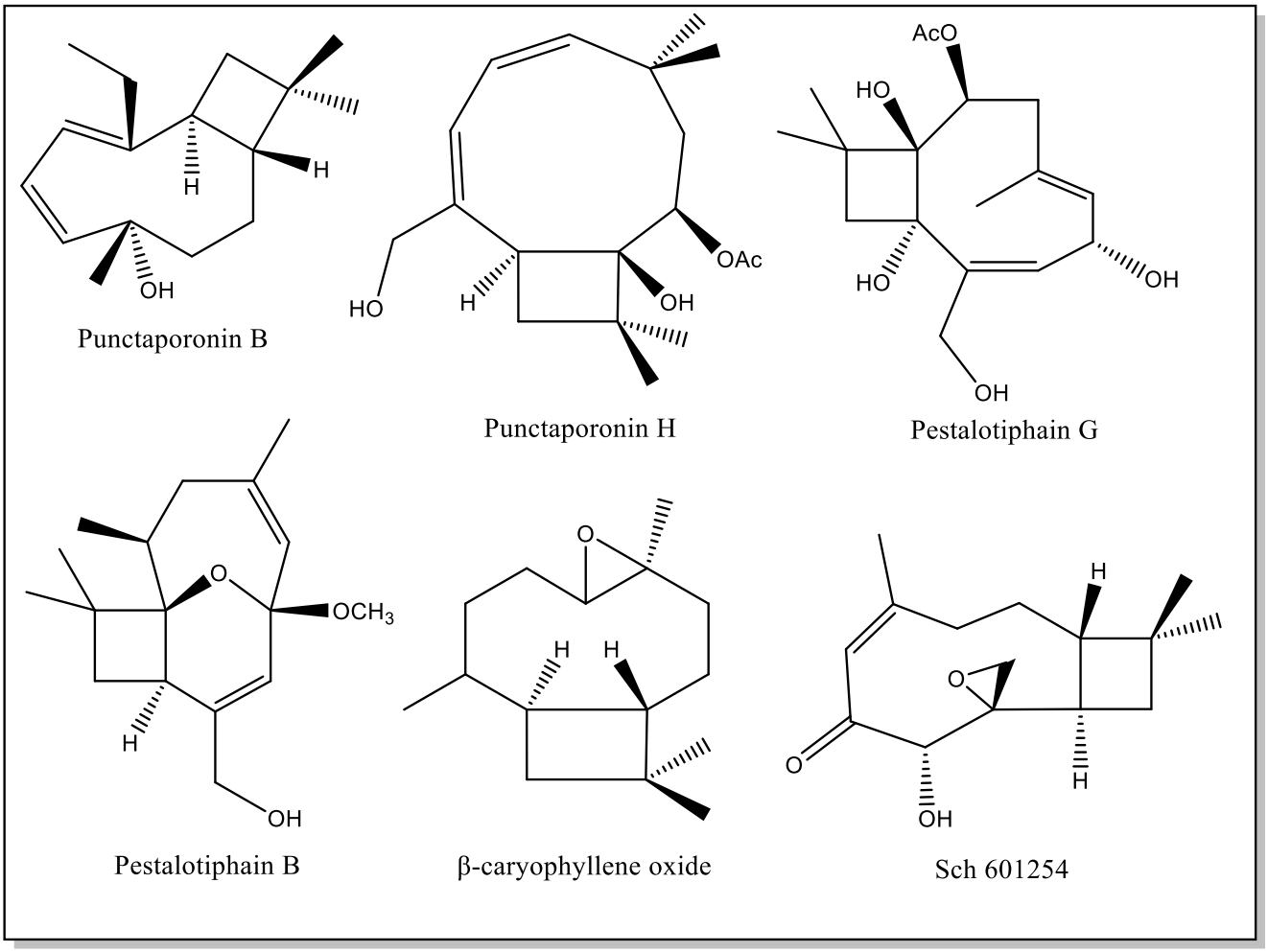

Fig. 2. Structural formulae of caryophyllene derivatives

Other examples include highly oxygenated caryophyllene-type compounds (Zhang, et al., 2020), where prevailing oxygen-containing functional groups are carbonyl, acetoxy, hydroxy, ether, and epoxy.

1.2 Natural sources

β-Caryophyllene is a natural sesquiterpene hydrocarbon present in hundreds of plant species. Some examples of plant families include *Anacardiaceae*, *Annonaceae*, *Apiaceae*, *Apocynaceae*, *Asteraceae*, *Boraginaceae*, *Cannabaceae*, *Clusiaceae*, *Euphorbiaceae*, *Fabaceae*, *Lamiaceae*, *Lauraceae*, *Myrtaceae*, *Pinaceae*, *Rutaceae*, *Verbenaceae*, and *Zingiberaceae* (Maffei, 2020).

In nature, β-caryophyllene is usually found together with small quantities of its isomers α-caryophyllene and γ-caryophyllene or in a mixture with its oxidation product, β-caryophyllene oxide.

Caryophyllenes and their related analogues have been widely isolated from the plants such as black pepper (*Piper nigrum L.*) (Miloš, et al., 2015), cinnamon (*Cinnamomum spp.*) (Erich, et al., 2006; Khalid, Lêda, & Eugenio, 2017), oregano (*Origanum Vulgare, Origanum onites*) (Teixeira, et al., 2013; Kokkini, Karousou, Hanlidou, & Lanaras, 2004), rosemary (*Rosmarinus officinalis*) (Özcan & Chalchat, 2008; Boutekedjiret, Bentahar, Belabbes, & Bessiere, 2003), lavender (*Lavandula angustifolia*) (Białoń, Krzyśko-Łupicka, Nowakowska-Bogdan, & Wieczorek, 2019), hops (*Humulus lupulus*) (Eyres & Dufour, 2008), thyme (*Thymus vulgaris*) (Borugă, et al., 2014), and basil (*Ocimum tenuiflorum*) (Sims, Juliani, Mentreddy, & Simon, 2014).

The highest content of β-caryophyllene (50.2%-74.0%) has been detected in the species shown in **Table 2** (Maffei, 2020).

Table 2. Occurrence of β-caryophyllene in the essential oil of different species.

Family	Genus	Species	Part used	Content in EO, %
Annonaceae	*Cananga*	*odorata*	leaves	52.0
Apocynaceae	*Tabernaemontana*	*catharinensis*	leaves	56.9
Asteraceae	*Tagetes*	*patula*	flowers	53.5
Boraginaceae	*Cordia*	*multispicata*	leaves	56.6
Burseraceae	*Bursera*	*microphylla*	oleo-gum-resin	72.9
Clusiaceae	*Pentadesma*	*butyracea*	barks	74.0
Euphorbiaceae	*Croton*	*glandulosus*	aerial parts	53.2
Fabaceae	*Copaifera*	*langsdorffii desf.*	oleoresins	72.0
Fabaceae	*Copaifera*	*multijuga*	oleoresins	57.5
Fabaceae	*Copaifera*	*reticulata*	oleoresins	68.0
Lamiaceae	*Colquhounia*	*coccinea*	flower	53.2
Lamiaceae	*Hyptis*	*mutabilis*	aerial parts	59.4
Lamiaceae	*Leucas*	*indica*	aerial parts	51.1
Lamiaceae	*Nepeta*	*curviflora*	aerial parts	50.2
Lamiaceae	*Orthodon*	*dianfhera*	aerial parts	52.9
Lamiaceae	*Ocotea*	*duckei*	leaves	60.5
Piperaceae	*Piper*	*guineense*	seeds	57.6
Piperaceae	*Pothomorphe*	*peltata*	leaves	68.0
Rutaceae	*Murraya*	*paniculata*	leaves	57.6
Zingiberaceae	*Aframomum*	*corrorima*	leaves	60.7
Zingiberaceae	*Renealmia*	*breviscapa*	rhizomes	62.3

Caryophyllenes can be found in cloves oil (*Caryophyllus aromaticus L.*) (Jirovetz, et al., 2006), from which these compounds take their name (Caryophyllus. In Merriam-Webster.com dictionary, n.d.).

Caryophyllenes and their derivatives are major constituents of essential oil of *Cannabis sativa*, e.g., α-caryophyllene, β-caryophyllene, γ-caryophyllene, γ-caryophyllene oxide, β-caryophyllene oxide,

α-caryophyllene epoxide (I, II and III), caryophylladienol II, caryophyllenol (I and II), and 3,6-caryolanediol (ElSohly, 2020).

Highly oxygenated caryophyllene-type sesquiterpenoids can also be isolated from ascomycete fungi such as plant pathogens *Pestalotiopsis hainanensis* (Zhang, et al., 2020), marine-derived fungus *Ascotricha sp.* ZJ-M-5 (Wang, et al., 2014), sponge-associated fungus *Hansfordia sinuosae* (Wu, Liu, Proksch, Guo, & Lin, 2014), and coprophilous fungus *Poronia punctata* (Anderson, Edwards, Poyser, & Whalley, 1988).

In plants, the probable biosynthetic pathway of α-caryophyllene, β-caryophyllene, β-caryophyllene oxide, and γ-caryophyllene is based on the cyclisation of a farnesyl pyrophosphate precursor to a humulyl carbocation (**Fig. 3**), which is catalysed by sesquiterpene cyclase QHS1 (Kollner, et al., 2008).

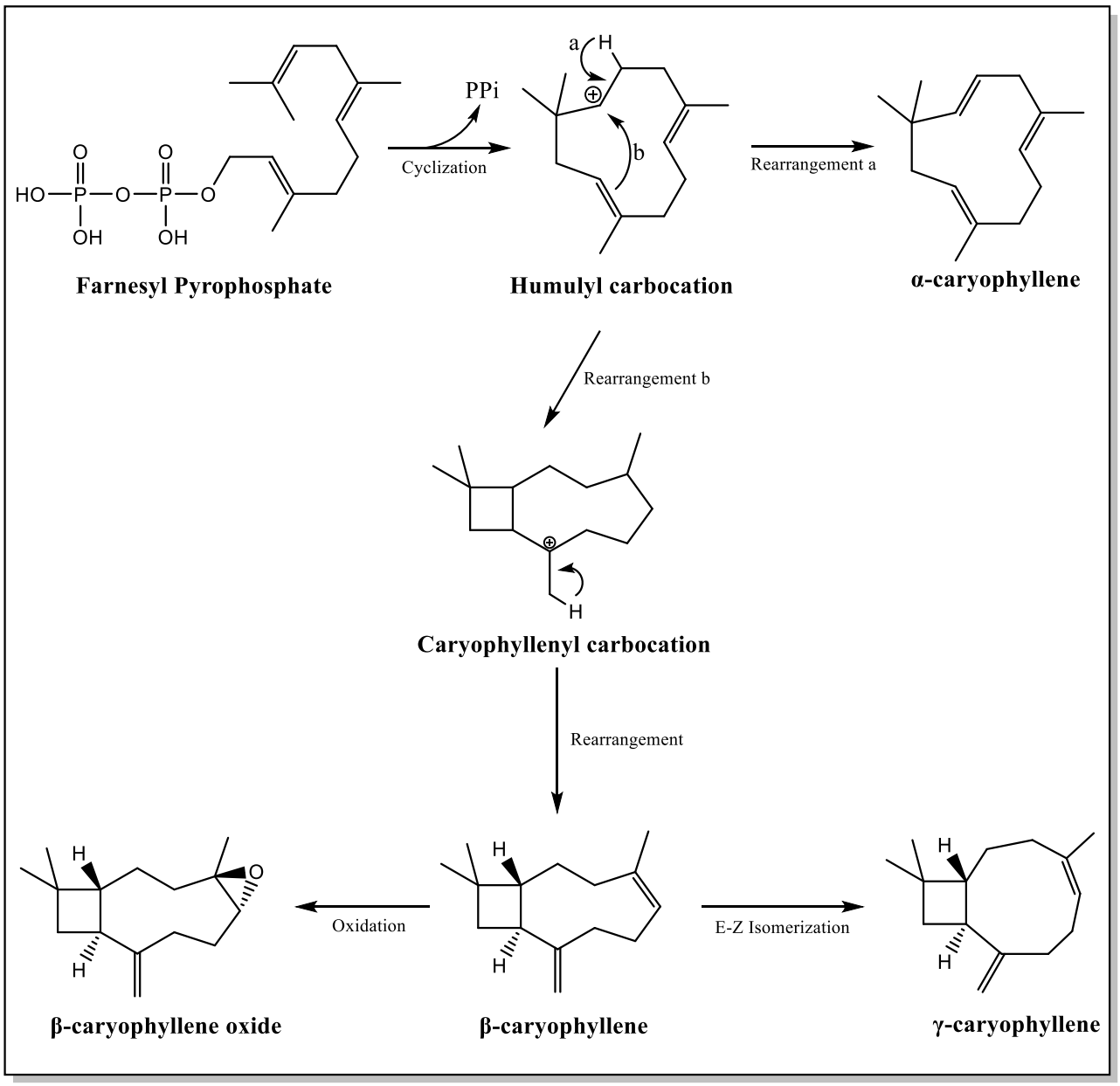

Fig. 3. Biosynthetic pathways of caryophyllenes

After cyclisation, proton abstraction from the humulyl carbocation intermediate forms the macrocyclic triene α-caryophyllene (rearrangement a). β-caryophyllene synthesis requires a further conversion of a humulyl carbocation into a caryophyllenyl carbocation (rearrangement b). γ-Caryophyllene is obtained by an anticlockwise rotation of β-caryophyllene (enzymatic E-Z isomerisation), whereas β-caryophyllene oxide derives from the 4-5 oxidation of β-caryophyllene (**Fig. 3**) (Talapatra & Talapatra, 2015; Asakawa, Ishida, Toyota, & Takemoto, 1986)

1.3 Properties and applications

1.3.1 Binding to CB_2 receptor

Cannabinoid receptors (**Fig. 4**) (Brown & Farquhar-Smith, 2018) are a part of the endocannabinoid system and play a crucial role in numerous human physiological and pathological conditions (Kendall & Yudowski, 2017).

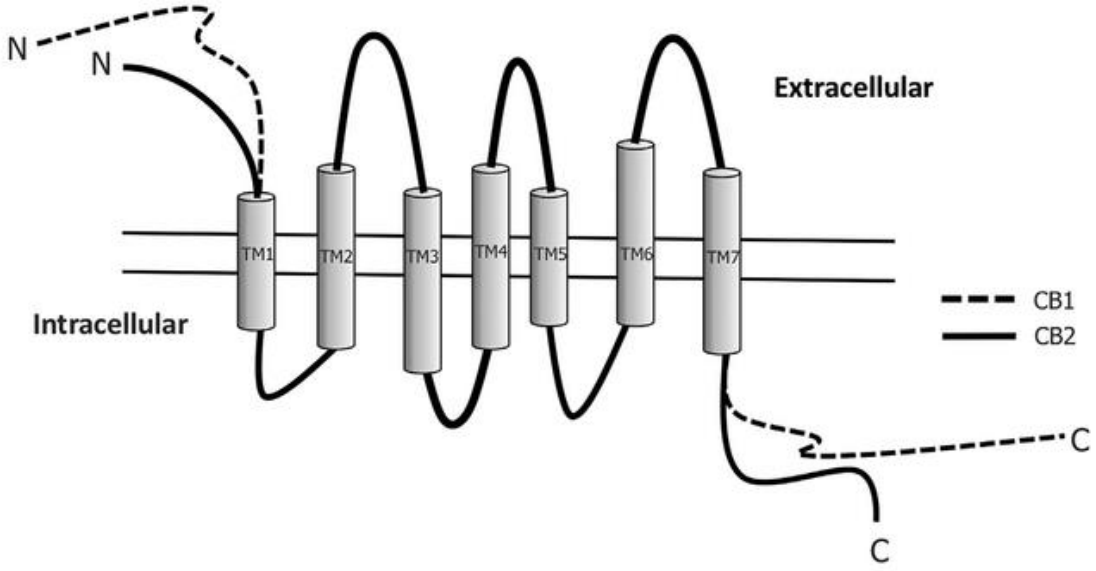

Fig. 4. Structural representation of CB_1 and CB_2 receptors

The psychoactive cannabinoids from *Cannabis sativa* and the arachidonic acid-derived endocannabinoids are non-selective natural ligands (except β-caryophyllene) for cannabinoid type 1 (CB_1) and type 2 (CB_2) receptors (**Fig. 5**).

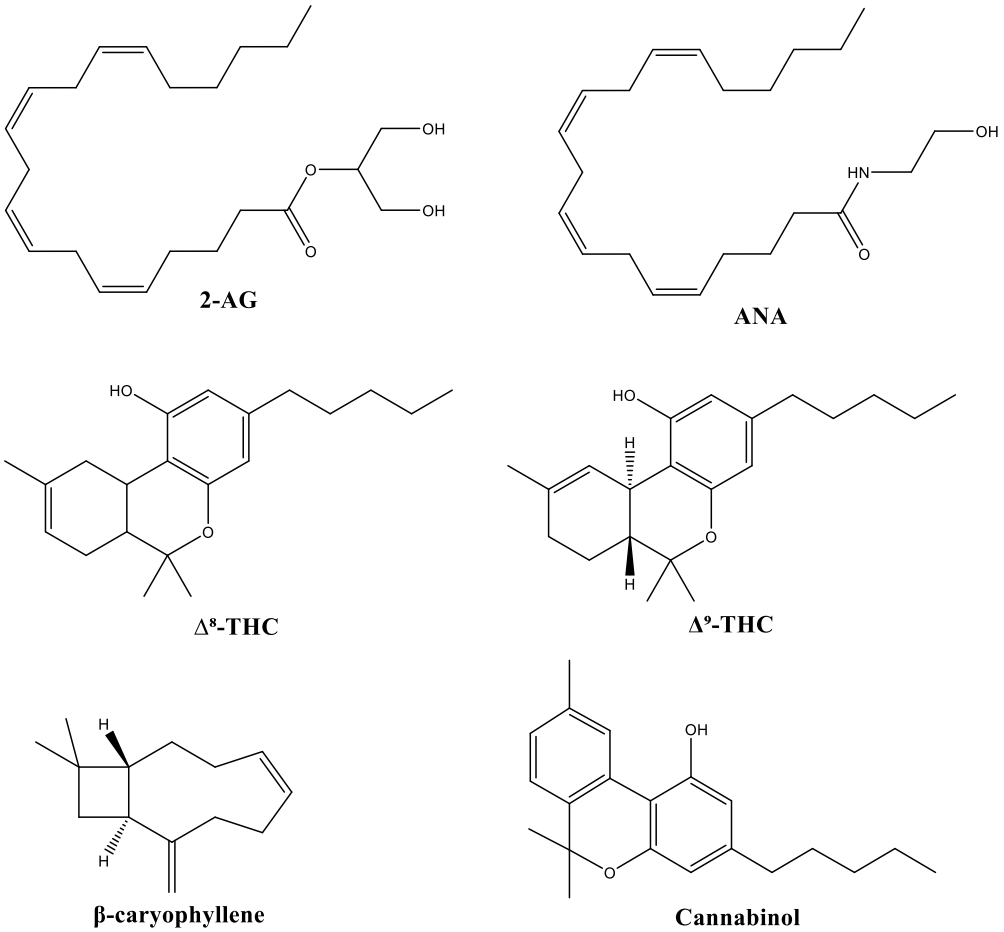

Fig. 5. Structural formulae of some cannabinoids.

The CB_1 receptor is one of the most abundant G protein-coupled receptors in the CNS and is found in particularly high levels in the neocortex, hippocampus, basal ganglia, cerebellum, and brainstem. CB_1 receptors are also found on peripheral nerve terminals and some extra-neural sites such as the testis, eye, vascular endothelium, and spleen (Kendall & Yudowski, 2017). The CB_2 receptor exhibits a more defined pattern of expression in the brain than CB_1 receptors and is found predominantly in cells and tissues of the immune system (lymphocytes, macrophages, mast cells) and to a lesser extent in the CNS (mainly expressed by microglial cells).

The activation of CB_1 is responsible for psychoactive effects, which is an important consideration for many clinicians and their patients. Although the CB_1 receptor is responsible for the psychomodulatory effects, activation of the CB_2 receptor is a potential therapeutic strategy for the treatment of inflammation, pain, atherosclerosis, and osteoporosis.

Interestingly, different CB_2 agonists (such as caryophyllenes) bind uniquely to CB_2 receptors and distinctly regulate multiple effectors, and at the same time don't cause psychoactive adverse effects by not possessing CB_1 affinity. This type of intracellular signalling has been described as agonist-directed trafficking of response (Shoemaker, Ruckle, Mayeux, & Prather, 2005). The ability of CB_2 ligands to selectively traffic intracellular responses, coupled with their selective expression profile in inflamed tissues, and pronounced anti-inflammatory and neuroprotective properties, suggest an exciting

future is approaching for the development of this novel class of drugs for the treatment of a variety of inflammatory disorders.

1.3.2 Anti-inflammatory and antioxidant activity

Caryophyllenes exert potent anti-inflammatory properties in all body organs (Scandiffio, et al., 2020; Francomano, et al., 2019), including the liver, kidneys, brain, heart, pancreas, and blood, and suppresses systemic inflammation by inhibiting proinflammatory cytokines in macrophages (e.g., IL-1β, TNF-α, IL-6, CRP) and other inflammatory mediators (e.g., iNOS, COX-1, COX-2, NF-κB, PGE-2), as well as signalling pathways (Chang, Kim, Lee, Kim, & Chun, 2013; Hub, Zenga, Wanga, & Guo, 2017).

Besides the immune-inflammatory changes, many diseases can cause the state of the body, where numerous ROS, including H_2O_2, (O^{2-}), (•OH) are produced, and this activates many signalling pathways for cell death in many organs. Caryophyllenes have been shown to augment the levels of endogenous antioxidants, exerting ferric reducing property, Fe^{2+} chelation, and radicals scavenging activity in DPPH, FRAP, ORAC, ABTS, •OH, and NO assays (Oboh, Olasehinde, & Ademosun, 2014; Pant, Maggi, Gyawali, & Dall'Acqua, 2019).

Some therapeutic effects appear due to the activation of nuclear peroxisome proliferator-activated receptors (PPAR-α, PPAR-γ) by caryophyllenes. These subtypes are encoded by distinct genes and are regulated by steroids and lipid metabolites and mainly control lipid and glucose homeostasis and inflammatory responses (O'Sullivan, 2016).

The above effects of caryophyllenes help to actively promote the inhibition of lipid accumulation, fatty acids oxidation, a decrease of the visceral fat index, reduction of total cholesterol, triglycerides, LDL levels, reduction of atherogenic and coronary risk index, an increase of plasma insulin, decrease in blood glucose, protective effect against doxorubicin-induced inflammation in the myocardium (Scandiffio, et al., 2020; Fernandes, et al., 2007). Thus, caryophyllenes are promising in the treatment of such diseases as type II diabetes, obesity, dyslipidaemia, NAFLD, NASH, and cardiovascular and neurological disorders.

1.3.3 Anticancer activity

Caryophyllenes have shown cytotoxic activity against various cancer cell lines (Francomano, et al., 2019). Currently, it is believed that all anticancer activities of caryophyllenes may be based on three different mechanisms such as induction of apoptosis, repression of the cell cycle, and inhibition of angiogenesis and metastasis.

S. Dahham et al. have shown that β-caryophyllene has significantly decreased the proliferation of two colon cancer cell lines HT-29 and HCT-116, and a pancreas cancer cell line PANC-1 (Dahham, et al., 2015). In the intestinal cancer cell line CaCo-2, α-caryophyllene has been able to exert a significant effect on cell growth (Fidyt, Fiedorowicz, Strządała, & Szumny, 2016).

In some cases, β-caryophyllene does not have cytotoxic activity, but its non-cytotoxic concentration significantly increases the anticancer activity of α-caryophyllene and γ-caryophyllene, for example, in human breast cancer MCF-7 cells: α-caryophyllene or γ-caryophyllene alone (32

mg/mL) inhibited cell growth by about 50% and 69%, respectively, compared with 75% and 90% when combined with 10 mg/mL β-caryophyllene (Legault & Pichette, 2007).

It has been shown that β-caryophyllene causes the activation of caspase-3 and determines nucleolus fragmentation and the consequent apoptosis in two different cell lines, BS-24-1 (murine cell line of lymphoma) and MoFir (human T cell transformed through Epstein-Barr virus) (Pavithra, Mehta, & Verma, 2018).

Further, the β-caryophyllene oxide is cytotoxic against several cell lines, including human cervical adenocarcinoma cells HeLa, human lung cancer cells AGS, human leukaemia cells HepG2, human stomach cancer cells SNU-1 and SNU-16 and human ovarian cancer cells A-2780. It modulates many fundamental pathways in tumour pathogenesis, such as those involving MAPK, PI3K/Akt, mTOR, and STAT3 (Fidyt, Fiedorowicz, Strządała, & Szumny, 2016).

Aside from the direct anticancer activities, β-caryophyllene and β-caryophyllene oxide can enhance the efficacy of classical anticancer drugs, such as paclitaxel or doxorubicin (Ambrož, et al., 2015).

1.3.4 Antifungal and antibacterial properties

Essential oils of species containing caryophyllenes have been found to possess antifungal and antibacterial (antimicrobial) activity.

The caryophyllene-rich (β-caryophyllene 42.2%, α-caryophyllene 27.7%) rhizome oil of *Zingiber nimmonii* showed significant inhibitory activity against the fungi *Candida glabrata*, *Candida albicans* and *Aspergillus niger* and the bacteria *Bacillus subtilis* and *Pseudomonas aeruginosa* (Baby, et al., 2006).

The β-Caryophyllene oxide was tested as an antifungal agent in an *in vitro* experimental model of onychomycosis and showed significant activity against *Trichophyton mentagrophytes var. mentagrophytes*, *Trichophyton mentagrophytes var. interdigitale* and *Trichophyton rubrum* dermatophytes (Yang, Michel, Chaumont, & Millet-Clerc, 2000).

J. Kamalpreet et al. investigated the antifungal potential of guava (*Psidium guajava*) essential oil major compounds β-caryophyllene (24.97%) and β-caryophyllene oxide (14.92%), and they were effective against *Rhizoctonia solani*, *Helminthosporium oryzae*, and *Fusarium moniliforme* fungi species (Jassal, Kaushal Rashmi, & Rani, 2021).

F. Pereira et al. have shown that non-oxygenated (α-caryophyllene) as well as oxygenated (β-caryophyllene oxide, 14-hydroxy-9-*epi*-β-caryophyllene) constituents of essential oil from leaves of *Casearia sylvestris* inhibit the growth of three yeast strains: *Candida glabrata*, *Saccharomyces cerevisiae*, and *Candida krusei* (Pereira, et al., 2017).

The antimicrobial assay demonstrated that the β-Caryophyllene can inhibit the growth of *Bacillus cereus* and *Proteus mirabilis*, and with a lower effect on *Enterococcus faecalis*, *Staphylococcus epidermidis* and *Staphylococcus aureus* (Juliani Jr., et al., 2002).

1.3.5 Other properties

Caryophyllenes and their derivatives have numerous applications besides those mentioned above. For example, β-Caryophyllene was approved by Food and Drug Administration (FDA) and European Food Safety Authority (EFSA) and it is used as a flavour enhancer and as a fragrance ingredient (woody-spicy, clove-like, turpentine aroma) in decorative cosmetics, fine fragrances, shampoos, toilet soaps and other toiletries as well as in non-cosmetic products such as household cleaners and detergents (Bhatia, Letizia, & Api, 2008).

Caryophyllenes can exhibit anti-allodynic, analgesic, anxiolytic, antidepressive, and sedative properties (Fidyt, Fiedorowicz, Strządała, & Szumny, 2016; Francomano, et al., 2019; Segat, et al., 2017; Bahi, et al., 214; Jha, et al., 2021) as well as a protective role in several nervous system-related disorders such as Alzheimer's and Parkinson's diseases, dementia, and multiple sclerosis (Jha, et al., 2021; Askari & Shafiee-Nick, 2019; Cheng, Dong, & Liu, 2014).

Due to the pandemics announced by WHO and the damage already done by SARS-COV-2, COVID-19 aroused tremendous interest in the scientific community. Caryophyllenes have shown to be promising therapeutic and/or preventive candidates to target the triad of infection, immunity, and inflammation in COVID-19 (Jha, et al., 2021).

2. DETERMINATION OF CARYOPHYLLENES

2.1 Sample extraction and preparation

Sample preparation and its proper execution are of paramount importance in achieving fast and accurate results (Dulski, 2016). The analysis of caryophyllenes and their derivatives usually comes from plants as a starting material, and usually can be divided into several basic steps: sampling, sample pre-treatment, extraction of target compounds, purification of crude extracts, qualitative identification, and quantitative determination (**Fig. 6**).

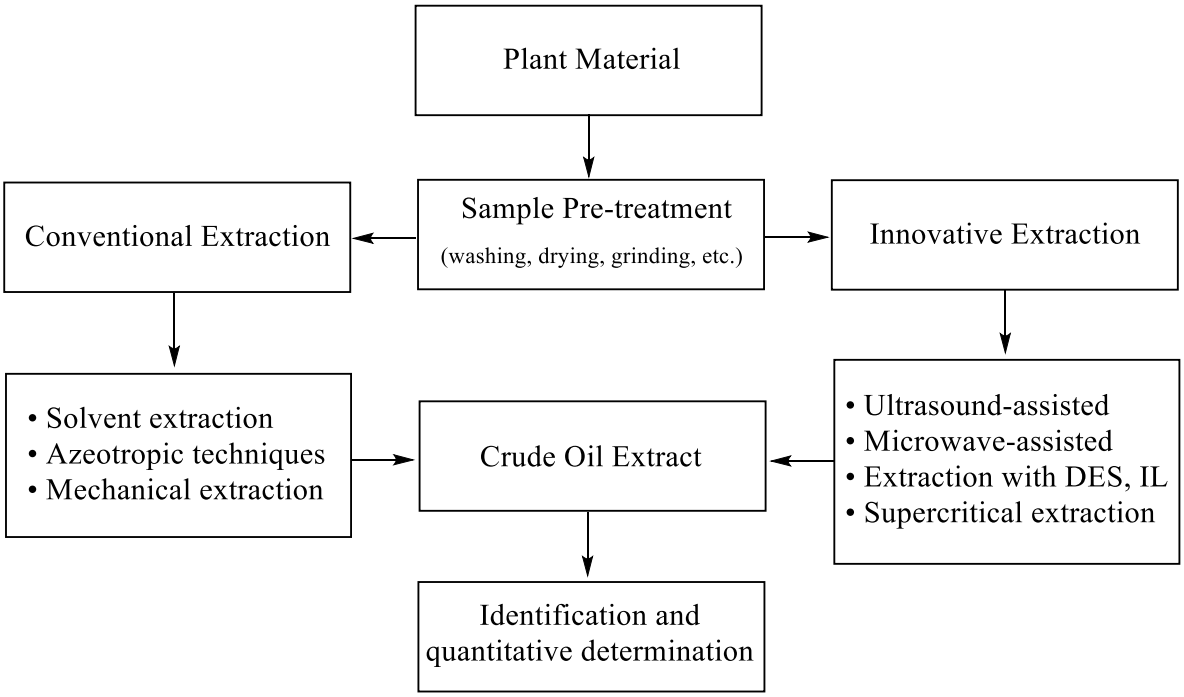

Fig. 6. Flow chart of sample extraction and preparation protocol

The extraction of target compounds can be done either by conventional or innovative techniques, which have their advantages and disadvantages.

Conventional techniques include ordinary cold-pressed extraction, solvent extraction (Soxhlet extraction, maceration, percolation, etc.), and azeotropic techniques (steam distillation, hydrodiffusion, hydrodistillation in Clevenger-type apparatus) (Rasul, 2018).

Cold-pressed extraction is a very simple solvent-free method, which uses only physical force to obtain the essential oil. It is a low-cost and rapid process, although the percentage of oil recovery is very low. This type of extraction is used to obtain hemp oil that contains caryophyllenes with yields up to 25-30% (Valizadehderakhshan, et al., 2021).

Solvent extraction is a separation process that separates liquid from a solid-liquid sample by using chemical solvents such as methanol, ethanol, n-hexane, chloroform, dichloromethane, glycerol, and benzene. Solvent extraction combines several methods that differ in the principle of operation.

Maceration (Sánchez-Muñoz, Aguilar, King-Díaz, Fausto Rivero, & Lotina-Hennsen, 2012; Mousavi, Nateghi, Dakheli, Ramezan, & Piravi-Vanak, 2022) is an old method used for medicinal

preparation and is driven only by molecular diffusion. The powdered solid materials are placed in a closed vessel and the solvent is added to initiate this process (**Fig. 7A**). The solvent diffuses through the cell wall and solubilises the plant constituents, occasional shaking could facilitate this process. After the desired amount of time has passed, the liquid is strained off, and the solid residue is pressed to recover as much solvent as possible. Maceration is a simple method using non-complicated utensils and equipment, it is an energy-saving process. Unfortunately, the duration of extraction time is long and sometimes takes up to weeks, it does not extract the drug exhaustively, and requires a big amount of solvent.

Percolation (Sadraei, Asghari, & Alipour, 2016) is the procedure used most frequently to extract active ingredients in the preparation of tinctures and fluid extracts. The moistened by the appropriate solvent mass is packed and the top of the percolator is closed. Additional solvent is added to form a shallow layer above the mass, and the mixture is allowed to macerate in the closed percolator for 12-24 h. Then the outlet of the percolator is opened, and the liquid contained there is allowed to drip slowly (**Fig. 7B**). The procedure of percolation requires less time than maceration and gives 10-30% more complete extraction, however, it requires a big amount of solvent, and special attention during preparation and throughout the process.

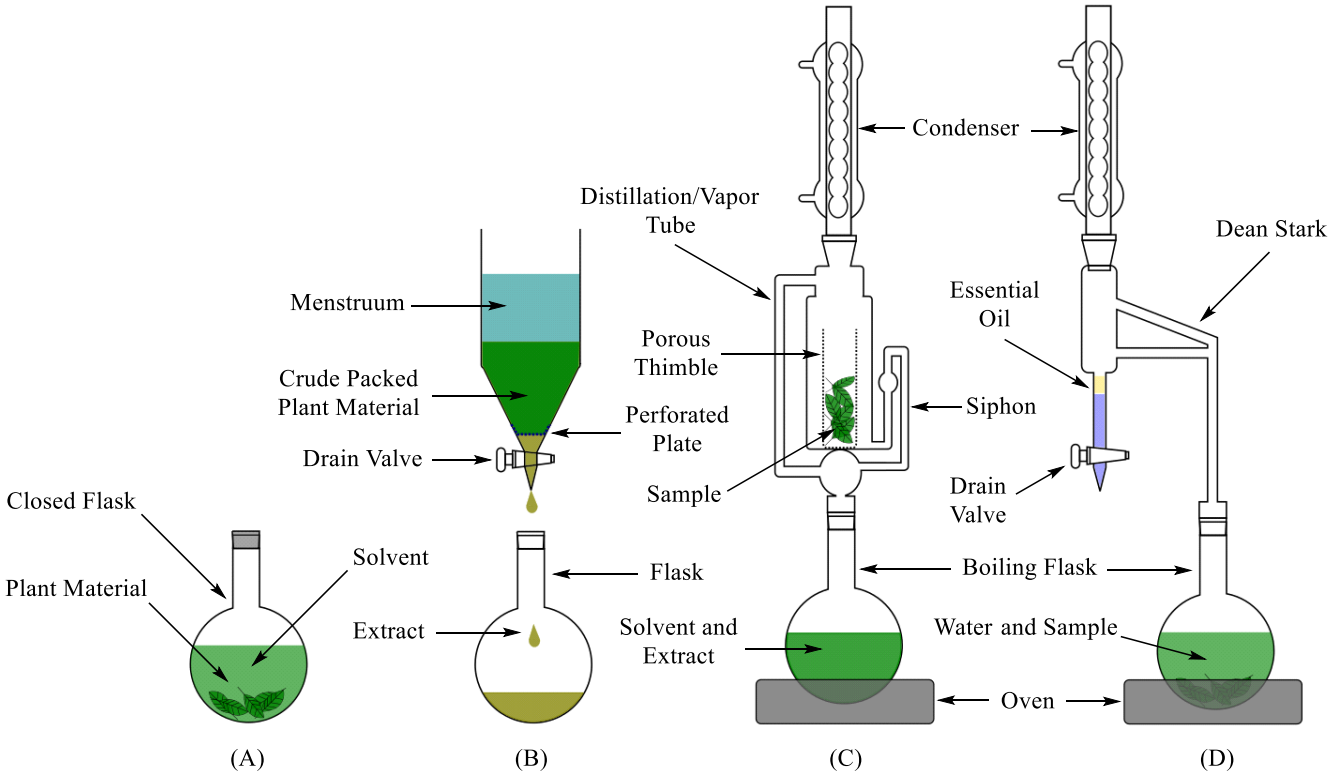

Fig. 7. Conventional extraction techniques (A – maceration, B – percolation, C – Soxhlet extraction, D – Clevenger-type distillation)

Soxhlet extraction (continuous hot percolation process) is now considered one of the best and most convenient methods. The plant material is placed inside the Soxhlet extractor in a thimble made of filter paper. This extractor is attached to a knockback condenser and a round-bottomed flask containing the solvent (**Fig. 7C**). The solvent in the flask is gently boiled, so the vapour rises through

the side tube, and being condensed falls into the thimble containing the material, gradually filling the Soxhlet apparatus. When the solvent reaches the top of the attached tube, it siphons over into the flask, removing the extracted portion of the substance. The procedure is repeated until the extraction is complete. The Soxhlet extraction requires less time than ordinary percolation: for example, 3 hours in n-hexane to extract caryophyllenes from Manuka leaves (Alsaud, Shahbaz, & Farid, 2021) or 6 hours in petroleum ether to extract caryophyllenes from tobacco leaves (Zhang, Gao, Zhang, Liu, & Ye, 2012). Although the technique is simple, it uses a big amount of solvent, yet long enough, and not appropriate for thermolabile compounds.

Azeotropic techniques have a few advantages over other conventional techniques. The main and only solvent is water, making this process cheaper and environmentally friendly. Most frequently used azeotropic techniques are hydrodistillation and steam distillation. The difference is that in hydrodistillation the plant material is fully immersed in water (Fig. 7D), while in steam distillation the steam passes through the plant biomass being generated in a separate water reservoir. Hydro- and steam distillation are traditional methods for the extraction of plant materials being used for a lot of time in science and industry. Hot water or steam act as the main influential factors to free bioactive compounds of plant tissue. Then the cold water condenses the vapour mixture of water and essential oil, which can be collected by opening the drain valve. Various parameters (weight of plant material, volume of water, size of raw material, nature of plants, time) determine the yield of essential oil. Azeotropic techniques work well for immiscible with water substances, and give relatively high-quality essential oil, but are still time-consuming. Thus, a lot of essential oils contain caryophyllenes (e.g., lemon basil (Ngamprasertsith, Menwa, & Sawangkeaw, 2018), rosemary (Özcan & Chalchat, 2008), thyme (Borugă, et al., 2014)) can be obtained by these techniques.

Valuable improvements in the extraction process have appeared with innovative techniques. For example, the implementation of microwave heating or ultrasound significantly increases the efficiency of extraction of conventional techniques, including low solvent volumes shorter extraction time, few instrumental requirements, and low economic and environmental impact. These techniques are also considered a contribution to a “cleaner technology”.

Ultrasound-assisted extraction (UAE) uses ultrasound energy (with frequencies between 20-100kHz) and solvents to extract target compounds from various plant matrices. The propagation of ultrasonic waves in any liquid medium entails the production of successive intermittent zones of high and low pressures, which are directly proportional to the power provided to the system and generate gas bubbles in this medium (Saien & Daneshamoz, 2018). The collapsing cavitation bubbles generate shockwaves and accelerated inter-particle collision causes the fragmentation of cellular structure. The rapid fragmentation leads to solubilisation of the bioactive component in the solvent due to a decrease in particle size, increased surface area and high mass transfer rates in the boundary layer of a solid matrix (Kusters, Pratsinis, Thoma, & Smith, 1994).

Microwave-assisted extraction (MAE) uses the energy of microwaves to disrupt the cell membrane and thus the intracellular lipids get released into the solvent. The moisture content of the sample matrix is the main target of microwave heating during MAE. As the water evaporates, the intracellular pressure increases, breaking the cell walls and increasing the leaching of high-value compounds (Gomez, Tiwari, & Garcia-Vaquero, 2020). The main advantage of this technique is the

ability to rapidly heat the sample reducing the time of extraction and making it possible to use with thermolabile compounds.

Supercritical fluid extraction (SFE) is one more environmentally clean alternative to conventional extraction methods, which uses substances in their critical state (e.g., CO_2, H_2O) as a solvent. Among all the solvent choices, supercritical fluids are more attractive compared to other organic solvents being able to overcome the limitations in traditional solvent extraction methods. The critical fluid is the state of the fluid, when it is pressurised above its critical pressure P_c and heated above its critical temperature T_c (**Fig. 8A, 8B**). This fluid is neither gas nor liquid anymore but keeps viscosity as in the gas state and density as in the liquid.

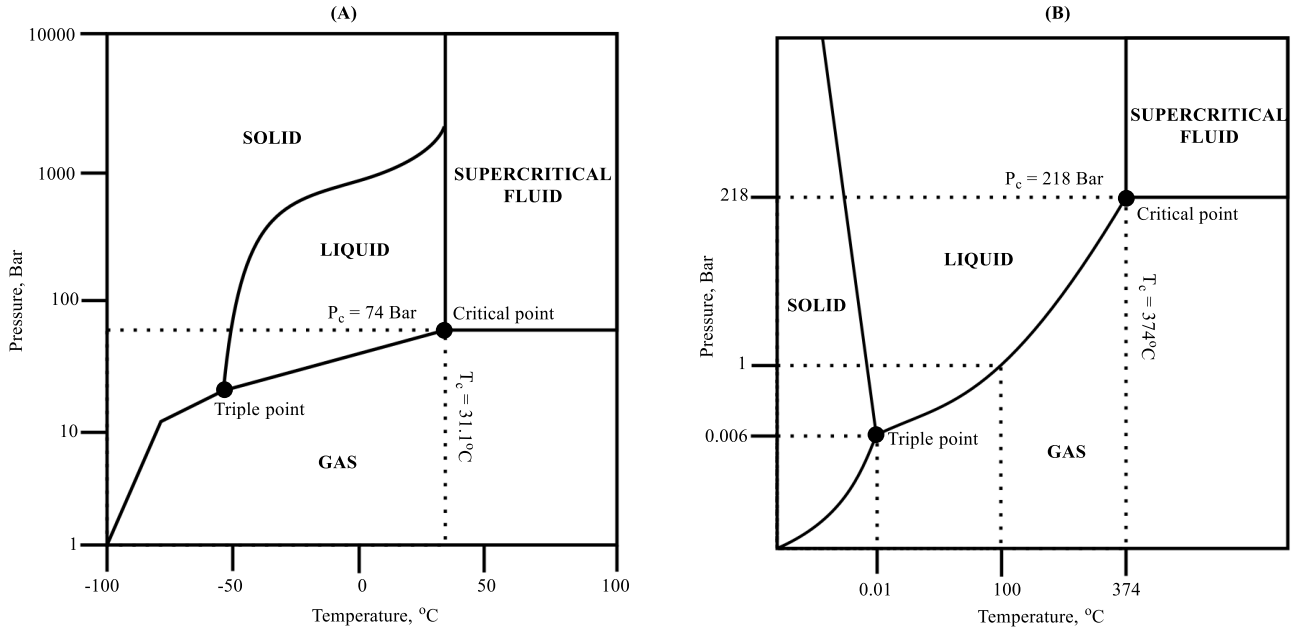

Fig. 8. Phase diagrams of carbon dioxide (A) and water (B)

The procedure of CO_2SFE is to some extent similar to steam distillation. The CO_2 is pressurised and pumped to a heating zone, where it is heated to supercritical conditions. Then it passes into the extraction vessel, where it rapidly diffuses into the solid matrix and dissolves the material meant to be extracted. This dissolved material is swept from the extraction cell into a separator at lower pressure, and the extracted material settles out while the CO_2 can then be cooled, re-compressed and recycled, or discharged into the atmosphere (Essien, Young, & Baroutian, 2020). A lot of advantages result from the properties of carbon dioxide: the mild critical temperature and the non-oxidative medium favour extraction of thermally unstable and easily oxidised compounds, while the gaseous state at room temperature greatly facilitates separation of solvent.

Recently, the potential of ionic liquids (ILs) and DESs as alternative solvents has grown up significantly. Ionic liquids are a combination of organic heterocyclic cations and organic or inorganic anions, while deep eutectic solvents are a combination of various hydrogen bond acceptors and hydrogen-bond donors (Płotka-Wasylka, de la Guardia, Andruch, & Vilkova, 2020). There are a few examples of the extraction ability of IL: Mezetta et al. (Mezzetta, et al., 2021) showed that [DMIM][DMP] as a pre-hydrodistillation maceration medium for *Cannabis sativa* L. gives a 10-20%

increase in yield of α-humulene, β-caryophyllene, β-caryophyllene oxide, humulene oxide, and caryophylla-4(14),8(15)-dien-5a-ol; Liu et al. (Liu, et al., 2011) demonstrated that ionic [BMIM][BF_4] microwave-assisted simultaneous extraction and distillation from *Rosmarinus officinalis* gives a slightly lower yield of β-caryophyllene and higher yield of β-caryophyllene oxide; Michalczyk et al. (Michalczyk, Cieniecka-Rosłonkiewicz, & Cholewińska, 2015) investigated the ability of benzalkonium lactate, didecyldimethyl lactate, and benzalkonium nitrate to extract β-caryophyllene from *Cinnamomum aromaticum* and these three ILs are more effective than ethyl acetate, hexane, methylene chloride, or methanol. DESs and their properties are discussed in a more detailed way in chapter 3 of this work.

2.2 Gas chromatography

Gas chromatography is an ideal technique for the quantitative and qualitative detection of semi-volatile organic bioactive compounds (i.e., caryophyllenes and their derivatives), whereas HPLC (Borges, Ribeiro, Anselmo, Cabral, & Pereirade Sousa, 2013) and HPTLC (Patra, Singh, Pareta, & Kumar, 2010) are less common due to their complexity. Identification of caryophyllenes with gas chromatography can vary and requires a thorough selection of sample injection/introduction method, sample injection mode, convenient type of detector and appropriate parameters for analysis performance.

2.2.1 Sample injection methods

Liquid injection method. Liquid sample injection in GC is nearly always carried out with microlitre syringes, see the example in **Fig. 9**.

Fig. 9. The examples of manual GC microlitre syringes

It is the most common and fast method for the sample introduction to the GC system, however, it has some disadvantages. The method is not solventless, as the sample should be dissolved in an appropriate solvent to be injected into the GC system. An additional amount of solvent is used to wash the syringe because the proper cleaning-washing procedure before and after injection, as well as proper maintenance of the syringe, significantly influences on accuracy and precision of analysis producing

better and more reliable analytical results. Selection of the correct syringe is required to meet sample and injection requirements, as there are different types of needles, volumes, and syringe accessories (Henshaw, 2006). The volumetric accuracy is considerably influenced by operating factors such as the speed of injection and the viscosity of the sample, as well as design factors such as the dead volume of the syringe needle and the clearance between the barrel and plunger. Automated devices can be used to reach excellent repeatability, reducing the human factor during the injection procedure.

Headspace injection. The term "headspace" (HS) in GC denotes the gas phase above the liquid or solid sample in a sealed vial (Fig. 10). Ideal candidates for HS-GC would be complex sample matrices, which are difficult to analyse directly or require time-consuming sample preparation. Usually, they contain volatile analyte in a less volatile matrix and can be placed directly into a vial without or with little preparation, which is a big advantage of headspace analysis.

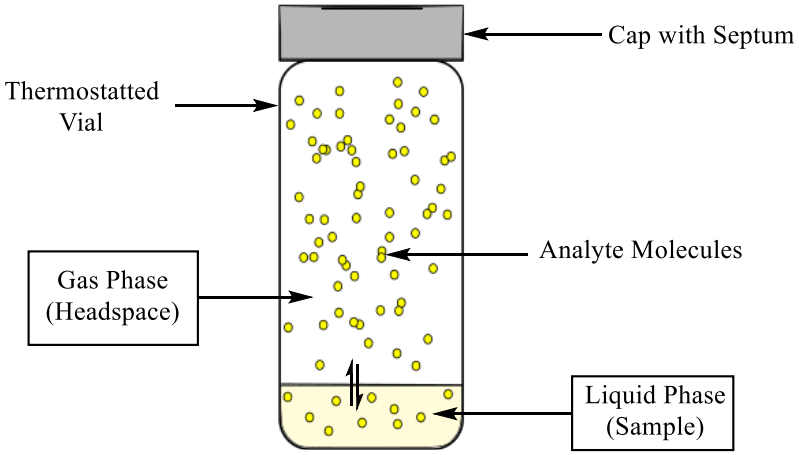

Fig. 10. The sealed thermostatted vial illustration

HS-GC sampling is generally classified as static or dynamic (Bicchi, 2000). In typical static HS-GC, a liquid or solid sample is placed in a sealed vial and heated to a predetermined temperature until equilibrium is reached, providing a constant composition mixture of gases in the vapour phase. The sample phase contains compounds of interest (volatile and semi-volatile molecules) which diffuse into the gas phase, while non-volatile heavy components remain in the sample phase (Sithersingh & Snow, 2012). An aliquot of this vapour-phase mixture is taken from the container and transferred to a gas chromatograph for separation and analysis of the components.

The headspace gas can be sampled manually using a gas-tight syringe, by an automated balanced-pressure system, or by an automated pressure-loop system. The manual technique is the least expensive and simple, but it has some reproducibility concerns. Recondensation of a sample can occur due to a difference in temperature of the syringe and heated oven; however, a heated syringe assembly could be used. In addition, an amount of sample can be lost while transferring it from the vial, because of pressure differences. The main steps of manual injection are shown in **Fig. 11**.

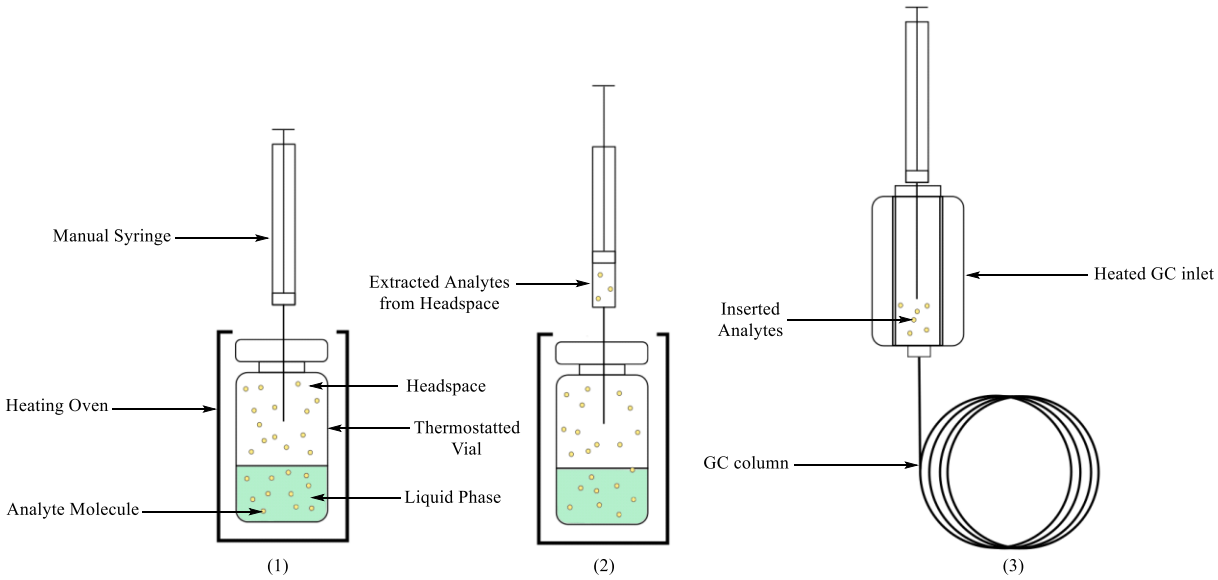

Fig. 11. Manual injection using a gas-tight syringe (1 – the needle is inserted upon equilibrium is reached, 2 – the amount of gas sample is extracted from headspace, 3 – the extracted sample is transferred to the GC column)

The balanced-pressure system can generate results with a high degree of repeatability compared to a gas-tight syringe injection, because the sample is transferred directly from the vial into the carrier gas stream, without additional moving parts other than a valve and a needle (Jochmann, Laaks, & Schmidt, 2014). It helps to decrease the chance for compound adsorption and loss via leaks. It should be noted that the absolute volume of the sample is unknown as this technique uses a theoretical amount of time to inject the sample (Restek Corp., 2000). A disadvantage of this system is the need for a dedicated instrument since the exchange of injection methods is not as easy as in syringe-based injection. The main steps of sample introduction using a balanced-pressure system are shown below in **Fig. 12**.

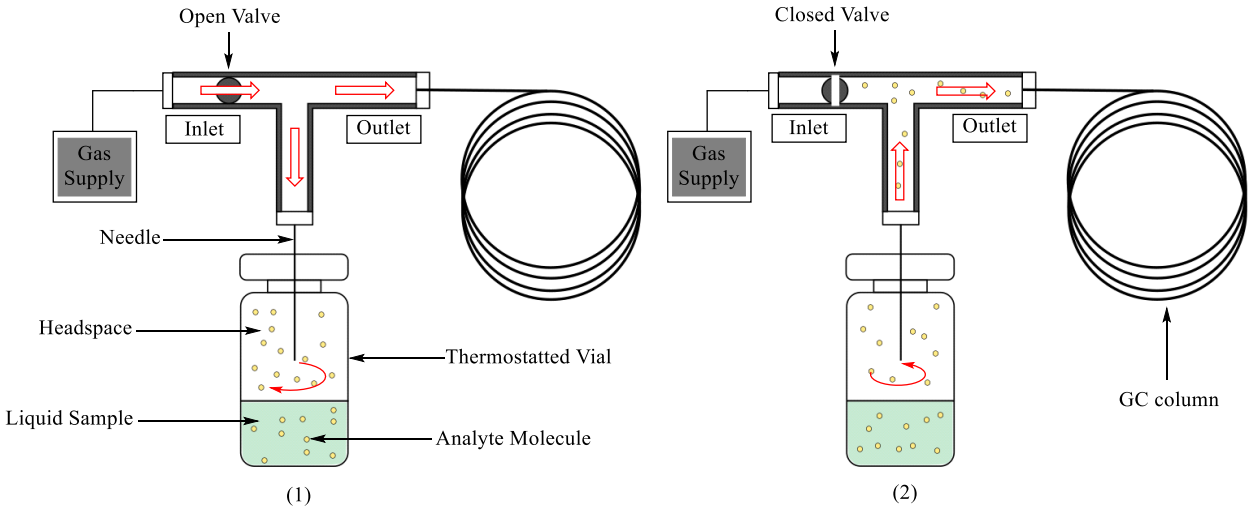

Fig. 12. Balanced-pressure system (1 – the needle is inserted upon equilibrium is reached and the sample is pressurised with a carrier gas, 2 – valve is switched for a specific amount of time to redirect the sample into the transfer line to the GC column)

The pressure-loop system has the same working principle as the balanced-pressure system. However, this technique typically uses a six-port valve: the sample is first extracted to loop and then is transferred to the GC column. Unlike a balanced-pressure system, the pressure-loop system uses a known amount of sample, that depends on the volume, pressure, and temperature of the loop (Jochmann, Laaks, & Schmidt, 2014; Kolb & Ettre, 2006).

One of the advantages is that loop can be thermostatted to high temperatures, which helps to lessen adsorption of higher molecular weight and sensitive compounds. The fixed volume of the sample loop also helps to improve run-to-run reproducibility. A disadvantage of a pressure-loop system is that it may cause ghost peaks because of sample carryover from a previous analysis (Restek Corp., 2000). The main steps of sample introduction using a balanced-pressure system are shown in **Fig. 13**.

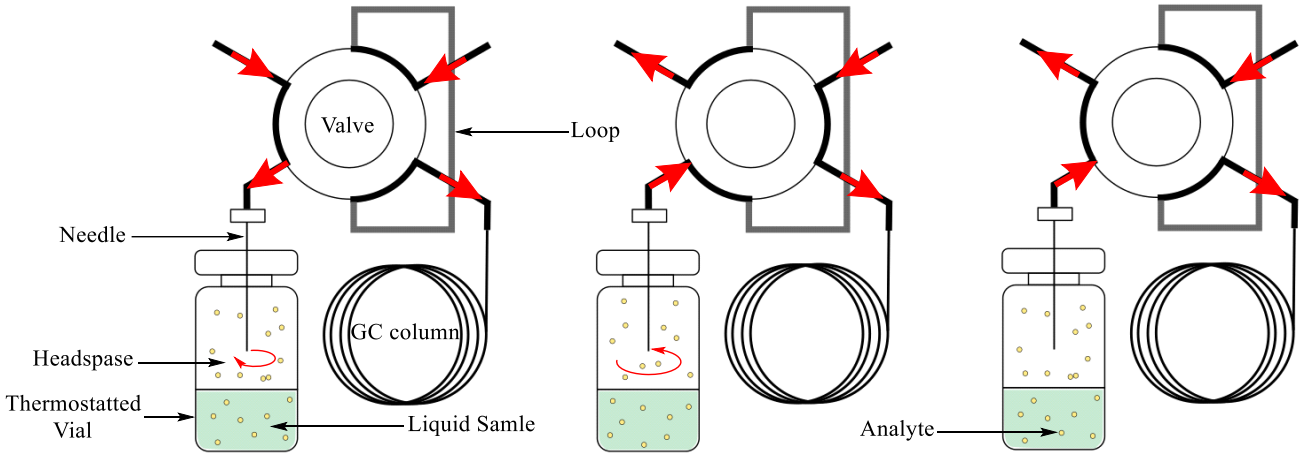

Fig. 13. Pressure-loop system (1 – the needle is inserted upon equilibrium is reached, and the sample is pressurised with a carrier gas, 2 – the valve is turned to fill the loop with the sample, 3 – the valve is turned again to redirect the gas flow and flush the sample into the transfer line to the GC column

Dynamic HS-GC provides an exhaustive extraction of analyte from the matrix, meaning that it is a non-equilibrium continuous process. In the ordinary dynamic headspace, the vial is pierced by a special double needle (gas supply, outlet) and a flow of carrier gas flushes the headspace. The volatile analytes flow through an outlet being captured by a suitable trapping system, such as cryotraps, solid adsorbents, liquid stationary phases or selective reagents for a given class of compounds, coated on a solid support. The trapped volatiles are then recovered through heat or solvent elution either on-line or offline to the GC.

Purge and Trap (P&T-HS) and Full Evaporation (FED-HS) are referred to as dynamic HS techniques having a slightly different principle of work from ordinary dynamic HS mentioned above (Jochmann, Laaks, & Schmidt, 2014). In P&T-HS the carrier gas is bubbled through a liquid sample and in FED-HS the sample is fully evaporated (**Fig. 14**).

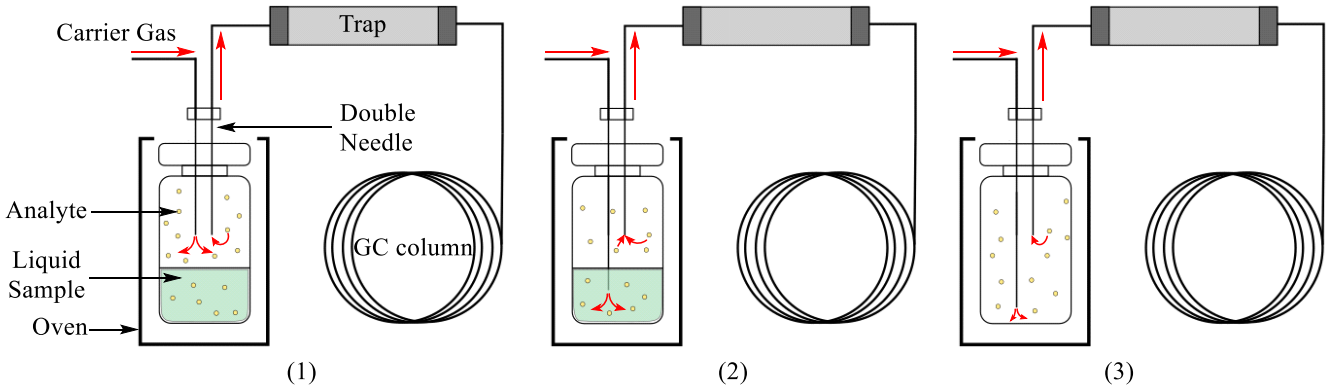

Fig. 14. Dynamic HS techniques (1 – ordinary dynamic HS, 2 – P&T-HS, 3 – FED-HS)

Dynamic HS was initially invented to overcome the relatively low sensitivity of static headspace. It can improve detection limits for analytes in samples by a factor of 100x or even more (Tipler, 2014). This technique is considered "green", solventless, and good for trace analysis. However, it is very expensive due to more sophisticated instrumentation, time- and energy-consuming due to the large number of parameters that must be standardised to achieve significant sampling repeatability and comparability, and it involves more complex procedures when quantitative analysis is required (Liberto, et al., 2019).

Headspace SPME. Several techniques such as stir-bar sorptive extraction (SBSE) (Ochiai, Sasamoto, David, & Sandra, 2018), single-drop microextraction (SDME) (Rincón, Pino, Ayala, & Afonso, 2011), liquid-phase microextraction (LPME) (Pawliszyn, 2012), solid phase microextraction (SPME) (Karačonji & Skender, 2007; Kataoka, 2017), direct immersion solid phase microextraction (DI-SPME), and high capacity sorptive extraction (HSSE) involve the addition of sorbents to trap analytes and transfer them to the GC.

SPME coupled with GC has become the most prominent, developed and widely used method for the analysis of volatile and semi-volatile analytes from various sources. Different standard procedures have been already implemented in the US and EU for plant treatment agents, biocides, their break-down products, and alkyl polycyclic aromatics in water. (Environmental Protection Agency, 2007; DIN EN ISO 17943:2016-10, 2016)

The SPME tool (**Fig. 15**) consists of a special SPME fibre holder, which enables the coated fibre to move in and out of the needle. The fragile fibre is encompassed in a fibre attachment needle for its protection during penetration of vial, GC injector septum, and movement along septum piercing needle. SPME fibres can be easily installed or replaced in the SPME holder, they are colour-coded and contain threads to screw into the holder barrel.

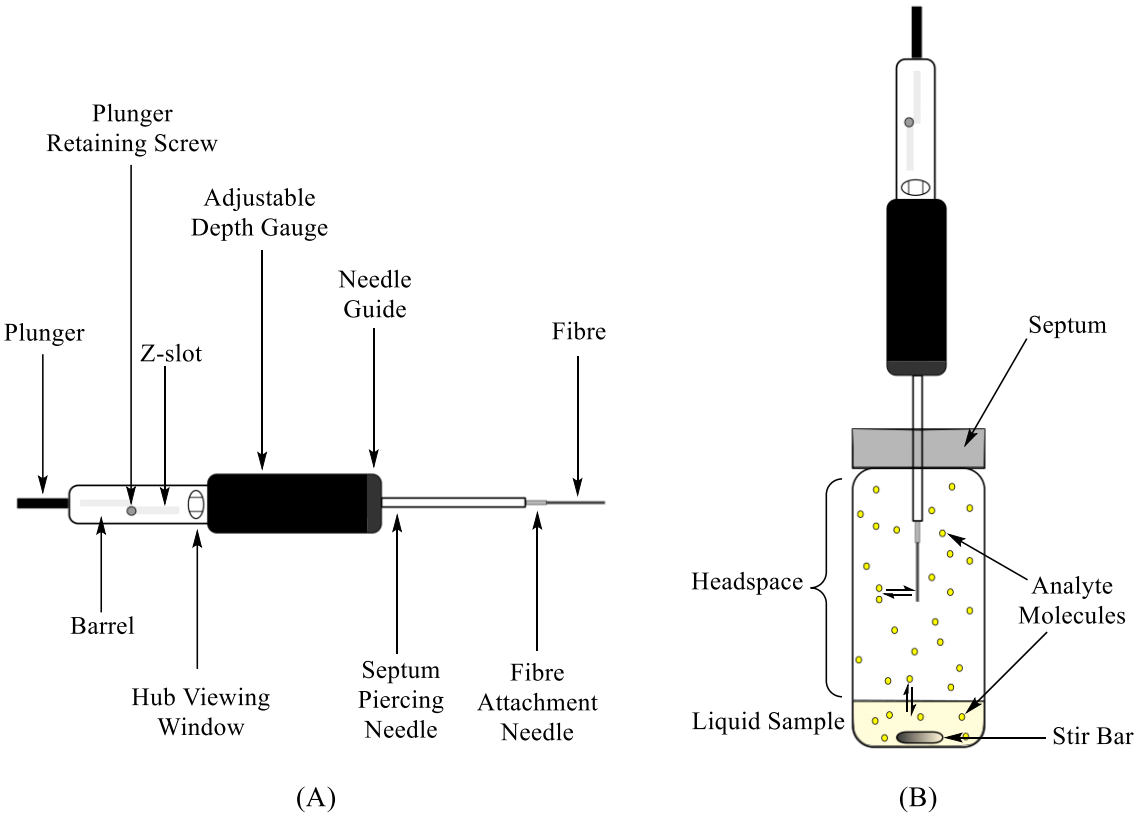

Fig. 15. Graphical representation of SPME tool (A) and equilibrated vial pierced by SPME tool (B)

HS-SPME combines several steps of sample preparation such as sampling, enrichment, and clean-up. It is an equilibrium-based technique and does not perform exhaustive extraction. Essentially, HS-SPME is a 3-phase system, consisting of a sample phase, headspace phase and fibre. The amount of a volatile analyte distributed between these three phases is shown in Equation 1.

$$C_0 \cdot V_s = (C_s \cdot V_s) + (C_g \cdot V_g) + (C_f \cdot V_f) \quad (1)$$

where C_0 – the concentration of the analyte in the original sample, V_s – volume of analyte in the original sample C_s, C_g, C_f – the concentrations of the analyte at equilibrium in the sample phase, gaseous phase, and fibre with volumes V_s, V_g, V_f respectively.

Two thermodynamic systems are at work simultaneously: analytes seek to achieve an equilibration between the sample and the headspace vapour with a concurrent equilibration taking place between the headspace vapour and the fibre coating (Equation 2).

$$[Analyte]_{sample} \leftrightarrow [Analyte]_{headspase} \leftrightarrow [Analyte]_{fibre} \quad (2)$$

It should be noted that equation 1 and equation 2 are only applicable for systems with a pure sample phase. If the sample containing the analyte is dissolved in the solvent, then an extra process (solid-liquid extraction) influences on 3-phase system equilibrium.

The typical SPME procedure includes the following steps of extraction and desorption: the septum of the sample vial is pierced by a needle after the equilibration of the system (Fig. 16, step 1), the fibre is exposed for sorption of analytes and related substances from headspace (Fig. 16, step 2), the fibre is retracted after a certain time and the needle is removed from the vial (Fig. 16, step 3), the needle is inserted into the GC injector (Fig. 16, step 4), the fibre is exposed for sorption of analytes and related compounds (Fig. 16, step 5), the fibre is retracted and the needle is removed from the GC injector (Fig. 16, step 6).

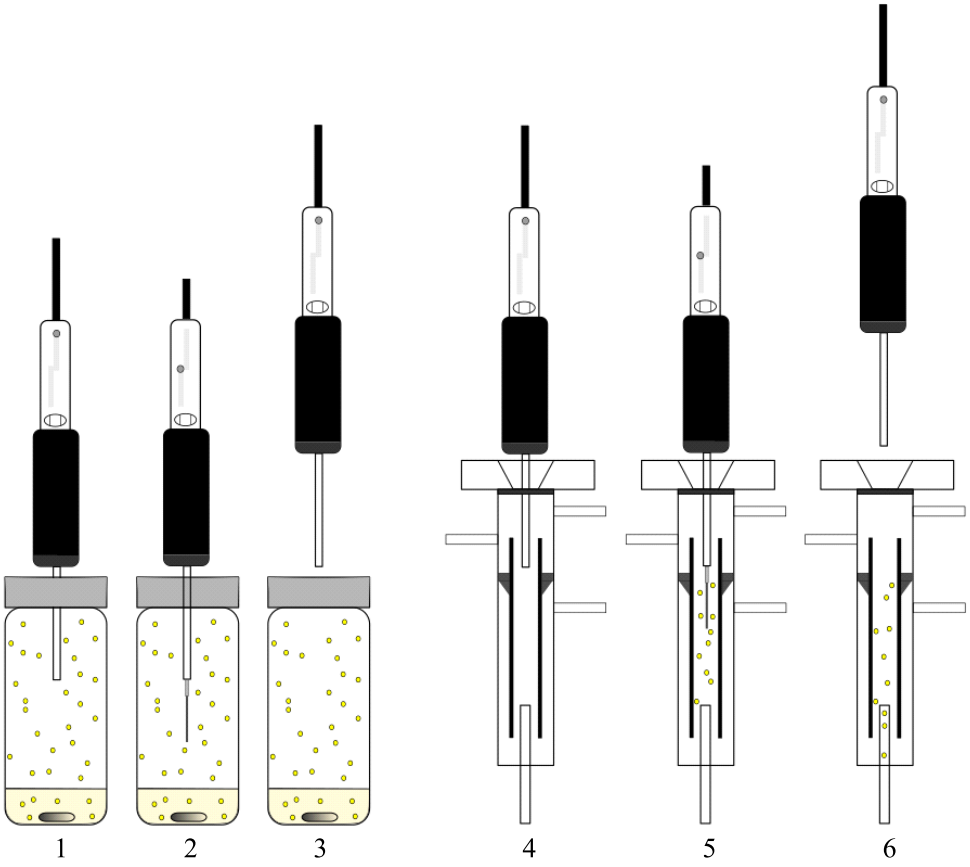

Fig. 16. Headspace SPME procedure scheme (1, 2, 3 – extraction; 4, 5, 6 – desorption)

SPME considerably simplifies the extraction of analytes as no gases and plumbing are required in comparison to other headspace techniques. The SPME method provides a good degree of pre-concentration of samples and is effective to get rid of the water effect on the GC column. It is considered “green” as there are no solvents needed and the fibre is reusable (all extracted compounds are transferred to GC and the fibre is cleaned up). The fibre can be used in two different ways: be directly immersed in the liquid sample or just in the headspace.

One of the challenges in SPME is that overlapped thermostatting cannot be performed with the fibre in the vial. The samples must first be thermostatted for some time to achieve equilibrium between the sample and the headspace phase, followed by an additional equilibration step once the fibre is inserted into the vial. This extra step reduces sample throughput significantly. The other potential issue with SPME concerns the kinetics in achieving equilibration (Reyes-Garcés, et al., 2018).

In terms of detection limits, typical extracts injected into the GC column will contain 0.1 to 1% of the compounds in the original sample (Tipler, 2014). Thus, SPME will provide a slight improvement in detection limits over conventional (equilibrium) headspace but will fall short of the detection limits provided by dynamic headspace (Povolo & Contarini, 2003).

2.2.2 Injection modes

Split and splitless injection modes are the two most frequently used injection modes in gas chromatography. Their use is determined by the concentration of the sample, the sensitivity of the detector, or any technique requirements. The split-splitless inlet is depicted in **Fig. 17**.

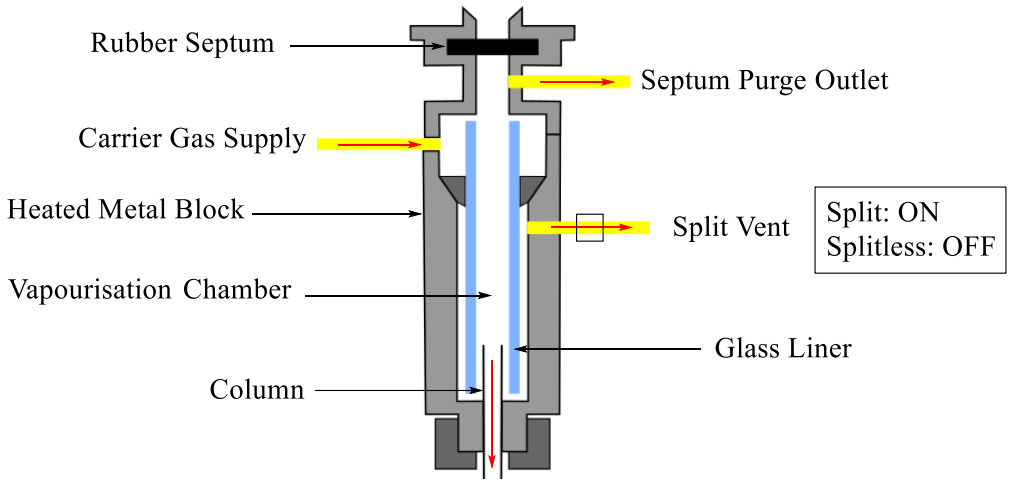

Fig. 17. Split-splitless inlet sketch

Because of its adaptability along with a wide range of analyses, the split mode is more popular. Only a part of the sample enters the column from a hot liner where it is introduced. For example, suppose the gas enters the inlet at a rate of 54 mL/min. A small amount (3 mL/min) passes through the septum purge to reduce the possibility of septum contamination, while the remainder continues to the liner. A small amount of gas (1 mL/min) flows into the column, but the majority (50 mL/min) is swept away via the split vent.

The split ratio (Equation 3) is the main characteristic parameter of the split injection mode, and it is calculated as the quotient of the column carrier gas flow rate and the flow rate into the split vent. It usually varies from 1:5 to 1:500.

$$Split\ Ratio = \frac{Q_{column}}{Q_{total} - Q_{septum\ purge} - Q_{column}} = \frac{Q_{column}}{Q_{split\ vent}} \quad (3)$$

The split injection is ideal for a high concentration of the analyte to meet required detection limits after sample dilution. Higher flow rates through the inlet produce sharp and narrow peaks while also shortening the amount of time needed for adverse interactions to occur.

In a splitless injection, the split vent is left closed before and during the injection, resulting in no split flow and a drastically reduced total flow. For example, if the total flow is set to 4 mL/min and 3 mL/min passes through the septum purge, the remaining 1 mL/min enters the column.

Because of the lower flow rate, the sample remains within the liner for a longer period before entering the column during a splitless injection. The splitless hold time is the time interval between injection and the opening of the split vent to purge the inlet. It is long enough to ensure that analytes are transferred to the column.

Splitless injections perform exceptionally well in trace analyses. Since the entire flow is directed to the column, you can transfer the major portion of the sample. However, the slower flow rate into the column can cause active analytes to degrade through adsorption and breakdown. It also causes increased diffusion, which causes band broadening.

2.2.3 Types of GC detectors

The selection of the GC detector is an important step of the analysis because it should have a universal response, high reliability, high sensitivity, large linear dynamic range, low noise, short response time, etc. Although the physical principle of action[1] of FID (Sabulal, et al., 2006; de O.Dias, et al., 2012) and MS (Sabulal, et al., 2006; Sudeep, et al., 2021; Al-Fatimi, 2020) are different, these detectors are among the most frequently used for the determination or identification of caryophyllenes in complex matrices. And it is worth mentioning that the MS detector allows applying SIR to reach better identification and high sensitivity (Stauffer, Dolan, & Newman, 2008).

[1] The FID measures the current of ions formed during combustion, while the MS detection is based on the intensity of fragments produced by ionisation.

3. DEEP EUTECTIC SOLVENTS

3.1 Definition, classification, and synthesis

Sample preparation techniques are an essential part of any analysis. The main aims of the sample preparation step are purification of the sample, extraction, enrichment of the analytes, and possibly modification of the sample to adapt it to the requirements of the analytical apparatus. The main trend is devoted to "green" extraction techniques, which focus on the elimination of toxic and volatile organic solvents. To be qualified as a green medium, these solvents must meet different criteria such as availability, non-toxicity, biodegradability, recyclability, flammability, and low price.

In recent years, the new generation of solvents (so-called deep eutectic solvents) has attracted the attention of scientific society. The number of publications is growing exponentially every year as shown in **Fig. 18** based on the data of search engine query = "deep eutectic solvents" in the American Chemical Society (https://www.acs.org/content/acs/en.html), Royal Society of Chemistry (https://pubs.rsc.org/), and PubMed databases (https://pubmed.ncbi.nlm.nih.gov/).

	2022	2021	2020	2019	2018	2017	2016	2015	2014	2013	2012	2011	2010	2009	2008	2007	2006	2005	2004	2003
ACS	98	253	251	198	137	106	61	42	33	16	5	10	12	3	3	1	2	0	1	0
RSC	124	291	215	153	120	101	100	84	57	32	31	24	4	7	2	2	2	0	0	1
PubMed	215	436	350	229	178	139	84	55	30	24	11	9	6	6	2	1	2	0	1	0

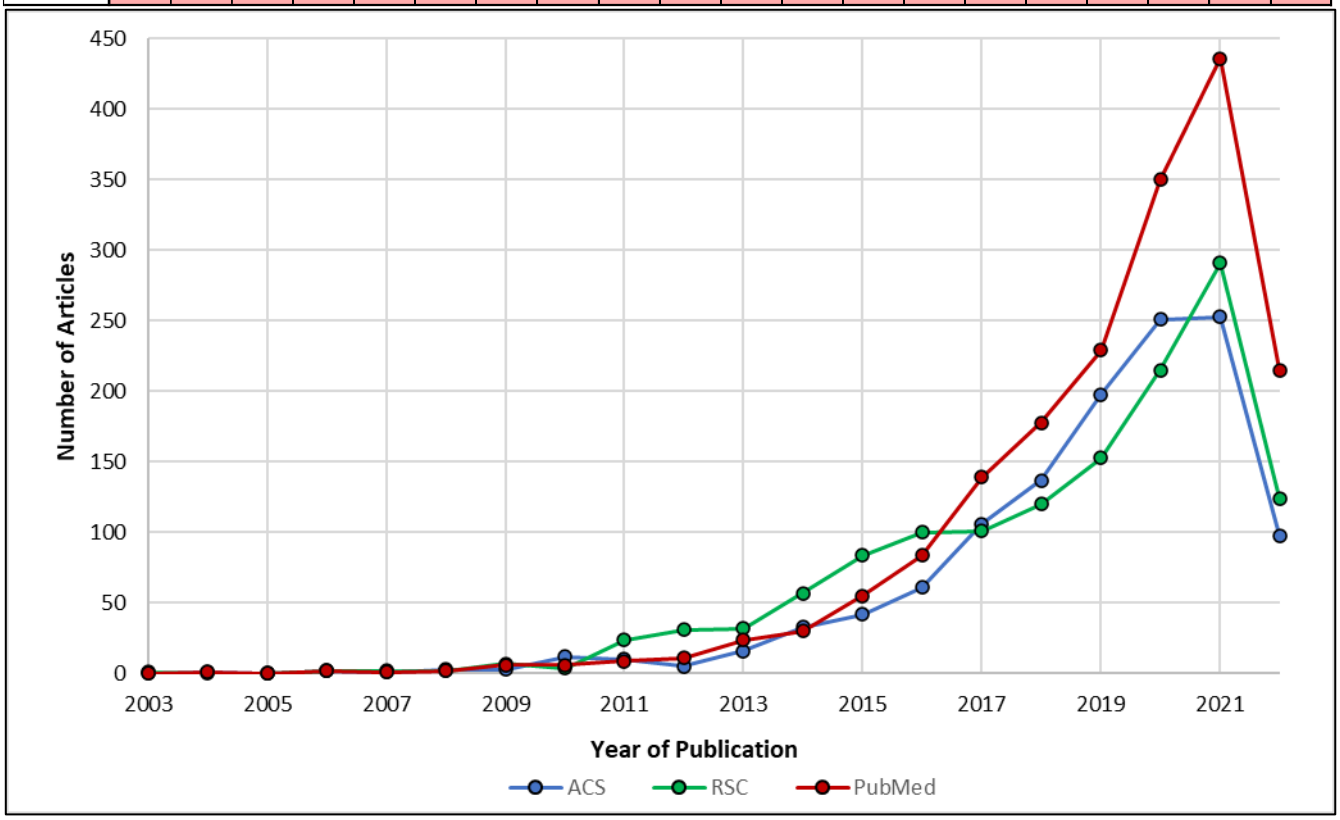

Fig. 18. The chart and table of the number of publications (search engine query: "deep eutectic solvents") from 2003 to 2022 (May 8)

In 2003 Abbott et al. investigated the mixtures of urea with a variety of quaternary ammonium salts (2:1), that are liquid at room temperature and have interesting solvent properties. Those mixtures were called "deep eutectic solvents" and defined as "a type of ionic liquids that decrease lattice energy and the freezing point of the system" (Abbott, Capper, Davies, Rasheed, & Tambyrajan, 2003).

Although some authors define DESs to be a subclass of ILs (He, et al., 2014) and others use the terms interchangeably (Hayyan, Mjalli, Hashim, & AlNashef, 2010), it is important to highlight that they are not quite the same types of solvents. The composition of the starting materials and the processes of synthesis distinguish DESs from ILs:

1. Ionic liquids are usually made up of organic heterocyclic cations and organic or inorganic anions, whereas DESs are made up of diverse hydrogen bond acceptors (HBA) and hydrogen bond donors (HBD).
2. The preparation of ILs is more expensive and difficult than that of DESs. The reaction time is relatively long, and the synthesis includes cation formation and anion exchange (Płotka-Wasylka, de la Guardia, Andruch, & Vilkova, 2020). DESs can be easily prepared through heating or grinding. The production of DESs is relatively simple and inexpensive, with no significant post-purification or disposal issues.

Deep eutectic solvents can be described by the general formula (4) and are largely classified into 5 types depending on the nature of the complexing agent used (**Table 3**).

$$Cat^+X^-zY \tag{4}$$

where Cat^+ – any ammonium, phosphonium or sulfonium cation; X^- – a Lewis base, usually halide anion; Y – either a Lewis or Brønsted acid; z – the number of Y molecules that interact with the anion.

Table 3. Classification of DESs and general formulae.

Type	Formula	Terms	Example
I	$Cat^+X^-zMCl_x$	$M = Zn, Sn, Fe, Al, Ga, In$	$ChCl + AlCl_3$
II	$Cat^+X^-zMCl_x \cdot yH_2O$	$M = Cr, Co, Cu, Ni, Fe$	$ChCl + CrCl_3 \cdot 6H_2O$
III	Cat^+X^-zRZ	$Z = CONH_2, COOH, OH$	$ChCl + Urea$
IV	$MHal_x + RZ = [MCl_{x-1}]^+ \cdot RZ \cdot [MCl_{x+1}]^-$	$M = Al, Zn; Z = CONH_2, OH$	$ZnCl_2 + Urea$
V	$HBA + HBD$	HBA *is non-ionic*	$Menthol + Octanoic\ acid$

Type I DESs formed with anhydrous metal chlorides (e.g., AgCl, $CuCl_2$, $CdCl_2$, LiCl) and quaternary ammonium salts can be considered analogous to the well-studied (metal halide)/(imidazolium salt) systems.

Type II DESs are identical to type I, however, metal halides are used in the form of hydrates (e.g., $CrCl_3 \cdot 6H_2O$, $CuCl_2 \cdot 2H_2O$).

DESs related to type III are now the most popular and widely investigated, especially those formed from choline chloride and hydrogen bond donors (e.g., amides, carboxylic acids, alcohols, and saccharides). Some examples of type III DESs are shown in **Fig. 19** below.

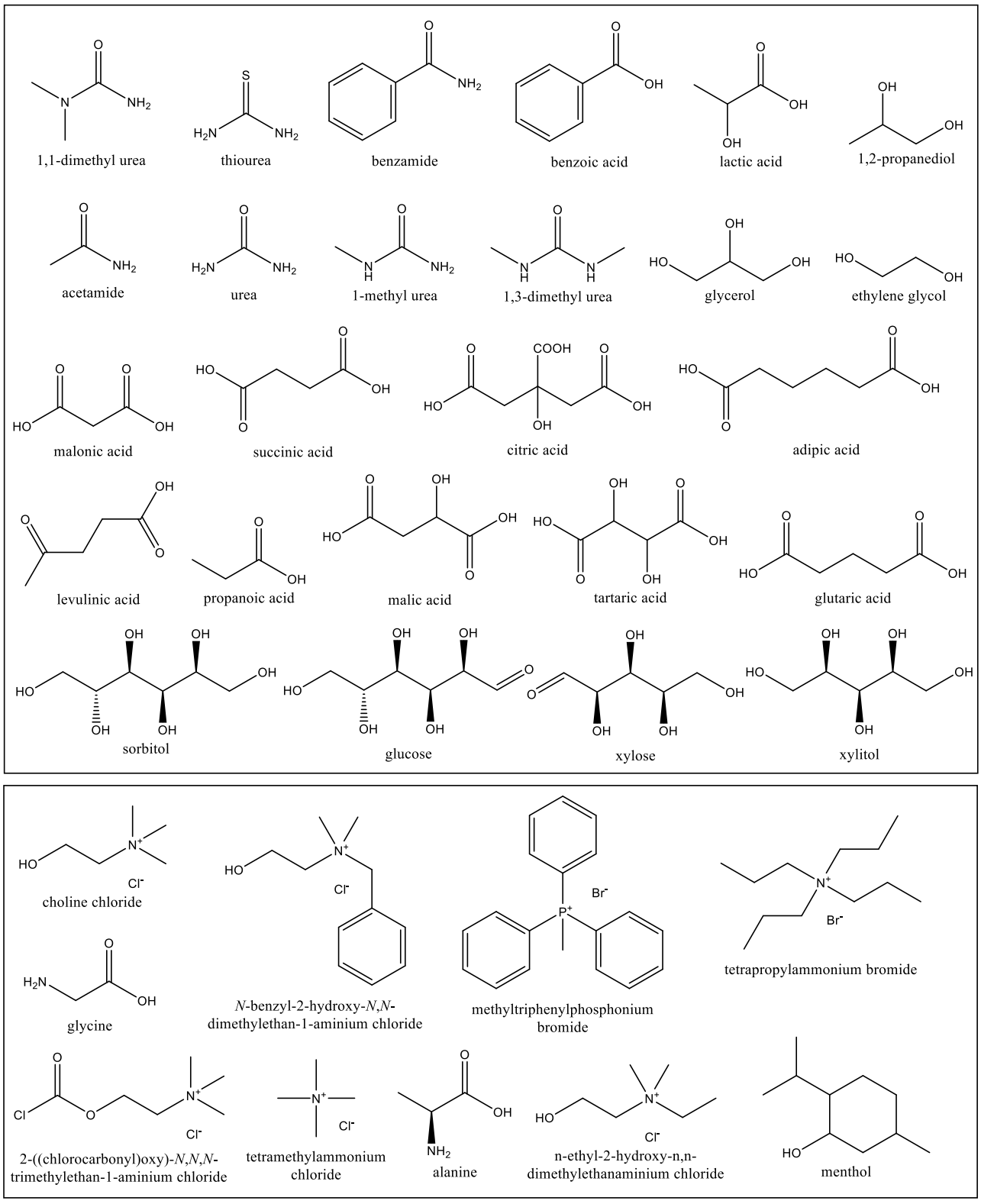

Fig. 19. The structures of the most common HBD (top) and HBA (bottom)

While most DESs include a quaternary ammonium ion as the cationic component, it has been shown recently that eutectics can also be formed between a metal hydrate (or metal halide hydrate) and a simple amide or alcohol to form a metal-containing solution composed of cations and anions via

disproportionation processes (Abbott, Barron, Ryder, & Wilson, 2007). Those DESs are classified as type IV DESs.

Type V is a relatively new type of DESs that could also be added to the classification. Type V DESs are formed with non-ionic molecular HBA (e.g., menthol, lidocaine, atropine, camphor, coumarin) and HBD (Ijardar, Singh, & Gardas, 2022). Those DESs are usually hydrophobic (van Osch, Dietz, Warrag, & Kroon, 2020).

As was previously mentioned, the synthesis of DESs is relatively simple. There are 4 main approaches to synthesising DESs:

1. *Heating method* is the most popular one, where the mixture of HBA and HBD is heated and stirred until the formation of a homogeneous liquid.
2. In the *vacuum evaporation method* the mixture of HBA and HBD is first dissolved in water, mixed, and then water is evaporated under vacuum at an elevated temperature and the resulting DES is dried in the desiccator.
3. *Grinding method* is based on continuous grounding until the formation of DES.
4. *Freeze-drying method* is used rarely. The HBA and HBD are first dissolved in water and then mixed, and frozen. The mixture is kept freeze-dried until the formation of DES.

A good example of the most common method is the preparation of DES from a mixture of choline chloride and urea (molar ratio 1:2), where it is heated for 15 minutes at 80 ^{o}C to form a transparent viscous liquid (**Fig. 20**).

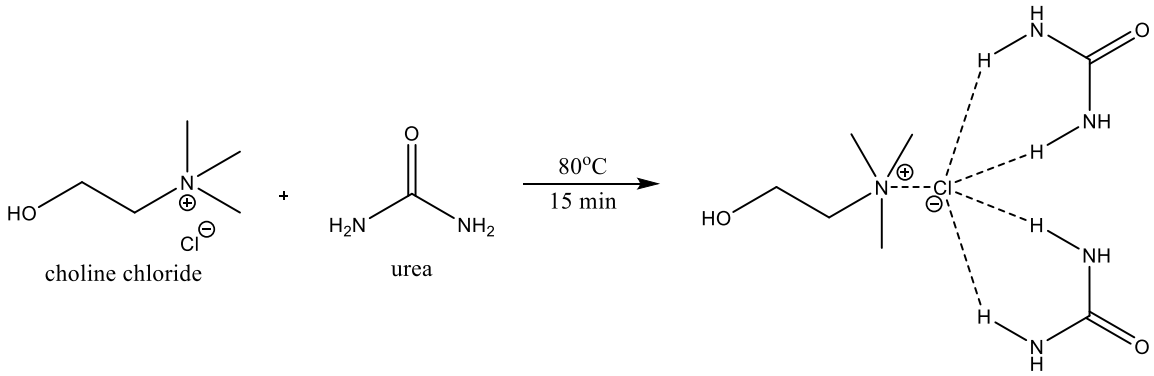

Fig. 20. The scheme of synthesis of DES from choline chloride and urea

The formation of DESs occurs due to hydrogen bonding of the precursors, together with intermolecular interactions involving Van der Waals and electrostatic forces (Espino, Fernández, Gomez, & Silva, 2016). In certain syntheses, water is added to the mixture of HBD and HBA to reduce viscosity and simplify the formation of DESs. It could be further evaporated, but sometimes it is strongly retained and fits into the hydrogen bond network of DESs.

3.2 Properties

Deep eutectic solvents are unique liquids and possess properties that differentiate them from convenient solvents. It should be noted that although DESs are different from ILs, their properties are

to some extent similar. The most important properties from the point of view of analytical chemistry include freezing point temperature, viscosity, polarity, extractability, and environmental friendliness. Other properties of DESs are surface tension, density, excess molar volume, enthalpy of mixing, excess molar Gibbs energy of activation, coordination number in structure, water absorption capacity, refractive index, and temperature of destruction.

Freezing point. DESs are characterised by a lower freezing point than that of the individual constituents. Some examples are shown below in **Table 4**.

Table 4. Freezing points of DESs

HBA	T_f (HBA), ^oC	HBD	T_f (HBD), ^oC	HBA : HBD	T_f (DES), ^oC
ChCl	303	Acetamide	222	1 : 2	51
ChCl	303	Oxalic acid	190	1 : 1	34
ChCl	303	D-glucose	146	2 : 1	15
ChCl	303	Urea	134	1 : 2	12
ChCl	303	Malonic acid	134	1 : 1	10
ChCl	303	Acetamide	80	1 : 2	52
Choline acetate	83	Glycerol	18	1 : 2	-40
$(n\text{-}Bu)_4NCl$	84	Ethylene glycol	-13	1 : 3	-31

The difference in the freezing point at the eutectic composition of a binary mixture of A + B compared to that of a theoretical ideal mixture – ΔT_f – strongly depends on the magnitude of the interaction between these two components (**Fig. 21**) (Smith, Abbott, & Ryder, 2014). The stronger the interaction of DES constituents the larger will be the value of ΔT_f, which also means the dependence of this parameter on the nature of HBD and HBA.

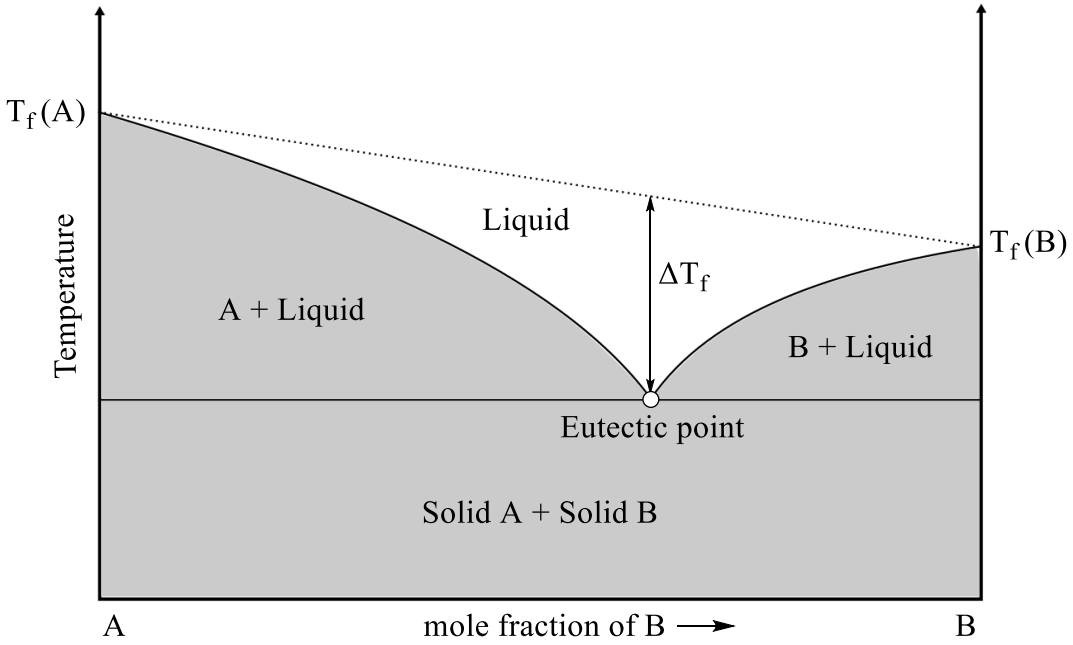

Fig. 21. Phase diagram of a eutectic mixture representing the eutectic point and ΔT_f

Colour. Most of the DESs are transparent liquids. Sometimes they have a whiteish-yellowish shade, which is due to the nature of starting materials.

Viscosity. Despite the potential of DESs, an obvious disadvantage is the high viscosity. Usually, DESs have dynamic viscosity higher than 100 cP at 25°C. For reference, the dynamic viscosity of water is 0.89 cP at 25°C. High viscosity influences extraction performance as it decreases the mass transfer between the sample and the extraction phase. At the same time, it limits the application of DESs in some analytical techniques. It has been found that the nature of the solvent, the molar ratio of HBA and HBD and temperature influence viscosity (**Table 5**) (Ramón & Guillena, 2019). For example, the viscosity of ChCl : Urea (1 : 2) decreases with heating from 25°C to 40°C by almost 5 times; type I and type II DESs usually have much greater dynamic viscosity than that of type III and type V; the viscosity of ChCl : Glycerol grows with a fraction of glycerol in DES.

Table 5. Dynamic viscosity of several DESs, water, methanol, and chloroform

Solvent	HBD : HBA	Dynamic viscosity, cP	Temperature, °C
ChCl : $ZnCl_2$	1 : 2	85000	25°C
ChCl : Urea	1 : 2	750	25°C
ChCl : Glycerol	1 : 2	259	25°C
ChCl : Glycerol	1 : 2	259	20°C
ChCl : Glycerol	1 : 3	450	20°C
ChCl : Glycerol	1 : 4	503	20°C
ChCl : Urea	1 : 2	449	30°C
ChCl : Urea	1 : 2	169	40°C
ChCl : Ethylene glycol	1 : 2	37	25°C
Choline acetate : Urea	1 : 2	2214	40°C
water	-	0.89	25°C
methanol	-	0.54	25°C
chloroform	-	0.54	25°C

Density. Density is an important thermophysical property that can be used in the evaluation of such parameters as mass transfer, expansion coefficient, viscosity, and isothermal compressibility (Ijardar, Singh, & Gardas, 2022). Usually, the density of most of the DESs varies between 1.0 and 1.6 g/cm^3 at 25°C, which is higher than the density of water. It depends on the nature of components of DESs and sometimes can be explained with the hole theory. For example, the density of ChCl-based DESs decreases with the longer alkyl chain of bifunctional carboxylic acid (oxalic > malonic > levulinic acids) (Florindo, Oliveira, Rebelo, Fernandes, & Marrucho, 2014). The density of DESs also depends on the temperature and decreases with higher the latter.

Polarity. Polarity is another property of DESs that correlates with the extraction performance According to the principle of similar miscibility, matched polarity between DES and analyte could increase its solubility in DES and hence promote the extraction (Xu, et al., 2019).

Conductivity. Due to high viscosity, the ionic conductivity of DESs is quite poor and usually not higher than 2 mS/cm at room temperature. The relationship between viscosity and conductivity can be

determined on a $\log\frac{1}{\eta} - \log\Lambda$ scale Walden plot, where low-viscous DESs have higher molar conductivity values and high-viscous are closer to the ideal linear-like pattern with slope = 1 (Ramón & Guillena, 2019). Conductivity also increases with the temperature.

Environmental friendliness. This property is multi-component and can be assessed in a few different ways. Usually, criteria such as biodegradability, synthesis, toxicity, ozone depletion, stability, recyclability/reusability, volatility, and low cost are used to determine the environmental impact of DES and decide whether they are considered green or not. The most common group of DESs is type III, especially ChCl-based. They are readily biodegradable and have low toxicity (Wen, Chen, Tang, Wang, & Yang, 2015). For example, ChCl is an important food additive for animal growth, and a lot of complementary HBDs are quite harmless as urea is a fertiliser, glycerol is additive in alcohol production, and saccharides are a part of our diet. Some DESs are used in therapeutics (THEDES – therapeutic deep eutectic solvents) such as menthol-ibuprofen and lidocaine-ibuprofen or have 100% natural components and are named NADES (natural deep eutectic solvents), which includes proline-malic acid, xylitol-ChCl-quercetin, urea-glucose-fructose, etc. The synthesis of DESs is quite simple, doesn't require a lot of energy, is cheap and has a very low E-factor[2]. DESs are usually very stable even when heated at relatively high temperatures, have negligible volatility, are non-flammable, and are non-ozone-depleting.

Surface tension. As the surface tension depends on strength of intermolecular forces in the hydrogen bond network of DESs, it is remarkably high and usually lies in the range of 40-75 mN/m. For reference, the surface tension of water is very high and is equal to 72.8 mN/m, and for the most common organic solvents, it is about 10-45 mN/m.

Extractability. The ability of DES to extract compounds differs significantly due to changes in polarity and viscosity. There is no common trend and conditions should be investigated for each DES and analyte.

Refractive index. Refractive indices of DESs studied to date have relatively high values between 1.4400 and 1.5000 (Chen, et al., 2022). For reference, the refractive index of water is equal to 1.3335.

3.3 The influence of water on the properties

Adjustment of DES properties can be reached by changing HBA or HBD, their molar ratio, temperature, or with addition. Water can be utilised as a cosolvent in various DESs/NADESs to modify their physicochemical properties.

It is important to mention that although water content in DESs has a big impact on its properties, there is not enough experimental data to properly describe them. Considering the lack of experimental data, most explanations are based on logic, chemical and physical laws, and mathematical modelling.

Near a dozen of articles was published in the last 5 years, which can give primary information about structural changes, viscosity, density, polarity, conductivity, and freezing point of most common DESs such as ChCl : Urea (1 : 2), ChCl : diethylene glycol (1 : 2), ChCl : ethylene glycol (1 : 2), ChCl : glycerol (1 : 2), ChCl : 1,2-propanediol (1 : 1) and a few NADESs such as lactic acid : glucose, proline : malic acid, ChCl : glucose, etc.

[2] E-factor is the ratio of the mass of waste products to the mass of the product. The lower E-factor the better.

Structural changes. Although water addition is good for tailoring properties of DESs, an excessive amount of water might cause severe weakening of the interaction between DES components and lead to full disruption of DESs (Vilková, Płotka-Wasylka, & Andruch, 2020). FTIR spectroscopy, Raman spectroscopy, X-ray diffraction, neutron diffraction, and NMR are the most popular techniques to study interaction and structural changes in DESs from temperature, the addition of water and the change of composition. Besides those techniques, molecular dynamics simulations and quantum chemistry calculations are becoming popular to simulate nanostructures or determine multiple parameters such as spatial distribution function, radial distribution function, or coordination number. A few examples are discussed below.

FTIR spectra and the absorbance peaks of the O–H bands as a function of the amount of deuterium oxide added to ChCl : diethylene glycol (1 : 3) are shown in **Fig. 22** (Gabriele, Chiarini, Germani, Tiecco, & Spreti, 2019). Raman spectra of ChCl : urea (1 : 2) and ChCl : glycerol (1 : 2) are shown in **Fig. 23** (Pandey & Pandey, 2014).

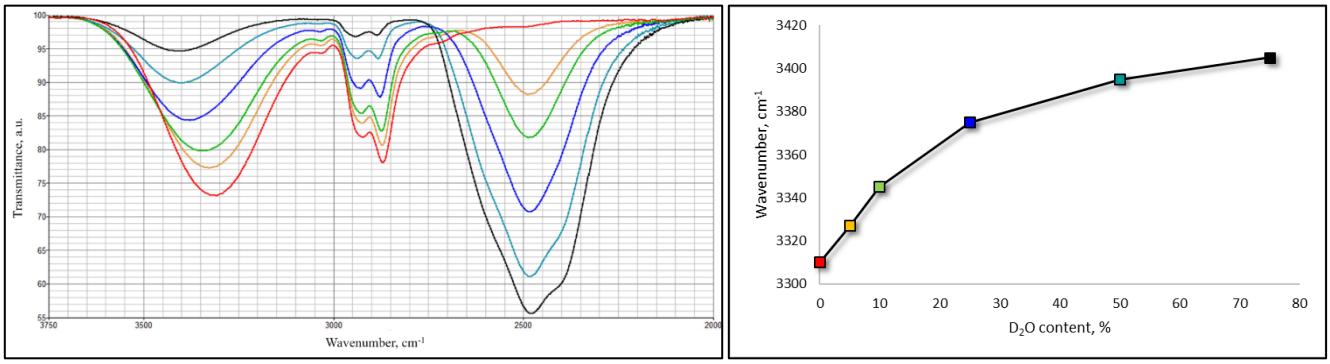

Fig. 22. FTIR spectra of ChCl : diethylene glycol (1 : 3) and the plot of wavenumber $(O–H)_\nu$ with different amounts of D_2O added (0% – red, 5% – orange, 10% – green, 25% – blue, 50% – aquamarine, 75% – black)

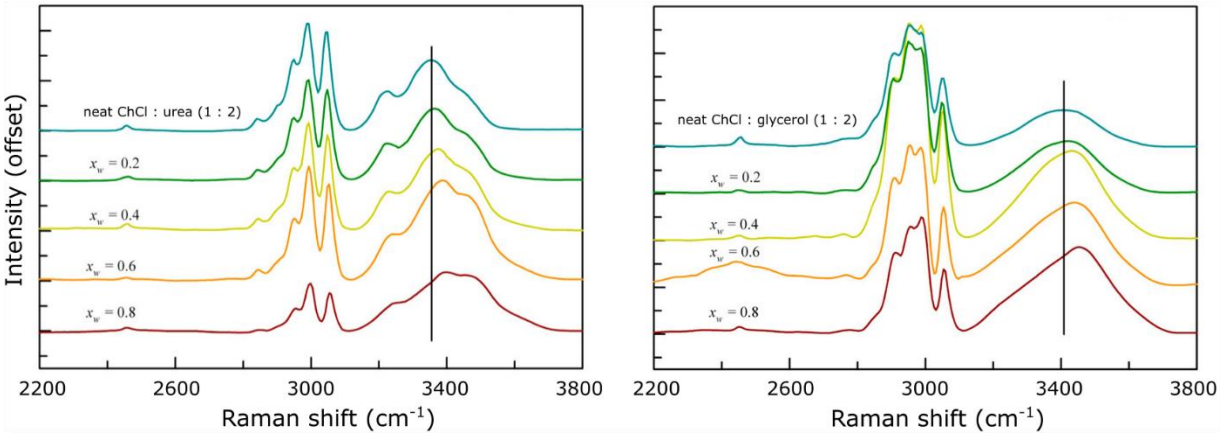

Fig. 23. Raman spectra of ChCl : urea (1 : 2) and ChCl : glycerol (1 : 2) vs $\chi(H_2O)$

The trend of the FTIR curves clearly shows the hypsochromic shift (up to 85 cm^{-1}) of the absorbance peaks of O–H stretching vibrations, which indicates that the interactions between the DES

components are weakened. The dependence of wavenumber is non-linear and has a greater growth tendency at lower D_2O amount, then it slows down after DES-DES interactions are disrupted.

The Raman spectra demonstrate that the region representing hydrogen bonding interactions of ChCl : urea (the highest energy band) does not change significantly when water is added. On other hand, the combined peaks representing all -OH functionalities present in the system have a shift, with even more noticeable for ChCl : glycerol (vertical line in Fig. 23 is added to highlight the shift). It could indicate that ChCl : glycerol has more hydrogen bonding interspecies than ChCl: urea, where interstitial water accommodation within the ChCl: urea molecular network appears to be more important.

Some NMR studies also observe a progressive rupture of hydrogen bonding interaction in DES with water dilution as a downfield shift of all signals (except methyl and methylene groups) was observed together with the reduced relative number of detected protons (Dai, Witkamp, Vertpoorte, & Choi, 2015; El Achkar, Fourmentin, & Greige-Gerges, 2019; D'Agostino, et al., 2015).

Computer simulations can help to better understand the distribution of hydrogen bonding in DESs-H_2O mixtures and to see structural changes visualised (Kaur, Kumari, & Kashyap, 2020; Zhekenov, Toskanbayev, Kazakbayeva, Shal, & Mjalli, 2017; Sapir & Harries, 2020).

Kaur and co-workers investigated the hydration effect on the microscopic structural morphology in (ChCl : ethylene glycol)–water mixtures by employing all-atom molecular dynamics simulations (Kaur, Gupta, & Kashyap, 2020) (**Fig. 24**).

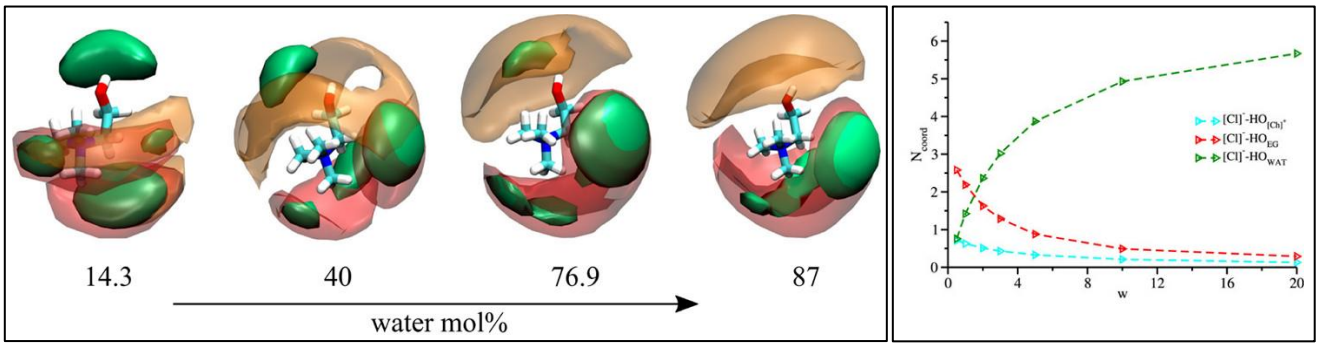

Fig. 24. (left) SDFs representing 3D spatial distribution variations of ChCl : ethylene glycol components (Cl^- in green, ethylene glycol in orange and H_2O in red) around central choline cation; (right) Variation in coordination number of constituent hydroxyl hydrogens ($[Ch]^+$, ethylene glycol, and water) around chloride as a function of the degree of hydration.

Kaur and co-workers found that the isosurface of water surrounds the ammonium group of the $[Ch]^+$ not only at minimum hydration level (14.3% water) but also at increasing water levels up to 87%. It means that water molecules preferably solvate the polar ammonium group of the $[Ch]^+$. However, the isodensity surface of ethylene glycol moved the from near-ammonium position (at 14.3% water) to the near-hydroxyl position of the $[Ch]^+$ at 87%. At the same time, the Cl^- isodensity surface gradually disappears near the hydroxyl group of $[Ch]^+$, due to the weakening of the intermolecular hydrogen bonding interactions and is still located around the ammonium group of $[Ch]^+$. In **Fig. 24**, the nonlinear increase in the N_{coord} of $[Cl]^-$–HO_{water} and decrease in the N_{coord} of $[Cl]^-$–HO_{EG} and $[Cl]^-$–HO[Ch]+ are shown. Hence At higher concentrations, water solvates the $[Cl]^-$ through H-bonding and fully breaks

the $[Ch]^+$–Cl^-–EG bridge responsible for DES structural stability and diminishes the long-range as well as short-range interactions (Kaur, Kumari, & Kashyap, 2020).

Zhekenov and co-workers ran some molecular dynamics simulations of ChCl-based DESs and demonstrated the number of hydrogen bonds between HBD, choline ion, chloride ion, and water with decreasing water fraction (Zhekenov, Toskanbayev, Kazakbayeva, Shal, & Mjalli, 2017) (**Fig. 25**).

The simulations of (Sapir & Harries, 2020) also correlate with the other authors. In **Fig. 25** as water content increases, the structures become progressively hydrated but retain their basic configuration in terms of intermolecular distances. Water molecules gradually replace urea around chloride in the nanostructure, but the overall cluster has similar connectivity and hydrogen bonding (at 5-30% water). In contrast, the highly hydrated structures show a chloride-water-chloride motif. The replacement of urea molecules by water molecules is likely driven by the strong H-bonding propensity of the Cl^-.

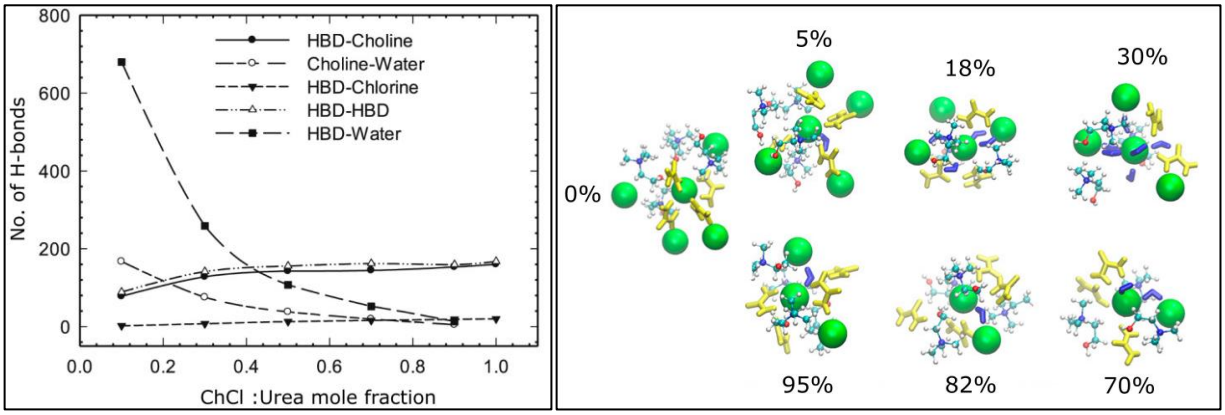

Fig. 25. Number of hydrogen bonds in ChCl : urea vs its mole fraction (left); Solvation-clustering snapshots of ChCl : urea with the amount of water indicated (right).

Viscosity. Dilution of DESs with water can lead to the weakening of hydrogen bond interactions, thus influencing the viscosity of these mixtures. The diagrams of viscosity vs water content are show below for ChCl : urea (1:2), ChCl : 1,2-propanediol (1 : 1), ChCl : ethylene glycol (1 : 1), and ChCl : glycerol (1 : 1) (Dai, Witkamp, Vertpoorte, & Choi, 2015; Rozas, Benito, Alcalde, Atilhan, & Aparicio, 2021; D'Agostino, et al., 2015) (**Fig. 26**).

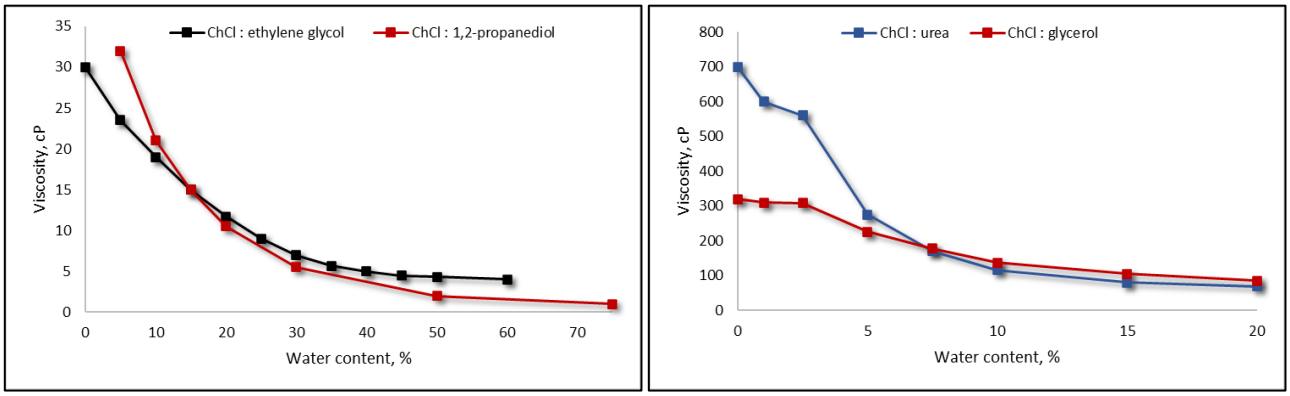

Fig. 26. The viscosity of selected DESs vs water content

In most cases, a non-linear decrease in viscosity is obtained with water addition, and the evolution of the property is following: the value drops significantly at the region of low water content (0-15%), then has a lower slope in the region of 15-35% water content, and slightly decreases at a high amount of water.

Polarity. Polarity is a relevant property for DESs because is it directly connected with the solubilizing capability and, hence, influences extraction efficiency. The estimation of polarity as a property is rather complicated and can be done with solvatochromic parameters[3], or sometimes with dielectric constant. But nowadays, a lot of researchers use polarity-dependent extraction of analytes to demonstrate the efficiency of extraction within DESs-H_2O systems, referring to changes in the polarity of DES by H_2O addition. For example, the extraction yield of flavonoids using ChCl : Levulinic acid : N-methyl urea (1 : 1.2 : 0.8) was the best with 20% water addition compared to pure DES (Xu, et al., 2019). In the same way, ChCl : 1,4-Butanediol with 30% of water demonstrated the highest extraction yield of several phenolic compounds from *Pyrola incarnata* Fisch. (Yao, et al., 2015).

Freezing point. As water molecules can fit into the hydrogen bond network of DES up to a certain moment, without disruption of this network, they probably could create "ternary" DES, which decreases the freezing point of such systems (Smith, Arroyo, Hernandez, & Goeltz, 2019). The diagram of freezing point vs mole fraction of water of well-studied ChCl : urea (1 : 2) is shown in **Fig. 27** below.

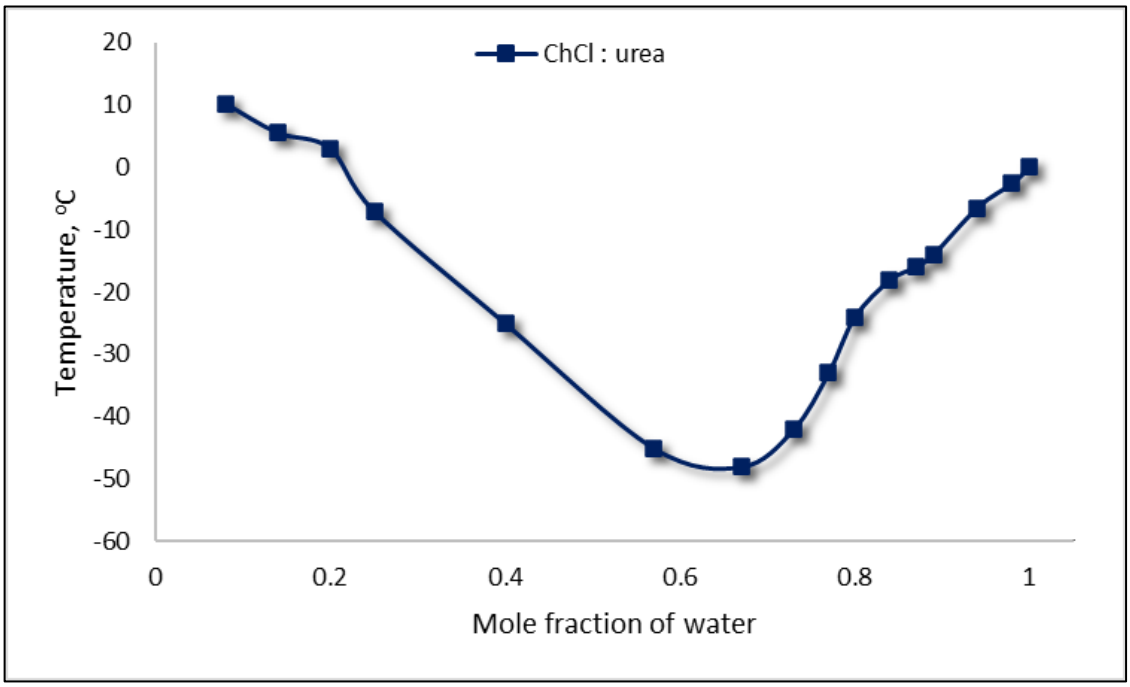

Fig. 27. Temperature vs mole fraction of water of ChCl : urea DES

The freezing points of these eutectic mixtures decrease as water is added. At the ratio, $\mathrm{ChCl : urea : H_2O = 0.11 : 0.22 : 0.67}$, the freezing point of the mixture reaches its minimum at

[3] Hypsochromic (blue) shift or bathochromic (red) shift of UV−vis bands for the negatively solvatochromic dyes or the positively solvatochromic dyes, respectively, as a function of the solvent's polarity.

about -48 °C. With greater mole fractions of water, the freezing point begins to increase. And in the end, approaches to the infinitely diluted urea and choline chloride in water. For reference, the eutectic temperature of ChCl : urea (1 : 2) is equal to 12°C, which corresponds to the first data point on the diagram.

Conductivity. The conductivity of DESs has a strong correlation with viscosity. There are a few diagrams below demonstrate the conductivity vs water content for ChCl : urea (1:2), lactic acid : glucose (5 : 1), proline : malic acid (1 : 1), ChCl : 1,2-propanediol (1 : 1), ChCl : diethylene glycol (1 : 2) (Al-Murshedi, Alesary, & Al-Hadrawi, 2019; Dai, Witkamp, Vertpoorte, & Choi, 2015; Du, Zhao, Chen, Birbilis, & Yang, 2016) (**Fig. 28**).

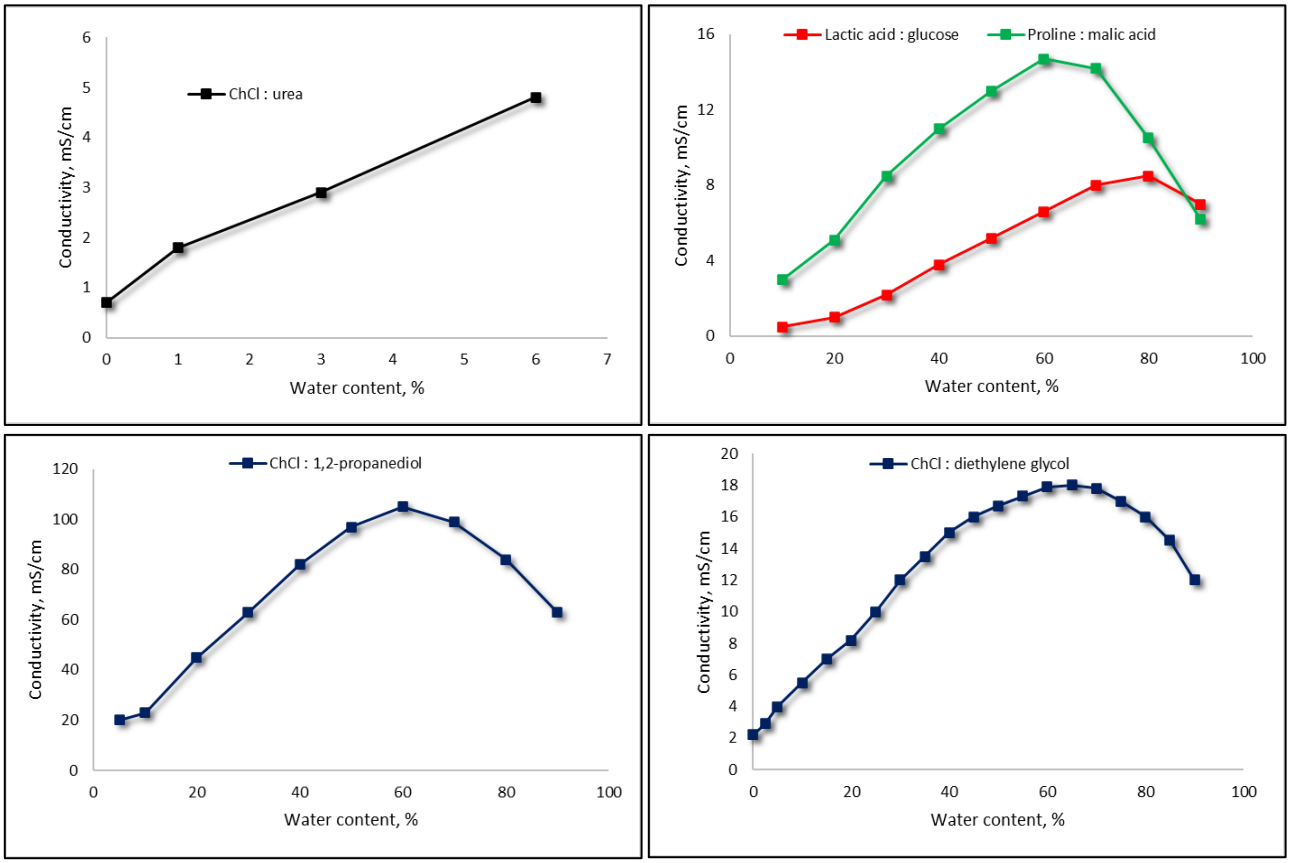

Fig. 28. The conductivity of selected DESs vs water content

In all cases, due to the lowering of viscosity, the conductivity increases with the amount of water added to DES, then it reaches its maximum, and decreases due to the huge water (dielectric) amount.

Density. Unlike conductivity and viscosity, density is less sensitive to water addition. There are diagrams of density dependencies on water content for ChCl : urea (1 : 2), ChCl : ethylene glycol (1 : 1), ChCl : glycerol (1 : 1), and ChCl : ethylene glycol (1 : 1) shown in **Fig. 29** (Al-Murshedi, Alesary, & Al-Hadrawi, 2019; Dai, Witkamp, Vertpoorte, & Choi, 2015).

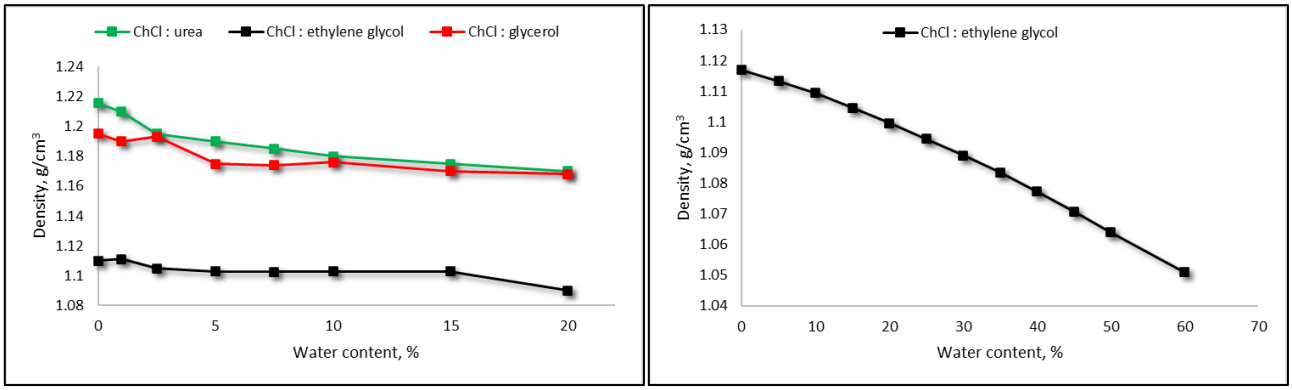

Fig. 29. The density of selected DESs vs water content

Usually, density linearly decreases from the initial value of density of DES (0% H_2O) to 1 g/cm^3 (100% H_2O) with the amount of water added.

3.4 Applications and perspectives

Multiple properties and green features of DESs let them be a subject of investigation in a wide range of applications.

The high solubility and electrical conductivity of metal salts and oxides in DESs, make them a promising candidate in the metal industry, which can be used for extraction/recycling of metals in solution, ore refining, electroplating, and electrodeposition (Smith, Abbott, & Ryder, 2014). DESs are being considered potential electrolytes for Li-ion and redox flow batteries owing to their suppressed flammability, wide *liquidus* range, and high conductivity (Boisset, Menne, Jacquemin, Balducci, & Anouti, 2013; Cong & Lu, 2018).

Potential applications of deep eutectic solvents in nanotechnology have been investigated in the last years. DESs can be used as structure-directing agents, dispersants, electrolytes, nano-confinement, or media in the chemical synthesis of nanoparticles (Abo-Hamad, Hayyan, AlSaadi, & Hashim, 2015; Oh & Lee, 2014).

DESs and NADES have demonstrated potential in biomass processing as they exhibit high dissolving, extraction, recycling and recovering abilities. In particular, DESs have been investigated in biomass pre-treatment, biomass conversion, and extraction of value-added chemicals (e.g., carbohydrates, proteins, phenolic compounds) as an alternative to expensive and toxic ILs (Chen & Mu, 2019; Kim, Eudes, Jeong, Yoo, & Kim, 2019).

DESs have been widely used in organic transformation reactions and catalysis. For example, atom-economic and odourless thia-Michael addition in ChCl : urea medium (Azizi & Yadollahy, 2014), direct C-3 alkenylation/alkylation of indoles with ChCl : oxalic acid as a solvent (Sanap & Shankarling, 2014), Addition of organolithium or Grignard reagent to ketones in ChCl-based eutectic mixtures (Vidal, García-Álvarez, Hernán-Gómez, Kennedy, & Hevia, 2014), high-yield Pechmann condensation for the synthesis of functionalised coumarins in ChCl : tartaric acid (Rather & Ali, 2022), several syntheses in ChCl : urea medium (aminooxazoles, dihydropyrimidinones, *gem*-diureas), one-pot fluorination of acetophenones catalysed by ChCl : p-TsOH and esterification of carboxylic acids

with alcohols catalysed by ChCl : $ZnCl_2$ (Alonso, et al., 2016). To date, there are numerous scientific articles dedicated to organic synthesis and catalysis with DESs.

Considering “green” properties of DESs, they have been being tested for different applications in ecological areas, such as water treatment, to remove pesticides and transition metal ions (Chabib, et al., 2022).

A new term THEDES was introduced for bioactive eutectic systems composed of an active pharmaceutical ingredient (API) as one of the DES constituents. These systems can overcome issues associated with drug solubility and permeability, which improves the efficiency of the delivery of the API (Aroso, et al., 2015).

DESs have some prerequisites for use in the molecular biology – biochemistry field as they can be used in the extraction of biological material, DNA and RNA preservation, and enzyme-catalysed reactions (Ramón & Guillena, 2019).

Probably the largest share of DESs (NADES, hydrophobic DESs) applications relates to analytical chemistry which mainly includes extraction techniques (solid-liquid, liquid-liquid, microextraction), and to a lesser extent chromatographic techniques (modification of stationary phases, additive to mobile phases, media for the synthesis of stationary phases). The use of DESs in extraction techniques is of growing interest due to their environmental friendliness and the possibility of tailoring their physicochemical properties. They have a lot of advantages in comparison to ordinary organic solvents and ILs. Thus, plenty of studies were conducted to check the ability and the efficiency of DESs to extract different natural compounds. Some examples are shown in Appendix 1, which include the identification and quantification of several groups of compounds (hormones, phenolic compounds, amino acids, cannabinoids, vitamins, flavonoids, terpenoids, etc.) in biological or plant sources by analytical techniques.

4. EXPERIMENTAL PART

4.1 Reagents and samples

The reagents, that were used for the practical experiment include several HBDs, HBAs, stock β-caryophyllene solution, and the sample for analysis. Their structural formulae are depicted in Appendix 2.

1. Hemp seed oil (Local market)
2. β-Caryophyllene, CAS No. 87-44-5, ≥ 80%, (Sigma-Aldrich, Germany)
3. Choline chloride, CAS No. 67-48-1, ≥ 99%, (Glentham Life Sciences, UK)
4. Urea, CAS No. 57-13-6, ≥ 99%, (Sigma-Aldrich, Germany)
5. Citric acid monohydrate, CAS No. 5949-29-1, p.a., (Eurochemicals)
6. (2R, 3R)-(+)-Tartaric acid, CAS No. 526-83-0, ≥ 99%, (Merck, Germany)
7. (±)-Menthol, CAS No. 89-78-1, ≥ 98%, (Sigma-Aldrich, Germany)
8. Propanoic acid, CAS No. 79-09-4, ≥ 99,5%, (Sigma-Aldrich, Germany)
9. Octanoic acid, CAS No. 124-07-2, ≥ 98%, (Sigma-Aldrich, Germany)
10. Distilled water

4.2 Equipment and conditions

Microwave-assisted synthesis of DESs was performed in a microwave reactor Monowave 450 (Anton Paar) in a G30 Wide-Neck vial (Anton Paar) with parameters shown in **Table 6** below.

The DES of ChCl : urea (2 : 1) without water additive was synthesised by the ordinary heating method in the temperature-holding water vessel/bath with a magnetic stirrer, connected to water heater UH4 (MLV Medingen, GDR).

Table 6. The composition and synthesis conditions of DESs

HBD	HBA	Molar ratio	Water additive, %	Temperature, ºC	Time, s
Citric acid	ChCl	1 : 1	15	80	30
Citric acid	ChCl	1 : 1	20	80	30
Tartaric acid	ChCl	1 : 2	15	80	30
Tartaric acid	ChCl	1 : 2	20	80	30
Octanoic acid	Menthol	1 : 1	0	70	120
Propionic acid	Menthol	1 : 1	0	70	120
Urea	ChCl	2 : 1	0	80	5 min

SPME procedure includes equilibration and sorption steps. Equilibration of the sample was achieved in a 20 ml vial closed with a Screw Cap N18 with silicone rubber septum (Macherey-Nagel, Germany). The vial was thermostatted in the water bath for some time and subsequent sorption of the analyte was performed with a Supelco 50/30 μm DVB/CAR/PDMS SPME fibre assembly (Supelco, Bellefonte, PA, USA) housed in a manual SPME holder (Supelco, Bellefonte, PA, USA).

Desorption of analyte was performed in the GC injector at 250ºC for 5 min. GC-MS experiments were performed on a PerkinElmer Clarus 580 series gas chromatograph (PerkinElmer, Shelton, USA) coupled to a PerkinElmer Clarus 560 S mass spectrometer (PerkinElmer, Shelton, USA). The system is equipped with an Elite-5 capillary GC column (30 m × 0.25 mm id, 0.25 µm film thickness, crossbond 5% diphenyl – 95% polydimethylsiloxane) (PerkinElmer, USA). The carrier gas is helium with a constant rate of 1.92 mL/min. The injection mode was either split (1:10) or splitless depending on the purpose of analysis. The temperature of the oven was dynamic and programmed as follows: from 45 to 100 ºC at the rate of 2 ºC/min, from 100 to 250 ºC at the rate of 5 ºC/min and held on at 250 ºC for 5 min (**Fig. 30**). The duration of the GC-MS run is 62.50 minutes.

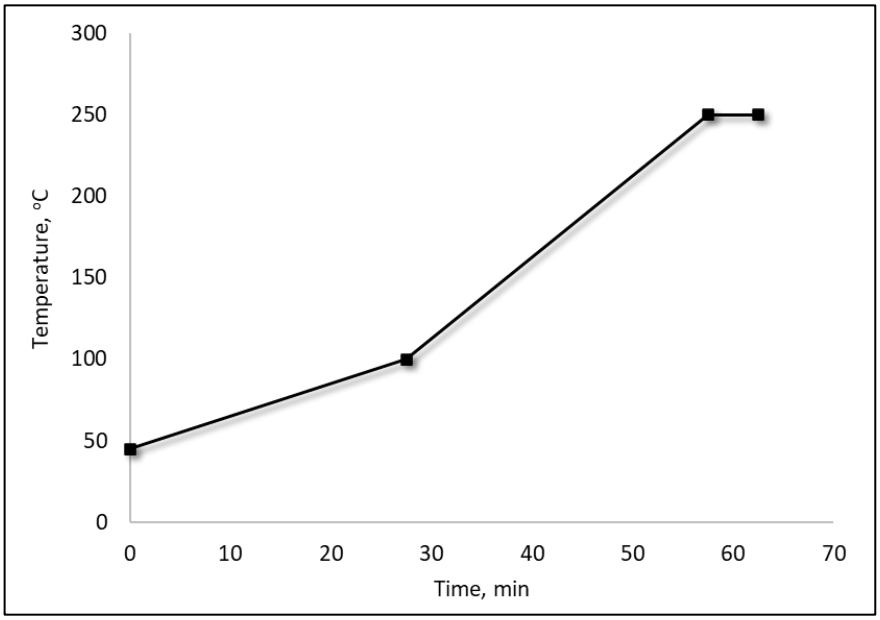

Fig. 30. Programmed oven temperature

The temperature of the transfer line was 250 ºC. Electron ionisation source temperature is 180 ºC and ionisation energy is 70 eV. Data were acquired in two modes: full scan mode with the m/z range of 45-500 from 0 to 62.50 min and selected ion recording of β-caryophyllene fragments with m/z 93 and 133 from 32 to 34 min (**Fig. 31**). Obtained spectra were compared with those of the NIST library.

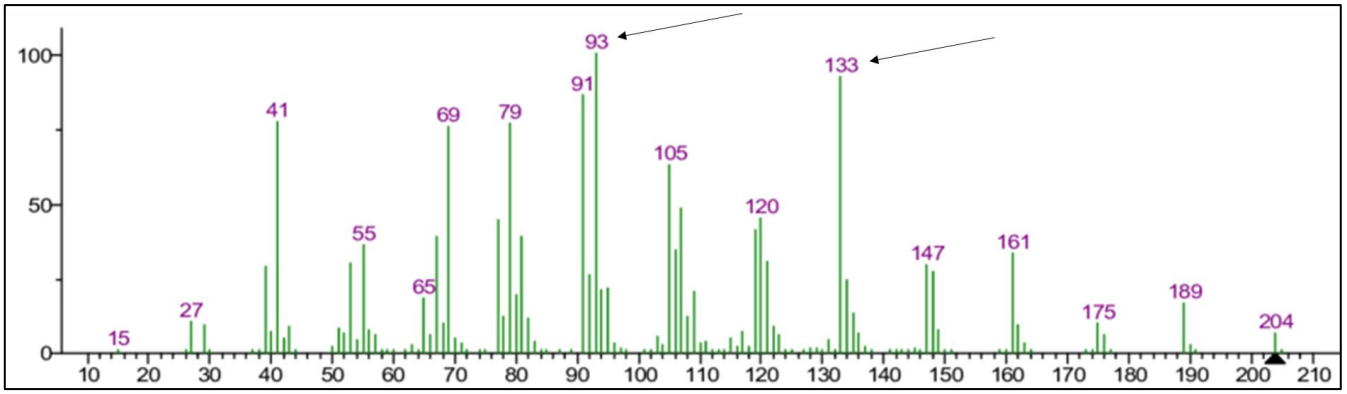

Fig. 31. Theoretical mass spectra of β-caryophyllene (NIST library)

TurboMass 6.1 GC/MS Software was used for the setting up of GC-MS analysis and chromatogram processing. Diagrams and graphs were built in Microsoft Excel. Graphical schemes and chemical structures were drawn in Inkscape 1.1 and ChemDraw 19.0, respectively.

4.3 Detailed experiment description

4.3.1 Synthesis of DESs.

The necessary mass amounts of DESs from molar ratios were recalculated with the eq.5 below:

$$n_1 \cdot M_1 + n_2 \cdot M_2 = mf \quad \rightarrow \quad f = \frac{n_1 \cdot M_1 + n_2 \cdot M_2}{m} \tag{5}$$

where n_1 – the amount of substance of component 1; n_2 – the amount of substance of component; M_1 – the molar mass of component 1; M_2 – the molar mass of component 2; m – total mass of DES; f – dilution factor.

Then the mass amounts can be found using f, as $[(n_1 \cdot M_1)/f] + [(n_2 \cdot M_2)/f]$ and the water amount was simply calculated as a total mass of substance multiplied by water percentage needed. For example, the required masses of components for the preparation of 10 g of DES and the corresponding amount of water are shown below in **Table 7**.

Table 7. Composition of 10 g DESs and amount of water added to DESs

HBA	HBD	Molar ratio	HBA+HBD, g	Water, %	Water, g
Citric acid	ChCl	1 : 1	5.7912 + 4.2088	15	1.5
Citric acid	ChCl	1 : 1	5.7912 + 4.2088	20	2.0
Tartaric acid	ChCl	1 : 2	3.4956 + 6.5044	15	1.5
Tartaric acid	ChCl	1 : 2	3.4956 + 6.5044	20	2.0
Octanoic acid	Menthol	1 : 1	4.7993 + 5.2007	0	-
Propionic acid	Menthol	1 : 1	3.2160 + 6.7840	0	-
Urea	ChCl	2 : 1[4]	4.6244 + 5.3755	0	-

The calculated masses of components (HBD, HBA, water) were placed in a vial with a magnetic stir-bar and were subject to microwave-assisted synthesis (except ChCl : Urea). Water additives were necessary in some cases to reduce the viscosity of DESs and hence simplify stirring and their formation. The procedure of synthesis in a microwave reactor includes three steps: heating with microwave radiation to a required temperature (**Table 6**), holding at the required temperature for an amount of time (**Table 6**), and cooling to 50°C.

[4] (Du, Zhao, Chen, Birbilis, & Yang, 2016); (Abbott, Capper, Davies, Rasheed, & Tambyrajan, 2003)

4.3.2 Standard solutions preparation.

The standard solution is a solution with the known concentration of β-caryophyllene in DES. β-Caryophyllene standard solutions were prepared by weighting, in 2 steps.

First, β-caryophyllene stock solution (≥80%) was pre-diluted by [ChCl : urea (2 : 1)] to 10 mg/g. This step is crucial to make further solubilisation possible as β-caryophyllene is poorly soluble in water-containing DES. Then, the necessary concentrations for calibration curve were prepared from 10 mg/g solution and [ChCl : Tartaric acid (2 : 1) + 15% H_2O]. After each dilution, the vial was heated and properly mixed to reach homogeneity.

The range of concentrations was selected during analysis based on the peak area obtained from GC-MS analysis and is as follows: 0.176 µg/g, 0.96 µg/g, 4.88 µg/g, and 7.52 µg/g.

4.3.3 Solid phase microextraction

For method adjustment, a closed 20 ml vial with 2.5 g of DES and 0.5 g of hemp seed oil was thermostatted at 80ºC before sorption. The different equilibration time was checked: 10, 20, and 30 min. Then the vial septum was pierced by the SPME holder needle, and the fibre was exposed for sorption of analyte and related substances at the same temperature for either 5, 10, 20, 25 or 30 min. For the calibration curve, 3 g of the standard solutions of [ChCl : Tartaric acid (2 : 1) + 15% H_2O] with a known amount of β-caryophyllene were subject to SPME.

4.3.4 Gas chromatography – mass spectrometry

GC-MS measurements were done according to the parameters in chapter 4.2. Both split and splitless were used in the case of ChCl : urea to evaluate and choose injection mode for further measurements. Splitless injection mode was used for evaluation of SPME with different DESs media and calibration curve with standard solutions.

4.4 Results and discussions

Hemp seed oil is a complex mixture and, hence, the chromatogram has a lot of peaks from volatile and semi-volatile compounds (Appendix 4). The sample chromatogram segment is shown below in **Fig. 32**, representing the region of interest.

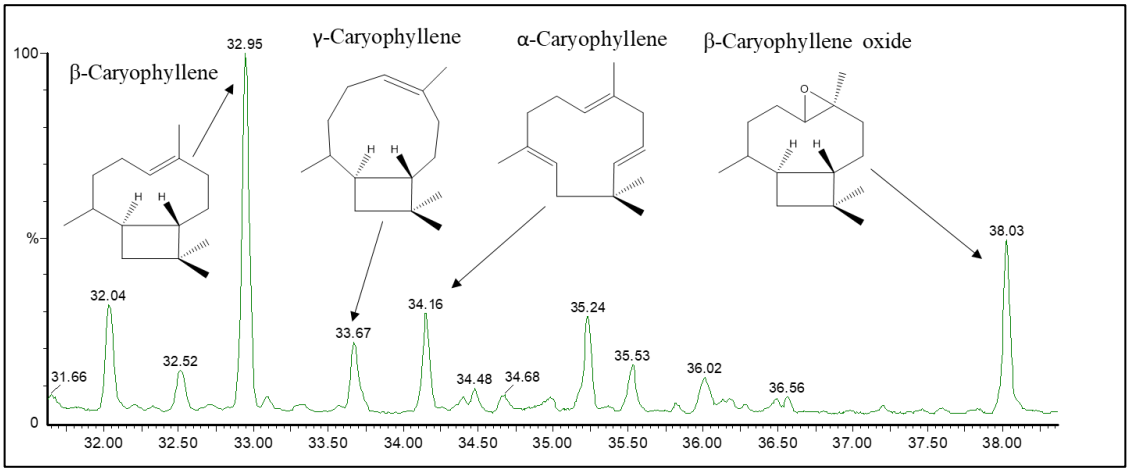

Fig. 32. The region of interest and identified caryophyllenes (Sample chromatogram)

The compound of interest is β-caryophyllene (retention time = 32.95 min), however other caryophyllenes can be identified as well: Z-stereoisomer γ-caryophyllene (retention time = 33.67 min), monocyclic isomer α-caryophyllene (retention time = 34.16 min), and oxidised form β-caryophyllene oxide (retention time = 38.08 min).

4.4.1 Split/splitless

Fig. 33 below represents integrated peaks of chromatograms of splitless and split (1:10) injection modes for the SPME of β-caryophyllene from hemp seed oil in ChCl : urea medium.

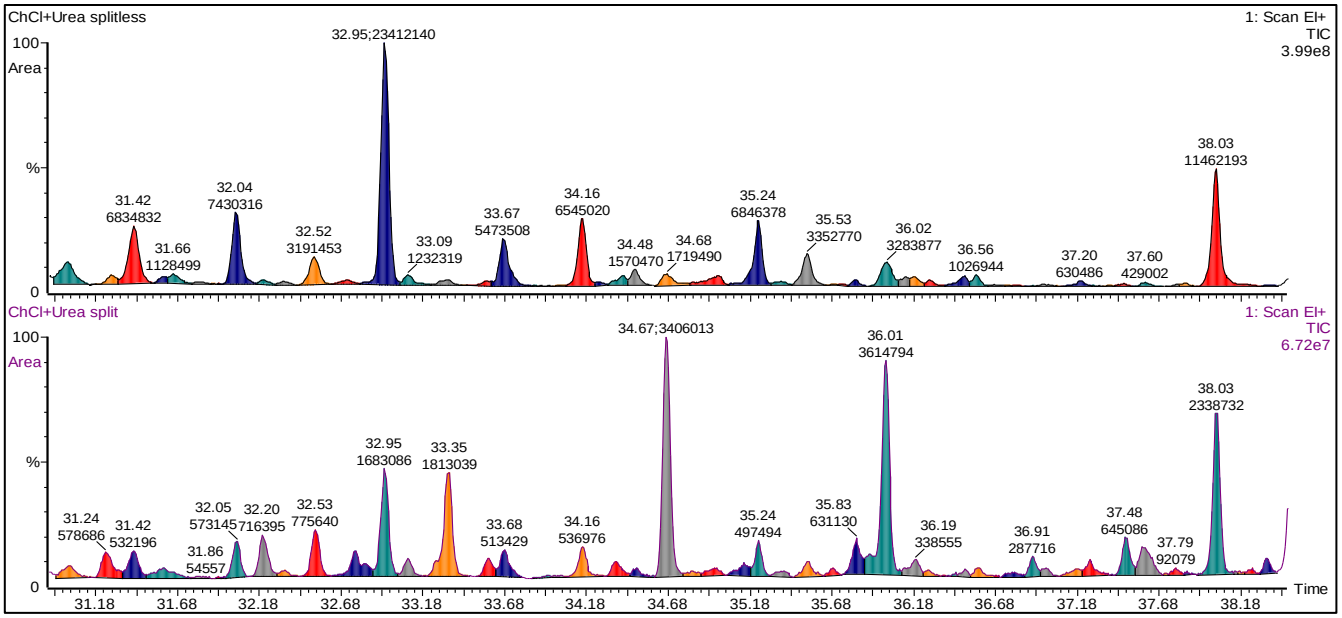

Fig. 33. Integrated peaks of splitless (top) and split (bottom) in full scan mode

The area of the β-caryophyllene peak (retention time = 32.95 min) in splitless injection mode is predictably higher (23,412,140 relative units) than in split (1,683,086 relative units). Moreover, the sample remains within the liner for a longer period before entering the column because of the lower

flow rate in splitless mode. And since desorption was done for long period of time (5 min), the worsening in efficiency was expected in splitless mode, however the results didn't show this effect. Therefore, the use of splitless gives some advantage over split injection mode, in addition, the entire amount of sample is injected, which increases the detection limit of β-caryophyllene.

4.4.2 DES selection

The efficiency of 7 DESs as a media for SPME was tested (see Appendices 5 and 6) . The results in **Table 8** and **Fig. 35** demonstrate the peak areas of β-caryophyllene (SIR mode). The relative peak area was calculated as a ratio:

$$(Relative\ peak\ area)_i = \frac{(Peak\ area)_i}{(Peak\ area)_{MAX}} \cdot 100\% \quad (6)$$

Table 8. The peak area of β-caryophyllene of DESs used as extraction media in SPME.

DES composition HBA : HBD (ratio) + water %	**Peak area of β-caryophyllene (SIM mode), relative units**	**Relative peak area, % (100% – the highest peak)**
ChCl : Citric acid (1:1) + 15% H_2O	222903	77
ChCl : Citric acid (1:1) + 20% H_2O	177135	62
ChCl : Tartaric acid (2:1) + 15% H_2O	284627	**100**
ChCl : Tartaric acid (2:1) + 20% H_2O	230590	81
ChCl : Urea (1:2)	219286	78
Menthol : Octanoic acid (1:1)	ND	0
Menthol : Propionic acid (1:1)	ND	0

The efficiency of SPME greatly depends on several parameters such as viscosity, polarity, and extraction media (DESs) composition. It has been found that the use of hydrophilic ChCl-based DESs as extraction media demonstrated better results in contrast to the use of hydrophobic menthol-based DESs. This could be for 2 reasons: partial decomposition of hydrophobic menthol-based DESs at 80^{o}C and strong retention of highly hydrophobic β-caryophyllene in liquid DES-phase as a result of matching hydrophobicity. Although, the main benefit of DES in HS-SPME analysis should be low volatility (Dwanema, 2019), but in this case, there are broad peaks going through the entire chromatogram and corresponding to the components of DES: menthol and propionic or octanoic acid (**Fig. 34**).

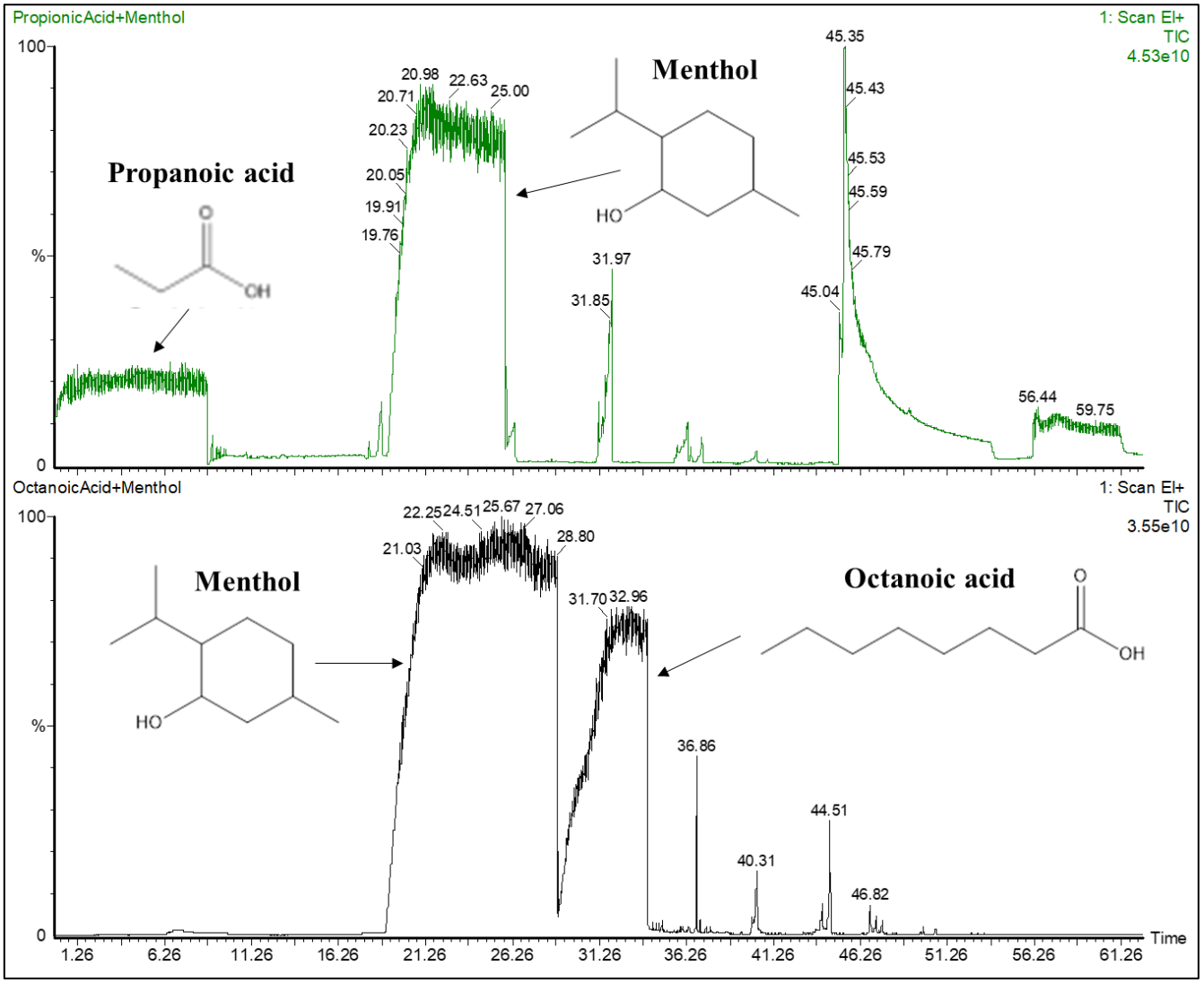

Fig. 34. Chromatograms (MS Full scan) with integrated peaks (hydrophobic DESs)

It is also worth noting the effect of water on the peak area. Although water is an essential component of some DES and is necessary for simplifying their synthesis, it is seen that transition from the 15% to 20% water content in [ChCl : citric acid] and [ChCl : tartaric acid] DESs reduced peak area by about 15-19% (**Fig. 35**). This may be related to the weakening of hydrogen bonding network interactions ($[Ch]^+$–$[Cl]^-$–OH_{acid}) since water forms clusters with chloride ions. (Kaur, Kumari, & Kashyap, 2020; Zhekenov, Toskanbayev, Kazakbayeva, Shal, & Mjalli, 2017; Sapir & Harries, 2020)

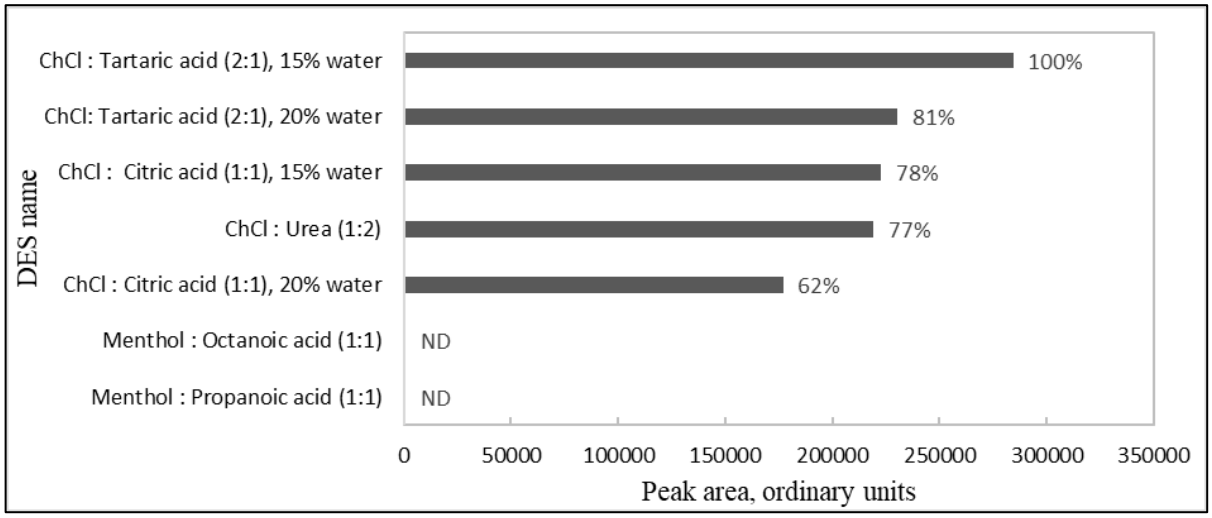

Fig. 35. The peak area diagram of β-caryophyllene of all DESs used as extraction media in SPME

[ChCl : tartaric acid + 15% H_2O] DES was selected for further investigations and calibration curve preparation as the best SPME media. Also, a few attempts were made to synthesise [ChCl : tartaric acid] and [ChCl : citric acid] in microwave reactor without water, because it could have improved SPME performance. But the viscosity of such components is too high, which significantly hardens synthesis (especially stirring) and makes it not suitable for extraction purposes. Water addition was crucial to lower viscosity in those cases.

4.4.3 SPME conditions optimisation

The conditions of SPME with [ChCl : tartaric acid + 15% H_2O] DES were optimised (see Appendices 7-9), i.e., equilibration and sorption time (**Table 9**, **Table 10**).

Table 9. Peak area of β-caryophyllene (SIR mode) vs equilibration time

Equilibration time, min	**Peak area of β-caryophyllene, relative units**	**Relative peak area, % (100% – the highest peak)**
10	212871	99.7
20	201796	94.5
30	213513	100

Table 10. Peak area of β-caryophyllene (SIR mode) vs equilibration time

Sorption time, min	**Peak area of β-caryophyllene, relative units**	**Relative peak area, % (100% – the highest peak)**
5	41594	18
10	73332	31
20	133757	56
25	213513	90
30	237403	100

The analysis of data (**Fig. 36**) shows that the peak area of β-caryophyllene has no significant change over equilibration time, meaning that equilibrium is reached quickly between DES and headspace phases. Shorter equilibration time were not investigated, because certain amount of time is needed for sample to heat up. On the other hand, the peak area of β-caryophyllene grows gradually over sorption time, has a dramatic increase from 20 to 25 min, and then levels off. Likely, the peak area changes slightly after 25 minutes of sorption, because the system is getting closer to the equilibrium in the 3-phase system (Tankevièiûtë, Panavaitë, Kazlauskas, & Vièkaèkaitë, 2004; Bielská & Hoffman, 2015).

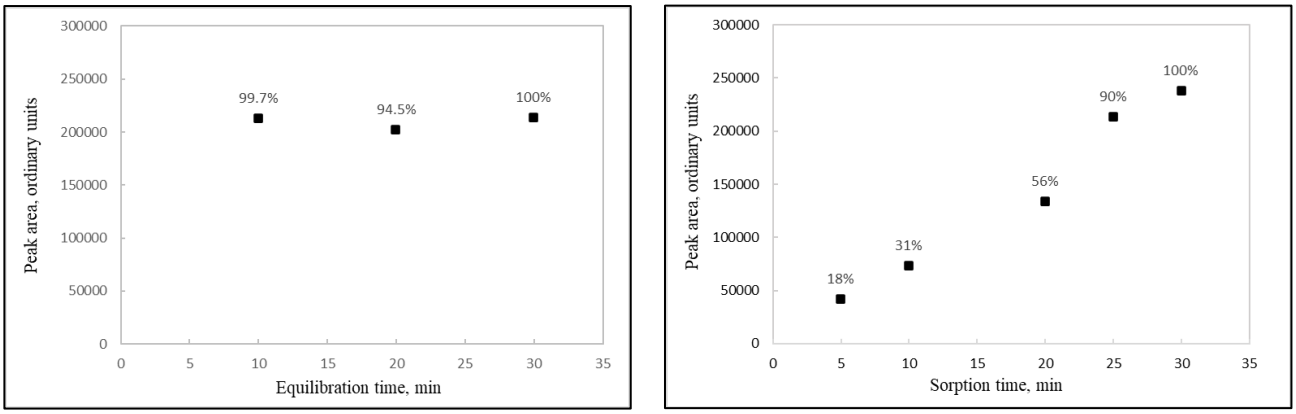

Fig. 36. Peak area of β-caryophyllene vs equilibration time (left) and peak area of β-caryophyllene vs sorption time (right) diagrams; maximum peak area values represented as 100%

The most suitable conditions for SPME were selected as follows: 10 min equilibration time and 25 minutes sorption time.

4.4.4 Calibration curve

The calibration curve is necessary for the quantification of β-caryophyllene in the hemp seed oil sample. Therefore, the 4-point calibration curve was built. The peak area of β-caryophyllene (SIR mode) obtained from the chromatograms (Appendix 10) is shown below in **Table 11**.

Table 11. The peak area of β-caryophyllene vs concentration of the substance in DES.

Concentration, µg/g	Peak area of β-caryophyllene (SIR mode), relative units
0.176	51,517
0.96	208,863
4.88	1,409,750
7.52	1,927,605

All the data points were used to build the calibration curve of β-caryophyllene. The linear trendline having the formula $y = ax + b$ was superimposed on the chart (**Fig. 37**). The slope and intercept of the trendline were found automatically in Excel and are $a = 264984.47$ and $b = 2726.30$,

respectively. The coefficient of determination (R-squared) is relatively high and equals 0.9921, meaning that the fitted trendline is very close to the data and is representative.

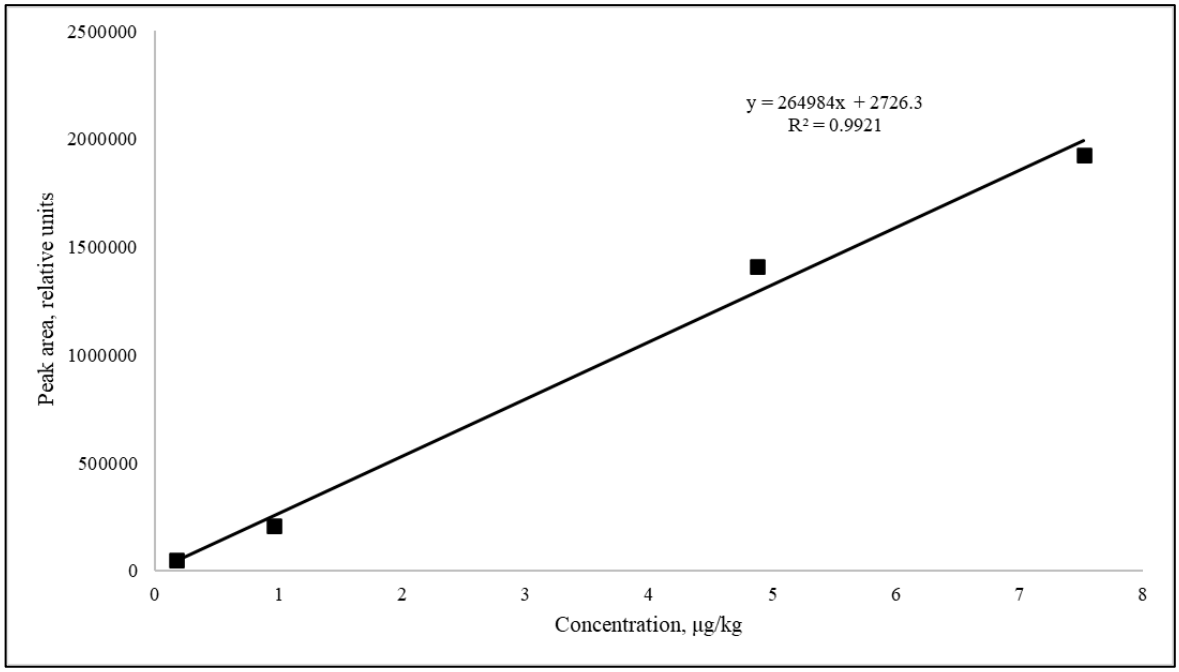

Fig. 37. Calibration curve of β-caryophyllene

The obtained equation $y = 264984.47x + 2726.30$ was used to quantify the amount of β-caryophyllene in the hemp seed oil sample. Considering the peak area of β-caryophyllene from hemp seed oil sample ($y = 212871$ relative units), the concentration of β-caryophyllene is $x = \frac{y-b}{a} = \frac{212871-2726.3}{264984.47} = 0.79$ µg/g or 0.79 mg/kg of hemp seed oil.

CONCLUSIONS

1. The detailed literature review is provided and covers the following topics: caryophyllenes, their sources and properties; extraction methods, sample preparation, and sample introduction to the GC system; deep eutectic solvents, their properties, and applications.
2. Seven deep eutectic solvents were synthesised in a microwave reactor: [ChCl : Citric acid (1:1) + 15% H_2O], [ChCl : Citric acid (1:1) + 20% H_2O], [ChCl : Tartaric acid (2:1) + 15% H_2O], [ChCl : Tartaric acid (2:1) + 20% H_2O], [ChCl : Urea (1:2)], [Menthol : Octanoic acid (1:1)], [Menthol : Propionic acid (1:1)].
3. The performance of deep eutectic solvents as a calibration medium in solid phase microextraction was investigated. The assessment criterion was the GC-MS peak area of β-caryophyllene. It was found that ChCl-based deep eutectic solvent perform well, whereas menthol-based are ineffective. The peak area of β-caryophyllene decreases in the following series: [ChCl : Tartaric acid (2:1) + 15% H_2O] > [ChCl : Tartaric acid (2:1) + 20% H_2O] > [ChCl : Citric acid (1:1) + 15% H_2O] > [ChCl : Urea (1:2)] > [ChCl : Citric acid (1:1) + 20% H_2O] > [Menthol : Octanoic acid (1:1)] = [Menthol : Propionic acid (1:1)].
4. [ChCl : Tartaric acid (2:1) + 15% H_2O] was selected as the most appropriate deep eutectic solvent. The SPME equilibration and sorption time were optimised for this deep eutectic solvent and were set to 10 and 25 minutes, respectively.
5. The 4-point calibration curve was built for the quantification of β-caryophyllene in hemp seed oil. The calculated concentration is 0.79 mg/kg.

REFERENCES

Abbott, A. P., Barron, J. C., Ryder, K. S., & Wilson, D. (2007). Eutectic-Based Ionic Liquids with Metal-Containing Anions and Cations. *Chemistry—A European Journal*, 6495-6501.

Abbott, A. P., Capper, G., Davies, D. L., Rasheed, R. K., & Tambyrajan, V. (2003). Novel solvent properties of choline chloride/urea mixtures. *Chemical Communications*(1), 70-71.

Abo-Hamad, A., Hayyan, M., AlSaadi, M. A., & Hashim, M. A. (2015). Potential applications of deep eutectic solvents in nanotechnology. *Chemical Engineering Journal, 273*, 551-567. doi:10.1016/j.cej.2015.03.091

Al-Fatimi, M. (2020). β-Caryophyllene: A Single Volatile Component of n-Hexane Extract of Dracaena cinnabari Resin. *Molecules, 25*(21), 4943. doi:10.3390/molecules25214939

Al-Murshedi, A., Alesary, H., & Al-Hadrawi, R. (2019). Thermophysical properties in deep eutectic solvents with/without water. *Journal of Physics: Conference Series, 1294*(5), 052014. doi:10.1088/1742-6596/1294/5/052041

Alonso, D., Baeza, A., Chinchilla, R., Guillena, G., Pastor, I., & Ramón, D. (2016). Deep Eutectic Solvents: The Organic Reaction Medium of the Century. *European Journal of Organic Chemistry, 2016*(4), 612-632. doi:10.1002/ejoc.201501197

Alsaud, N., Shahbaz, K., & Farid, M. (2021). Evaluation of deep eutectic solvents in the extraction of β-caryophyllene from New Zealand Manuka leaves (Leptospermum scoparium). *Chemical Engineering Research and Design, 166*, 97-108. doi:10.1016/j.cherd.2020.11.028

Ambrož, M., Boušová, I., Skarka, A., Hanušová, V., Králová, V., Matoušková, P., . . . Szotáková, B. (2015). The Influence of Sesquiterpenes from Myrica rubra on the Antiproliferative and Pro-Oxidative Effects of Doxorubicin and Its Accumulation in Cancer Cells. *Molecules, 20*(8), 15343-15358. doi:10.3390/molecules200815343

Anderson, J. R., Edwards, R. L., Poyser, J. P., & Whalley, A. J. (1988). Metabolites of the higher fungi. Part 23. The punctaporonins. Novel bi-, tri-, and tetra-cyclic sesquiterpenes related to caryophyllene, from the fungus Poronia punctata(Linnaeus:Fries) Fries. *Journal of the Chemical Society, Perkin Transactions 1*, 823-831. doi:10.1039/P19880000823

Aroso, I. M., Craveiro, R., Rocha, Â., Dionísio, M., Barreiros, S., Reis, R. L., . . . Duarte. (2015). Design of controlled release systems for THEDES—Therapeutic deep eutectic solvents, using supercritical fluid technology. *International journal of pharmaceutics, 492*(1-2), 73-79. doi:10.1016/j.ijpharm.2015.06.038

Asakawa, Y., Ishida, T., Toyota, M., & Takemoto, T. (1986). Terpenoid biotransformation in mammals IV. Biotransformation of (+)-longifolene, (-)-caryophyllene, (-)-caryophyllene oxide, (-)-cyclocolorenone, (+)-nootkatone, (-)-elemol, (-)-abietic acid and (+)-dehydroabietic acid in rabbits. *Xenobiotica, 16*, 753-767.

Askari, V., & Shafiee-Nick, R. (2019). The protective effects of β-caryophyllene on LPS-induced primary microglia M1/M2 imbalance: A mechanistic evaluation. *Life Sciences, 219*, 40-73. doi:10.1016/j.lfs.2018.12.059

Aydin, F., Yilmaz, E., & Soylak, M. (2017). A simple and novel deep eutectic solvent based ultrasound-assisted emulsification liquid phase microextraction method for malachite green in

farmed and ornamental aquarium fish water samples. *Microchemical Journal, 132*, 280-285. doi:10.1016/j.microc.2017.02.014

Aydin, F., Yilmaz, E., & Soylak, M. (2018). Vortex assisted deep eutectic solvent (DES)-emulsification liquid-liquid microextraction of trace curcumin in food and herbal tea samples. *Food Chemistry, 243*, 442-447. doi:10.1016/j.foodchem.2017.09.154

Azizi, N., & Yadollahy, Z. R.-O. (2014). An atom-economic and odorless thia-Michael addition in a deep eutectic solvent. *Tetrahedron letters, 55*(10), 1722-1725. doi:10.1016/j.tetlet.2014.01.104

Baby, S., Mathew, D., Anil, J. J., Rajani, K., Nediyamparambu, S. P., Renju, K. V., & Varughese, G. (2006). Caryophyllene-rich rhizome oil of Zingiber nimmonii from South India: Chemical characterization and antimicrobial activity. *Phytochemistry, 67*(22), 2469-2473. doi:10.1016/j.phytochem.2006.08.003

Bahi, A., Al Mansouri, S., Al Memari, E., Al Ameri, M., Nurulain, S., & Ojha, S. (214). beta-Caryophyllene, a CB2 receptor agonist produces multiple behavioral changes relevant to anxiety and depression in mice. *Physiology & Behavior, 135*, 119-124. doi:10.1016/j.physbeh.2014.06.003

Barbieri, J. B., Goltz, C., Cavalheiro, F. B., Toci, A. T., Igarashi-Mafra, L., & Mafra, M. R. (2020). Deep eutectic solvents applied in the extraction and stabilization of rosemary (Rosmarinus officinalis L.) phenolic compounds. *Industrial Crops and Products, 144*, 112049. doi:10.1016/j.indcrop.2019.112049

Bhatia, S., Letizia, C., & Api, A. (2008). Fragrance material review on β-caryophyllene alcohol. *Food and Chemical Toxicology, 46*(11), S95-S96. doi:10.1016/j.fct.2008.06.030

Białoń, M., Krzyśko-Łupicka, T., Nowakowska-Bogdan, E., & Wieczorek, P. (2019). Chemical Composition of Two Different Lavender Essential Oils and Their Effect on Facial Skin Microbiota. *Molecules, 24*(18), 3270-3286.

Bicchi, C. (2000). ESSENTIAL OILS | Gas Chromatography. In *Encyclopedia of Separation Science* (pp. 2744-2755). Academic Press.

Bielská, L., & Hoffman, J. (2015). The kinetics of solid-phase microextraction measured for freshly added and aged hydrophobic compounds in two different soils. *International Journal of Environmental Analytical Chemistry, 95*(7), 635-649. doi:10.1080/03067319.2015.1048438

Boisset, A., Menne, S., Jacquemin, J., Balducci, A., & Anouti, M. (2013). .Deep eutectic solvents based on N-methylacetamide and a lithium salt as suitable electrolytes for lithium-ion batteries. *Physical Chemistry Chemical Physics, 15*(46), 20054-20063. doi:10.1039/C3CP53406E

Borges, V. R., Ribeiro, A. F., Anselmo, C. S., Cabral, L. M., & Pereirade Sousa, V. (2013). Development of a high performance liquid chromatography method for quantification of isomers β-caryophyllene and α-humulene in copaiba oleoresin using the Box-Behnken design. *Journal of Chromatography B, 940*, 35-41. doi:10.1016/j.jchromb.2013.09.024

Borugă, O., Jianu, C., Mişcăl, C., Goleţ, I., Gruia, A., & Horhat, F. (2014). Thymus vulgaris essential oil: chemical composition and antimicrobial activity. *Journal of Medicine and Life, 7*(3), 56-60.

Boutekedjiret, C., Bentahar, F., Belabbes, R., & Bessiere, J. M. (2003). Extraction of rosemary essential oil by steam distillation and hydrodistillation. *Flavour and Fragrance Journal, 18*(6), 481-484.

Brown, M., & Farquhar-Smith, W. (2018). Cannabinoids and cancer pain: A new hope or a false dawn? *European Journal of Internal Medicine, 49*, 30-36. doi:10.1016/j.ejim.2018.01.020

Caryophyllus. In Merriam-Webster.com dictionary. (n.d.). Retrieved October 16, 2021, from https://www.merriam-webster.com/dictionary/Caryophyllus

Chabib, C., Ali, J., Jaoude, M., Alhseinat, E., Adeyemi, I., & Al Nashef, I. (2022). Application of deep eutectic solvents in water treatment processes: A review. *Journal of Water Process Engineering, 47*, 102663. doi:10.1016/j.jwpe.2022.102663

Chang, H.-J., Kim, J.-M., Lee, J.-C., Kim, W.-K., & Chun, H.-S. (2013). Protective Effect of β-Caryophyllene, a Natural Bicyclic Sesquiterpene, Against Cerebral Ischemic Injury. *Journal of Medicinal Food, 16*(6), 471-480. doi:10.1089/jmf.2012.2283

Chen, Y., & Mu, T. (2019). Application of deep eutectic solvents in biomass pretreatment and conversion. *Green Energy & Environment, 4*(2), 95-115. doi:10.1016/j.gee.2019.01.012

Chen, Y., Zhao, D., Bai, Y., Duan, Y., Liu, C., Gu, J., . . . Zhang, L. (2022). Tuning refractive index of deep eutectic solvents. *Journal of Molecular Liquids, 348*, 118031. doi:10.1016/j.molliq.2021.118031

Cheng, Y., Dong, Z., & Liu, S. (2014). β-Caryophyllene ameliorates the Alzheimer-like phenotype in APP/PS1 Mice through CB2 receptor activation and the PPARγ pathway. *Pharmacology, 94*(1-2), 1-12. doi:10.1159/000362689

Chizzola, R. (2013). Regular Monoterpenes and Sesquiterpenes (Essential Oils). In K. Ramawat, & J. Mérillon (Eds.), *Natural Products.* Berlin: Springer.

Cong, G., & Lu, Y. (2018). Organic Eutectic Electrolytes for Future Flow Batteries. *Chem, 4*(12), 2732-2734. doi:10.1016/j.chempr.2018.11.018

Cox-Georgian, D., Ramadoss, N., Dona, C., & Basu, C. (2019). Therapeutic and Medicinal Uses of Terpenes. In S. Dhekney, & P. Parajuli (Eds.), *Medicinal Plants.* Cham: Springer.

D'Agostino, C., Gladden, L. F., Mantle, M. D., Abbott, A. P., Essa, I. A., Al-MurshedI, A. Y., & Harris, R. C. (2015). Molecular and ionic diffusion in aqueous – deep eutectic solvent mixtures: probing inter-molecular interactions using PFG NMR. *Physical Chemistry Chemical Physics, 17*(23), 15297-15304. doi:10.1039/C5CP01493J

Dahham, S., Tabana, Y., Iqbal, M., Ahamed, M., Ezzat, M., Majid, A., & Majid, A. (2015). The Anticancer, Antioxidant and Antimicrobial Properties of the Sesquiterpene beta-Caryophyllene from the Essential Oil of Aquilaria crassna. *Molecules, 20*(7), 11808-11829. doi:10.3390/molecules200711808

Dai, Y., Witkamp, G.-J., Vertpoorte, R., & Choi, Y. (2015). Tailoring properties of natural deep eutectic solvents with water to facilitate their applications. *Food Chemistry, 187*, 14-19. doi:10.1016/j.foodchem.2015.03.123

de O.Dias, D., Colombo, M., Kelmann, R. G., De Souza, T. P., Bassani, V. L., Teixeira, H. F., . . . Koester, L. S. (2012). Optimization of headspace solid-phase microextraction for analysis of β-caryophyllene in a nanoemulsion dosage form prepared with copaiba (Copaifera multijuga Hayne) oil. *Analytica Chimica Acta, 721*, 79-84. doi:10.1016/j.aca.2012.01.055

DIN EN ISO 17943:2016-10. (2016). Berlin: Beuth.

Du, C., Zhao, B., Chen, X.-B., Birbilis, N., & Yang, H. (2016). Effect of water presence on choline chloride-2urea ionic liquid and coating platings from the hydrated ionic liquid. *Scientific reports, 6*, 29225. doi:10.1038/srep29225

Dulski, T. (2016, Novenber). *Sample Preparation*. (Encyclopedia Britannica) Retrieved from https://www.britannica.com/science/sample-preparation

Dwanema, A. K. (2019). Recent Advances in Hydrophobic Deep Eutectic Solvents for Extraction. *Separations, 6*(1), 9. doi:10.3390/separations6010009

El Achkar, T., Fourmentin, S., & Greige-Gerges, H. (2019). Deep eutectic solvents: An overview on their interactions with water and biochemical compounds. *Journal of Molecular Liquids, 288*, 111028. doi:10.1016/j.molliq.2019.111028

ElSohly, M. A. (2020). Chemical Composition of Volatile Oils of Fresh and Air-Dried Buds of Cannabis chemovars, Their Insecticidal and Repellent Activities. *Natural Product Communications, 15*(5). doi:10.1177/1934578X20926729

Environmental Protection Agency. (2007). METHOD 8272. Parent and alkyl polycyclic aromatics in sediment pore water by solidphase microextraction and gas chromatography/mass spectrometry in selected ion monitoring. Washington. Retrieved 2022, from https://www.epa.gov/sites/default/files/2015-12/documents/8272.pdf

Erich, S., Leopold, J., Gerhard, B., Gernot A., E., Ivanka, S., Albert, K., . . . Margit, G. (2006). Composition and Antioxidant Activities of the Essential Oil of Cinnamon (Cinnamomum zeylanicum Blume) Leaves from Sri Lanka. *Journal of Essential Oil Bearing Plants, 9*(2), 170-182.

Espino, M., Fernández, M., Gomez, F., & Silva, M. (2016). Natural designer solvents for greening analytical chemistry. *Trends in Analytical Chemistry*, 126-136.

Essien, S. O., Young, B., & Baroutian, S. (2020). Recent advances in subcritical water and supercritical carbon dioxide extraction of bioactive compounds from plant materials. *Trends in Food Science & Technology, 97*, 156-169. doi:10.1016/j.tifs.2020.01.014

Eyres, G., & Dufour, J.-P. (2008). Hop Essential Oil: Analysis, Chemical Composition and Odor Characteristics. In V. R. Preedy (Ed.), *Beer in Health and Disease Prevention* (pp. 239-254). Academic Press.

Fernandes, E. S., Passos, G. F., Medeiros, R., da Cunha, F. M., Ferreira, J., Campos, M. M., . . . Calixto, J. B. (2007). Anti-inflammatory effects of compounds alpha-humulene and (−)-trans-caryophyllene isolated from the essential oil of Cordia verbenacea. *European Journal of Pharmacology, 569*(3), 228-236. doi:10.1016/j.ejphar.2007.04.059

Fidyt, K., Fiedorowicz, A., Strządała, L., & Szumny, A. (2016). β-caryophyllene and β-caryophyllene oxide—natural compounds of anticancer and analgesic properties. *Cancer Medicine, 10*(5), 3007-3017.

Florindo, C., Oliveira, F. S., Rebelo, L. P., Fernandes, A. M., & Marrucho, I. M. (2014). Insights into the Synthesis and Properties of Deep Eutectic Solvents Based on Cholinium Chloride and Carboxylic Acids. *ACS Sustainable Chemistry & Engineering, 2*(10), 2416-2425. doi:10.1021/sc500439w

Francomano, F., Caruso, A., Barbarossa, A., Fazio, A., La Torre, C., Ceramella, J., . . . Sinicropi, M. (2019). β-Caryophyllene: A Sesquiterpene with Countless Biological Properties. *Applied Sciences, 9*(24), 5420. doi:10.3390/app9245420

Gabriele, F., Chiarini, M., Germani, R., Tiecco, M., & Spreti, N. (2019). Effect of water addition on choline chloride/glycol deep eutectic solvents: Characterization of their structural and physicochemical properties. *Journal of Molecular Liquids, 291*, 111301. doi:10.1016/j.molliq.2019.111301

Gao, M. Z., Cui, Q., Wang, L. T., Meng, Y., Yu, L., Li, Y. Y., & Fu, Y. J. (2020). A green and integrated strategy for enhanced phenolic compounds extraction from mulberry (Morus alba L.) leaves by deep eutectic solvent. *Microchemical Journal, 154*, 104598. doi:10.1016/j.microc.2020.104598

García, A., Rodríguez-Juan, E., Rodríguez-Gutiérre, G., Rios, J., & Fernández, J. (2016). Extraction of phenolic compounds from virgin olive oil by deep eutectic solvents (DESs). *Food Chemistry, 197*, 554-561. doi:10.1016/j.foodchem.2015.10.131

Gomez, L., Tiwari, B., & Garcia-Vaquero, M. (2020). Emerging extraction techniques: Microwave-assisted extraction. In *Sustainable Seaweed Technologies: Cultivation, Biorefinery, and Applications* (pp. 207-224). Elsevier.

Guo, N., Ping-Kou, J., Wang, L. T., Niu, L. J., Liu, Z. M., & Fu, Y. J. (2019). Natural deep eutectic solvents couple with integrative extraction technique as an effective approach for mulberry anthocyanin extraction. *Food chemistry, 296*, 78-85. doi:10.1016/j.foodchem.2019.05.196

Hayyan, M., Mjalli, F. S., Hashim, M. A., & AlNashef, I. M. (2010). A novel technique for separating glycerine from palm oil-based biodiesel using ionic liquids. *Fuel Processing Technology, 91*(1), 116-120. doi:10.1016/j.fuproc.2009.09.002

He, Q., O'Brien, J. W., Kitselman, K. A., Tompkins, L. E., Curtis, G. C., & Kerton, F. M. (2014). Synthesis of cyclic carbonates from CO2 and epoxides using ionic liquids and related catalysts including choline chloride–metal halide mixtures. *Catalysis Science & Technology*, 1513-1528.

Henshaw, J. V. (2006). Syringes for Gas Chromatography. *LCGC Europe, 19*(10), 530-534.

Hub, Y., Zenga, Z., Wanga, B., & Guo, S. (2017). Trans-caryophyllene inhibits amyloid β (Aβ) oligomer-induced neuroinflammation in BV-2 microglial cells. *International Immunopharmacology, 51*, 91-98. doi:10.1016/j.intimp.2017.07.009

Ijardar, S., Singh, V., & Gardas, R. (2022). Revisiting the Physicochemical Properties and Applications of Deep Eutectic Solvents. *Molecules, 27*(4), 1368. doi:0.3390/molecules27041368

Jassal, K., Kaushal Rashmi, S., & Rani, R. (2021). Antifungal potential of guava (Psidium guajava) leaves essential oil, major compounds: beta-caryophyllene and caryophyllene oxide. *Archives of Phytopathology and Plant Protection*. doi:10.1080/03235408.2021.1968287

Jha, N., Sharma, C., Hashiesh, H., Arunachalam, S., Meeran, M. N., Javed, H., . . . Ojha, S. (2021). β-Caryophyllene, A Natural Dietary CB2 Receptor Selective Cannabinoid can be a Candidate to Target the Trinity of Infection, Immunity, and Inflammation in COVID-19. *Frontiers in Pharmacology, 12*, 590201. doi:10.3389/fphar.2021.590201

Jirovetz, L., Buchbauer, G., Stoilova, I., Stoyanova, A., Krastanov, A., & Schmidt, E. (2006). Chemical Composition and Antioxidant Properties of Clove Leaf Essential Oil. *Journal of Agricultural and Food Chemistry, 54*(17), 6303-6307.

Jochmann, M., Laaks, J., & Schmidt, T. (2014). Solvent-Free Extraction and Injection Techniques. In K. Dettmer-Wilde, & W. Engewald, *Practical Gas Chromatography* (pp. 371-412). Berlin: Springer. doi:10.1007/978-3-642-54640-2_11

Juliani Jr., H. R., Biurrun, F., Koroch, A. R., Oliva, M. M., Demo, M. S., Trippi, V. C., & Zygadlo, J. A. (2002). Chemical Constituents and Antimicrobial Activity of the Essential Oil of Lantana xenica. *Planta Medica, 68*(8), 762-764. doi:10.1055/s-2002-33803

Karačonji, I., & Skender, L. (2007). Comparison Between Dynamic Headspace and Headspace Solid-Phase Microextraction for Gas Chromatography of Btex in Urine. *Archives of Industrial Hygiene and Toxicology, 58*(4), 421-427. doi:10.2478/v10004-007-0035-1

Karimi, M., Dadfarnia, S., Shabani, A. M., Tamaddon, F., & Azadi, D. (2015). Deep eutectic liquid organic salt as a new solvent for liquid-phase microextraction and its application in ligandless extraction and preconcentraion of lead and cadmium in edible oils. *Talanta, 144*, 648-654. doi:10.1016/j.talanta.2015.07.021

Kataoka, H. (2017). Sample preparation for liquid chromatography. In *Liquid Chromatography* (2nd ed., pp. 1-37). Elsevier. doi:10.1016/B978-0-12-805392-8.00001-3

Kaur, S., Gupta, A., & Kashyap, H. K. (2020). How Hydration Affects the Microscopic Structural Morphology in a Deep Eutectic Solvent. *Journal of Physical Chemistry B, 124*(11), 2230-2237. doi:10.1021/acs.jpcb.9b11753

Kaur, S., Kumari, M., & Kashyap, H. K. (2020). Microstructure of Deep Eutectic Solvents: Current Understanding and Challenges. *The Journal of Physical Chemistry B, 124*(47), 10601-10616. doi:10.1021/acs.jpcb.0c07934

Kendall, D., & Yudowski, G. (2017). Cannabinoid Receptors in the Central Nervous System: Their Signaling and Roles in Disease. *Frontiers in Cellular Neuroscience, 10*(294). doi:10.3389/fncel.2016.00294

Khalid, H., Lêda, F., & Eugenio, O. (2017). Cinnamon Oil. In N. Leo M.L., & R. Hamir Singh (Eds.), *Green Pesticides Handbook Essential Oils for Pest Control* (1st ed., pp. 118-150). CRC Press Taylor & Francis Group.

Khezeli, T., & Daneshfar, A. (2015). Dispersive micro-solid-phase extraction of dopamine, epinephrine and norepinephrine from biological samples based on green deep eutectic solvents and Fe3O4@MIL-100 (Fe) core-shell nanoparticles grafted with pyrocatechol. *RSC Advances, 5*(80), 65264-65273. doi:10.1039/C5RA08058D

Kim, K. H., Eudes, A., Jeong, K., Yoo, C. G., & Kim, C. S. (2019). Integration of renewable deep eutectic solvents with engineered biomass to achieve a closed-loop biorefinery. *Proceedings of the National Academy of Sciences, 116*(28), 13816-13824. doi:10.1073/pnas.190463611

Kokkini, S., Karousou, R., Hanlidou, E., & Lanaras, T. (2004). Essential Oil Composition of Greek (Origanum vulgare ssp. hirtum) and Turkish (O. onites) Oregano: a Tool for Their Distinction. *Journal of Essential Oil Research, 16*(4), 334-338.

Kolb, B., & Ettre, L. E. (2006). *Static Headspace-Gas Chromatography: Theory and Practice* (2nd ed.). Hoboken, NJ: John Wiley and Sons, Inc.

Kollner, T., Held, M., Lenk, C., Hiltpold, I., Turlings, T., Gershenzon, J., & Degenhardt, J. (2008). A maize (E)-β-caryophyllene synthase implicated in indirect defense responses against herbivores is not expressed in most American maize varieties. *The Plant Cell, 20*, 482-494.

Křížek, T., Bursová, M., Horsley, R., Kuchař, M., Tůma, P., Čabala, R., & Hložek, T. (2018). Menthol-based hydrophobic deep eutectic solvents: Towards greener and efficient extraction of phytocannabinoids. *Journal of Cleaner Production, 193,* 391-396. doi:10.1016/j.jclepro.2018.05.080

Kusters, K. A., Pratsinis, S. E., Thoma, S. G., & Smith, D. M. (1994). Energy—size reduction laws for ultrasonic fragmentation. *Powder Technology, 80*(3), 253-263. doi:10.1016/0032-5910(94)02852-4

Legault, J., & Pichette, A. (2007). Potentiating effect of b-caryophyllene on anticancer activity of a-humulene, isocaryophyllene and paclitaxel. *Journal of Pharmacy and Pharmacology, 59*(12), 1643-1647. doi:10.1211/jpp.59.12.0005

Liberto, E., Bicchi, C., Cagliero, C., Cordero, C., Rubiolo, P., & Sgorbini, B. (2019). Headspace Sampling: An “Evergreen” Method in Constant Evolution to Characterize Food Flavors through their Volatile Fraction. In P. Q. Tranchida (Ed.), *Advanced Gas Chromatography in Food Analysis* (pp. 1-37). Croydon: CPI Group (UK) Ltd. doi:10.1039/9781788015752-FP001

Liu, T., Sui, X., Zhang, R., Yang, L., Zu, Y., Zhang, L., . . . Zhang, Z. (2011). Application of ionic liquids based microwave-assisted simultaneous extraction of carnosic acid, rosmarinic acid and essential oil from Rosmarinus officinalis. *Journal of Chromatography A, 1218*(47), 8480-8489. doi:10.1016/j.chroma.2011.09.073

López, R., D'Amato, R., Trabalza-Marinucci, M., Regni, L., Proietti, P., Maratta, A., . . . Pacheco, P. (2020). Green and simple extraction of free seleno-amino acids from powdered and lyophilized milk samples with natural deep eutectic solvents. *Food Chemistry, 326,* 126965. doi:10.1016/j.foodchem.2020.126965

Mabou, F., & Yossa, I. (2021). TERPENES : structural classification and biological activities. *IOSR Journal Of Pharmacy And Biological Sciences, 16*(3), 25-40.

Maffei, M. E. (2020). Plant Natural Sources of the Endocannabinoid (E)-β-Caryophyllene: A Systematic Quantitative Analysis of Published Literature. *International Journal of Molecular Sciences, 21*(18), 6540-6556.

Mezzetta, A., Ascrizzi, R., Martinelli, M., Pelosi, F., Chiappe, C., Guazzelli, L., & Flamini, G. (2021). Influence of the Use of an Ionic Liquid as Pre-Hydrodistillation Maceration Medium on the Composition and Yield of Cannabis sativa L. Essential Oil. *Molecules, 26*(18), 5654. doi:10.3390/molecules26185654

Michalczyk, A., Cieniecka-Rosłonkiewicz, A., & Cholewińska, M. (2015). APPLICATION OF IONIC LIQUIDS IN THE ULTRASOUND-ASSISTED EXTRACTION OF ANTIMICROBIAL COMPOUNDS FROM THE BARK OF CINNAMOMUM CASSIA. *Journal of the Chilean Chemical Society, 60*(4), 2698-2703.

Miloš, N., Dejan, S., Jasmina, G., Ana, Ć., Tatjana, M., Marija, S., & Marina, S. (2015). Could essential oils of green and black pepper be used as food preservatives? *Journal of Food Science and Technology, 52*(10), 6565-6573.

Mousavi, S. A., Nateghi, L., Dakheli, M. J., Ramezan, Y., & Piravi-Vanak, Z. (2022). Maceration and ultrasound-assisted methods used for extraction of phenolic compounds and antioxidant activity from Ferulago angulata. *Journal of Food Processing and Preservation, 46*(3), e16356. doi:10.1111/jfpp.16356

Ngamprasertsith, N., Menwa, J., & Sawangkeaw, R. (2018). Caryophyllene oxide extraction from lemon basil (Ocimum citriodorum Vis.) straw by hydrodistillation and supercritical CO2. *The Journal of Supercritical Fluids, 138*, 1-6. doi:10.1016/j.supflu.2018.03.024

Oboh, G., Olasehinde, T. A., & Ademosun, A. O. (2014). Essential Oil From Lemon Peels Inhibit Key Enzymes Linked to Neurodegenerative Conditions and Pro-Oxidant Induced Lipid Peroxidation. *Journal of Oleo Science, 63*(4), 373-381. doi:10.5650/jos.ess13166

Ochiai, N., Sasamoto, K., David, F., & Sandra, P. (2018). Recent Developments of Stir Bar Sorptive Extraction for Food Applications: Extension to Polar Solutes. *Journal of Agricultural and Food Chemistry, 66*(28), 7249-7255. doi:10.1021/acs.jafc.8b02182

Oh, J.-H., & Lee, J.-S. (2014). Synthesis of Gold Microstructures with Surface Nanoroughness Using a Deep Eutectic Solvent for Catalytic and Diagnostic Applications. *Journal of Nanoscience and Nanotechnology, 14*(5), 3753-3757. doi:10.1166/jnn.2014.8658

O'Sullivan, S. (2016). An update on PPAR activation by cannabinoids. *British Journal of Pharmacology, 173*(12), 1899-1910. doi:10.1111/bph.13497

Özcan, M. M., & Chalchat, J.-C. (2008). Chemical composition and antifungal activity of rosemary (Rosmarinus officinalis L.) oil from Turkey. *International Journal of Food Sciences and Nutrition, 59*(7-8), 691-698.

Pandey, A., & Pandey, S. (2014). Solvatochromic Probe Behavior within Choline Chloride-Based Deep Eutectic Solvents: Effect of Temperature and Water. *The Journal of Physical Chemistry B, 118*(50), 14652-14661. doi:10.1021/jp510420h

Pant, P., Maggi, F., Gyawali, R., & Dall'Acqua, S. (2019). Sesquiterpene Rich Essential Oil From Nepalese bael Tree (Aegle Marmelos (L.) Correa) as Potential Antiproliferative Agent. *Fitoterapia, 138*, 104266. doi:10.1016/j.fitote.2019.104266

Patra, K. C., Singh, B., Pareta, S., & Kumar, K. J. (2010). A validated HPTLC method for determination of trans-caryophyllene from polyherbal formulations. *Natural Product Research, 24*(20), 1933-1938. doi:10.1080/14786419.2010.497147

Pavithra, P., Mehta, A., & Verma, R. (2018). Synergistic interaction of beta-caryophyllene with aromadendrene oxide 2 and phytol induces apoptosis on skin epidermoid cancer cells. *International Journal of Phytotherapy and Phytopharmacology, 47*, 121-134. doi:10.1016/j.phymed.2018.05.001

Pawliszyn, J. (2012). *Comprehensive Sampling and Sample Preparation.* Academic Press.

Pereira, F., Marquete, R., Domingos, L., Rocha, M., Ferreira-Pereira, A., Mansur, E., & Moreira, D. (2017). Antifungal activities of the essential oil and its fractions rich in sesquiterpenes from leaves of Casearia sylvestris Sw. *Anais da Academia Brasileira de Ciências, 89*(4), 2817-2824. doi:10.1590/0001-3765201720170339

Płotka-Wasylka, J., de la Guardia, M., Andruch, V., & Vilkova, M. (2020). Deep eutectic solvents vs ionic liquids: Similarities and differences. *Microchemical Journal, 159*, 105539. doi:10.1016/j.microc.2020.105539

Povolo, M., & Contarini, G. (2003). Comparison of solid-phase microextraction and purge-and-trap methods for the analysis of the volatile fraction of butter. *Journal of Chromatography A, 985*(1), 117-125. doi:10.1016/s0021-9673(02)01395-x

Ramón, D. J., & Guillena, G. (2019). *Deep Eutectic Solvents: Synthesis, Properties, and Applications.* Weinheim, Germany: Wiley-VCH.

Rasul, M. G. (2018). Conventional Extraction Methods Use in Medicinal Plants, their Advantages and Disadvantages. *International Journal of Basic Sciences and Applied Computing, 2*(6), 10-14.

Rather, I., & Ali, R. (2022). An Efficient and Versatile Deep Eutectic Solvent-Mediated Green Method for the Synthesis of Functionalized Coumarins. *ACS Omega, 7*(12), 10649-10659. doi:10.1021/acsomega.2c00293

Restek Corp. (2000). *A Technical Guide for Static Headspace Analysis Using GC.* Restek. Retrieved 2022, from https://d1lqgfmy9cwjff.cloudfront.net/csi/pdf/e/rk67.pdf

Reyes-Garcés, N., Gionfriddo, E., Gómez-Ríos, G. A., Alam, M. N., Boyacı, E., Bojko, B., . . . Pawliszyn, J. (2018). Advances in Solid Phase Microextraction and Perspective on Future Directions. *Analytical Chemistry, 90*(1), 302-360. doi:10.1021/acs.analchem.7b04502

Rincón, A. A., Pino, V., Ayala, J. H., & Afonso, A. M. (2011). Headspace-single drop microextraction (HS-SDME) in combination with high-performance liquid chromatography (HPLC) to evaluate the content of alkyl- and methoxy-phenolic compounds in biomass smoke. *Talanta, 85*(3), 1265-1273. doi:10.1016/j.talanta.2011.05.046

Rozas, S., Benito, C., Alcalde, R., Atilhan, M., & Aparicio, S. (2021). Insights on the water effect on deep eutectic solvents properties and structuring: The archetypical case of choline chloride + ethylene glycol. *Journal of Molecular Liquids, 334*, 117717. doi:10.1016/j.molliq.2021.117717

Sabulal, B., Dan, M., John J, A., Kurup, R., Sukumaran Pradeep, N., Krishna Valsamma, R., & George, V. (2006). Caryophyllene-rich rhizome oil of Zingiber nimmonii from South India: Chemical characterization and antimicrobial activity. *Phytochemistry, 67*(22), 2469-2473. doi:10.1016/j.phytochem.2006.08.003

Sadraei, H., Asghari, G., & Alipour, M. (2016). Anti-spasmodic assessment of hydroalcoholic extract and essential oil of aerial part of Pycnocycla caespitosa Boiss. & Hausskn on rat ileum contractions. *Research in Pharmaceutical Sciences, 11*(1), 33-42.

Saien, J., & Daneshamoz, S. (2018). Experimental studies on the effect of ultrasonic waves on single drop liquid-liquid extraction. *Ultrasonics sonochemistry, 40*(A), 11-16. doi:10.1016/j.ultsonch.2017.06.020

Sain, S., K. Naoghare, P., Saravana Devi, S., Daiwile, A., Krishnamurthi, K., Arrigo, P., & Chakrabarti, T. (2014). Beta Caryophyllene and Caryophyllene Oxide, Isolated from Aegle Marmelos, as the Potent Anti-inflammatory Agents against Lymphoma and Neuroblastoma Cells. *Anti-Inflammatory & Anti-Allergy Agents in Medicinal Chemistry, 13*(1), 45-55.

Sanap, A., & Shankarling, G. (2014). Choline chloride based eutectic solvents: direct C-3 alkenylation/alkylation of indoles with 1,3-dicarbonyl compounds. *RSC Advances, 4*(66), 34938-34943. doi:10.1039/C4RA05858E

Sánchez-Muñoz, A., Aguilar, M. A., King-Díaz, B., Fausto Rivero, J., & Lotina-Hennsen, B. (2012). The Sesquiterpenes β-Caryophyllene and Caryophyllene Oxide Isolated from Senecio salignus Act as Phytogrowth and Photosynthesis Inhibitors. *Molecules, 17*(2), 1437-1447.

Sapir, L., & Harries, D. (2020). Restructuring a Deep Eutectic Solvent by Water: The Nanostructure of Hydrated Choline Chloride/Urea. *Journal of Chemical Theory and Computation, 16*(5), 3335-3342. doi:10.1021/acs.jctc.0c00120

Scandiffio, R., Geddo, F., Cottone, E., Querio, J., Antoniotti, S., Gallo, M., . . . Bovolin, P. (2020). Protective Effects of (E)-β-Caryophyllene (BCP) in Chronic Inflammation. *Nutrients, 12*(11), 3273. doi:10.3390/nu12113273

Segat, G., Manjavachi, M., Matias, D., Passos, G., Freitas, C., Costa, R., & Calixto, J. (2017). Antiallodynic effect of β-caryophyllene on paclitaxel-induced peripheral neuropathy in mice. *Neuropharmacology, 125*, 207-219. doi:10.1016/j.neuropharm.2017.07.015

Shoemaker, J. L., Ruckle, M. B., Mayeux, P. R., & Prather, P. L. (2005). Agonist-directed trafficking of response by endocannabinoids acting at CB2 receptors. *The Journal of Pharmacology and Experimental Therapeutics, 315*(2), 828-838. doi:10.1124/jpet.105.089474

Shu-Wei, Y., Tze-Ming, C., Joseph, T., Eric, B., Reena, P., Guodong, C., . . . Min, C. (2009). Caryophyllenes from a Fungal Culture of Chrysosporiumpilosum. *Journal of Natural Products, 72*(3), 484-487.

Sims, C. A., Juliani, H. R., Mentreddy, S., & Simon, J. E. (2014). Essential Oils in Holy Basil (Ocimum tenuiflorum L.) as Influenced by Planting Dates and Harvest Times in North Alabama. *Journal of Medicinally Active Plants, 2*(3), 33-41.

Sithersingh, M. J., & Snow, N. H. (2012). Headspace-Gas Chromatography. In C. F. Poole, *Gas Chromatography* (pp. 221-233). Elsevier.

Smith, E. L., Abbott, A. P., & Ryder, K. S. (2014). Deep Eutectic Solvents (DESs) and Their Applications. *Chemical Reviews, 114*(21), 11060-11082. doi:10.1021/cr300162p

Smith, P. J., Arroyo, C. B., Hernandez, F. L., & Goeltz, J. C. (2019). Ternary Deep Eutectic Solvent Behavior of Water and Urea–Choline Chloride Mixtures. *The Journal of Physical Chemistry B, 123*(25), 5302-5306. doi:10.1021/acs.jpcb.8b12322

Stauffer, E., Dolan, J. A., & Newman, R. (2008). Gas Chromatography and Gas Chromatography — Mass Spectrometry. In E. Stauffer, J. A. Dolan, & R. Newman (Eds.), *Fire Debris Analysis* (pp. 235-293). Academic Press. doi:10.1016/B978-012663971-1.50012-9

Sudeep, H. V., Gouthamchandra, K., Reethi, B., Naveen, P., Lingaraju, H., & Shyamprasad, K. (2021). A standardized black pepper seed extract containing β-caryophyllene improves cognitive function in scopolamine-induced amnesia model mice via regulation of brain-derived neurotrophic factor and MAPK proteins. *Journal of Food Biochemistry, 45*(12), e13994. doi:10.1111/jfbc.13994

Talapatra, S., & Talapatra, B. (2015). *Chemistry of Plant Natural Products.* Berlin, Germany: Springer Science and Business Media LLC.

Tankevièiûtë, A., Panavaitë, D., Kazlauskas, R., & Vièkaèkaitë, V. (2004). Solid phase microextraxtion fibers for alcohol determination. *Chemija, 15*(3), 39-44.

Teixeira, B., Marques, A., Ramos, C., Serrano, C., Matos, O., Neng, N. R., . . . Nunes, M. L. (2013). Chemical composition and bioactivity of different oregano (Origanum vulgare) extracts and essential oil. *Journal of the Science of Food and Agriculture, 93*(11), 2707-2714.

Tipler, A. (2014). An Introduction to Headspace Sampling in Gas Chromatography. Waltham: Perkin Elmer, Inc. Retrieved April 28, 2022, from https://resources.perkinelmer.com/corporate/pdfs/downloads/gde_intro_to_headspace.pdf

Valizadehderakhshan, M., Shahbazi, A., Kazem-Rostami, M., Todd, M. S., Bhowmik, A., & Wang, L. (2021). Extraction of Cannabinoids from Cannabis sativa L. (Hemp)—Review. *Agriculture, 11*(5), 384. doi:10.3390/agriculture11050384

van Osch, D., Dietz, C., Warrag, S., & Kroon, M. (2020). The Curious Case of Hydrophobic Deep Eutectic Solvents: A Story on the Discovery, Design, and Applications. *ACS Sustainable Chemistry & Engineering, 8*(29), 10591-10612. doi:10.1021/acssuschemeng.0c00559

Vidal, C., García-Álvarez, J., Hernán-Gómez, A., Kennedy, A., & Hevia, E. (2014). Introducing Deep Eutectic Solvents to Polar Organometallic Chemistry: Chemoselective Addition of Organolithium and Grignard Reagents to Ketones in Air. *Angewandte Chemie International Edition, 59*(23), 5969-5973. doi:10.1002/anie.201400889

Vilková, M., Płotka-Wasylka, J., & Andruch, V. (2020). The role of water in deep eutectic solvent-base extraction. *Journal of Molecular Liquids, 304*, 112747. doi:10.1016/j.molliq.2020.112747

Wang, W.-J., Li, D.-Y., Li, Y.-C., Hua, H.-M., Ma, E.-L., & Li, Z.-L. (2014). Caryophyllene Sesquiterpenes from the Marine-Derived Fungus Ascotricha sp. ZJ-M-5 by the One Strain–Many Compounds Strategy. *Journal of Natural Products, 77*(6), 1367-1371. doi:10.1021/np500110z

Wen, Q., Chen, J. X., Tang, Y. L., Wang, J., & Yang, Z. (2015). Assessing the toxicity and biodegradability of deep eutectic solvents. *Chemosphere, 132*, 63-39. doi:10.1016/j.chemosphere.2015.02.061

Wu, Z., Liu, D., Proksch, P., Guo, P., & Lin, W. (2014). Punctaporonins H–M: Caryophyllene-Type Sesquiterpenoids from the Sponge-Associated Fungus Hansfordia sinuosae. *Marine Drugs, 12*(7), 3904-3916. doi:10.3390/md12073904

Xiao, J., Lin, L., Hu, J., Jiao, F., Duan, D., Zhang, Q., . . . Wang, X. (2017). Highly oxygenated caryophyllene-type and drimane-type sesquiterpenes from Pestalotiopsis adusta, an endophytic fungus of Sinopodophyllum hexandrum. *RSC Advances, 7*(46), 29071-29079. doi:10.1039/C7RA04267A

Xu, M., Ran, L., Chen, N., Fan, X., Ren, D., & Yi., L. (2019). Polarity-dependent extraction of flavonoids from citrus peel waste using a tailor-made deep eutectic solvent. *Food Chemistry, 297*, 124970. doi:10.1016/j.foodchem.2019.124970

Yang, D., Michel, L., Chaumont, J., & Millet-Clerc, J. (2000). Use of caryophyllene oxide as an antifungal agent in an in vitro experimental model of onychomycosis. *Mycopathologia, 148*, 79-82. doi:10.1023/A:1007178924408

Yao, X., Zhang, D., Duan, M., Cui, Q., Xu, W., Luo, M., . . . Fu, Y. (2015). Preparation and determination of phenolic compounds from Pyrola incarnata Fisch. with a green polyols based-deep eutectic solvent. *Separation and Purification Technology, 149*, 116-123. doi:10.1016/j.seppur.2015.03.037

Zhang, X., Gao, H., Zhang, L., Liu, D., & Ye, X. (2012). Extraction of essential oil from discarded tobacco leaves by solvent extraction and steam distillation, and identification of its chemical composition. *Industrial Crops and Products, 39*, 162-169. doi:10.1016/j.indcrop.2012.02.029

Zhang, Y., Bai, J., Yan, D., Liu, B., Zhang, L., Zhang, C., . . . Hu, Y. (2020). Highly Oxygenated Caryophyllene-Type Sesquiterpenes from a Plant-Associated Fungus, Pestalotiopsis

hainanensis, and Their Biosynthetic Gene Cluster. *Journal of Natural Products, 83*(11), 3262-3269. doi:10.1021/acs.jnatprod.0c00501

Zhekenov, T., Toskanbayev, N., Kazakbayeva, Z., Shal, D., & Mjalli, F. (2017). Formation of type III Deep Eutectic Solvents and effect of water on their intermolecular interactions. *Fluid Phase Equilibria, 441*, 43-48. doi:10.1016/j.fluid.2017.01.022

SUMMARY

VILNIUS UNIVERSITY
FACULTY OF CHEMISTRY AND GEOSCIENCES
DEPARTMENT OF ANALYTICAL AND ENVIRONMENTAL CHEMISTRY

DMITRIJ GRITSOK

Investigation of Deep Eutectic Solvents for the Determination of β-Caryophyllene by Solid Phase Microextraction Technique

β-Caryophyllene is a natural bicyclic sesquiterpene found in many essential oils, including *Cannabis sativa* L. Due to its unique ability to selectively bind to the CB_2 receptor, β-caryophyllene has been identified as an anti-inflammatory, antimicrobial, antitumor, and antioxidant agent. Moreover, β-caryophyllene is known to relieve anxiety, pain and is a valuable candidate for the treatment of neurodegenerative disorders, cancer, and osteoporosis.

The determination of β-caryophyllene from essential oil requires time-consuming sample preparation and extraction from plant material. Solid phase microextraction (SPME) allows the determination of β-caryophyllene directly in the solid or liquid sample. Nevertheless, selecting appropriate calibration media is crucial in this technique.

In this work, seven deep eutectic solvents (DESs) were synthesised in a microwave reactor and investigated as a calibration media in SPME of β-caryophyllene from the complex matrix – hemp seed oil. The analyte was further identified by gas chromatographic – mass spectrometric analysis (GC-MS) and the selection criterion for the extraction efficiency was its peak area.

Among 7 DESs, the hydrophilic ChCl-based DES demonstrated better suitability for HS-SPME, whereas hydrophobic menthol-based DESs were ineffective. The combination of [ChCl : tartaric acid (2 : 1)] with 15% water additive demonstrated the largest peak area. Equilibration and sorption time at the SPME step were optimised for this DES and further selected for the preparation of the calibration curve to quantify β-caryophyllene in hemp seed oil. The equation of the trendline with a good coefficient of determination was obtained and the calculated concentration of β-caryophyllene in hemp seed oil is 0.79 mg/kg.

Thus, the application of DESs as a calibration media in SPME has been proved to be effective for the direct quantification of β-caryophyllene in a complex matrix and has the potential to be employed for other volatile and semi-volatile compounds.

APPENDICES

Appendix 1

Application of DESs in extraction techniques

Analytes	DESs	Sample matrix	Extraction and identification techniques		References
Pb, Cd	ChCl : urea (1:2)	Edible oils	Liquid-phase microextraction	ETAAS	(Karimi, Dadfarnia, Shabani, Tamaddon, & Azadi, 2015)
Dopamine, epinephrine, norepinephrine	ChCl : urea (1:2)	Human urine and serum	Dispersive solid-phase microextraction	HPLC-UV	(Khezeli & Daneshfar, 2015)
Methadone	ChCl : TNO (1:2)	Water, urine and plasma	Ultrasound-assisted liquid-phase microextraction	GC-FID	(Aydin, Yilmaz, & Soylak, 2017)
Phenolic compounds	ChCl : xylitol (2:1)	Virgin olive oil	Liquid-liquid extraction	HPLC-UV	(García, Rodríguez-Juan, Rodríguez-Gutiérre, Rios, & Fernández, 2016)
Cannabidiol, cannabidiolic acid, THC	Menthol : acetic acid (1:1)	*Cannabis sativa* L. plant powder	Ultrasound-assisted solid-liquid extraction	CE	(Křížek, et al., 2018)
Caffeic acid, rutin, astragalin, isoquercetin,	ChCl : glycerol (1:2)	*Morus alba* Leaves	Microwave-assisted solid-liquid extraction	HPLC-UV	(Gao, et al., 2020)
Curcumin	ChCl : phenol (1:4)	Turmeric root herbal tea, Turmeric drug	Emulsification liquid-liquid extraction	UV-Vis, HPLC	(Aydin, Yilmaz, & Soylak, 2018)
β-caryophyllene	Menthol: LA (1:2)	Leptospermum scoparium leaves	Solid-liquid extraction	HPLC-DAD	(Alsaud, Shahbaz, & Farid, 2021)
β-caryophyllene	ChCl : Tartaric acid (2:1)	Hemp seed oil	Solid phase microextraction	GC-MS	This work
Rosmarinic caffeic, ferulic acid, naringin, rutin	ChCl : OA (1:1) + 10% H_2O, ChCl : 1,2-propanediol (2:1) + 10% H_2O	*Rosmarinus officinalis* L. leaves	Ultrasound-assisted solid-liquid extraction	HPLC-DAD	(Barbieri, et al., 2020)
Vitamins, minerals, flavonols and anthocyanins	ChCl : citric acid : glucose (1:1:1) + 10% H_2O	Fresh mulberry (*Fructus Mori*)	High-speed homogenization and cavitation-burst extraction	HPLC-UV	(Guo, et al., 2019)
Selenoamino acids	LA : glucose (5:1) + 25% H_2O	Powdered and lyophilised milk	Ultrasound-assisted solid-liquid extraction	HPLC-ICP-MS	(López, et al., 2020)

ETAAS – electrothermal atomic absorption spectroscopy; HPLC – high-performance liquid chromatography; TNO – tetrahydro-5,5,8,8-tetramethylnaphthalene-2-ol; GC – gas chromatography; FID – flame ionization detector; CE – capillary electrophoresis; MS – mass spectrometry; DAD – diode-array detector; ICP – inductively coupled plasma; OA – oxalic acid; LA – lactic acid.

Appendix 2

Structural formulae of substances used in the experimental part

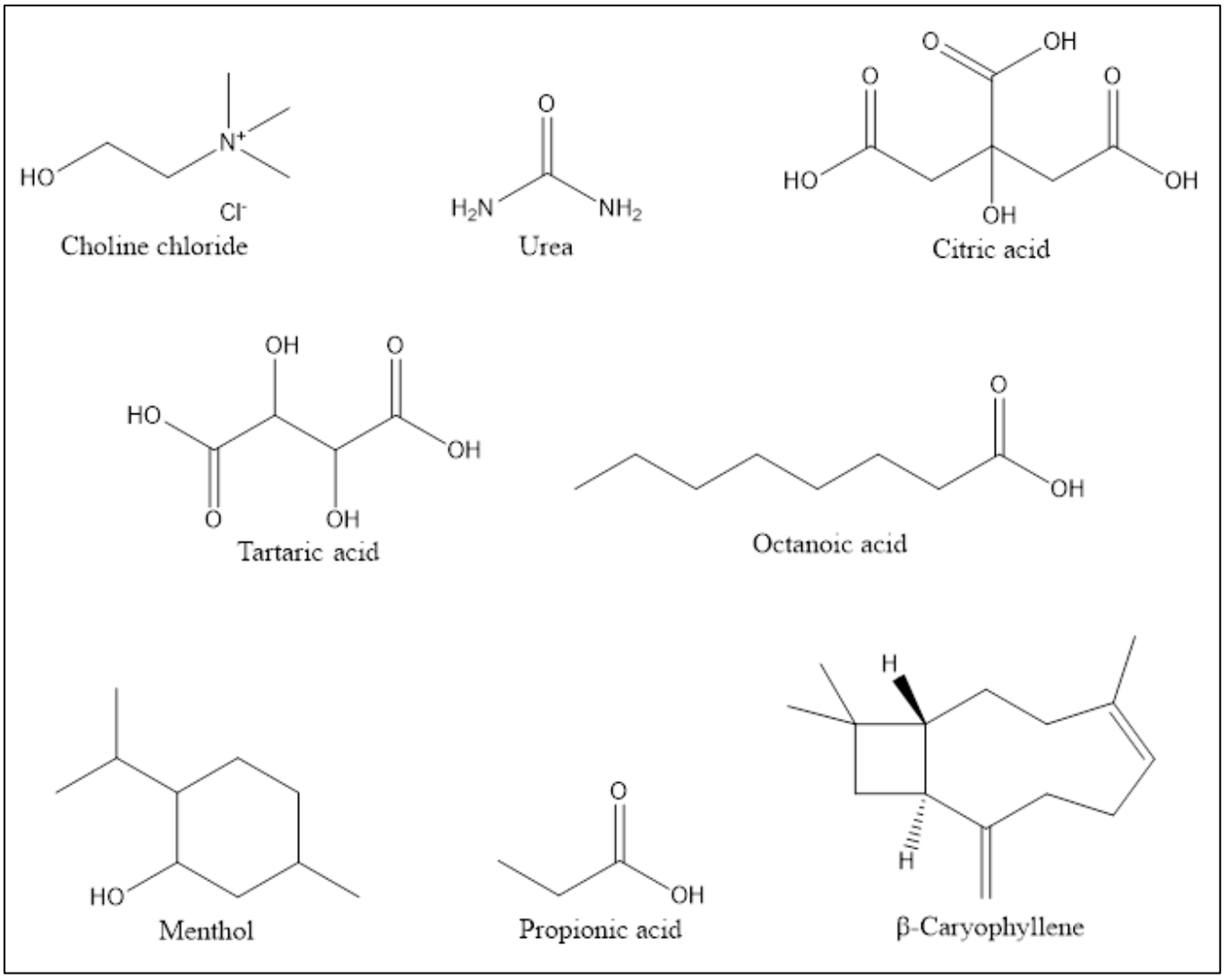

Appendix 3

Photographs of laboratory equipment

A –water vessel/bath connected to water heater; B – HBA and HBD in the vial before microwave-assisted synthesis; C – sorption step of SPME; D – GC-MS system with PC; E – SPME fibre holder; F – SPME fibre assembly; G – microwave reactor.

Appendix 4

Sample chromatogram

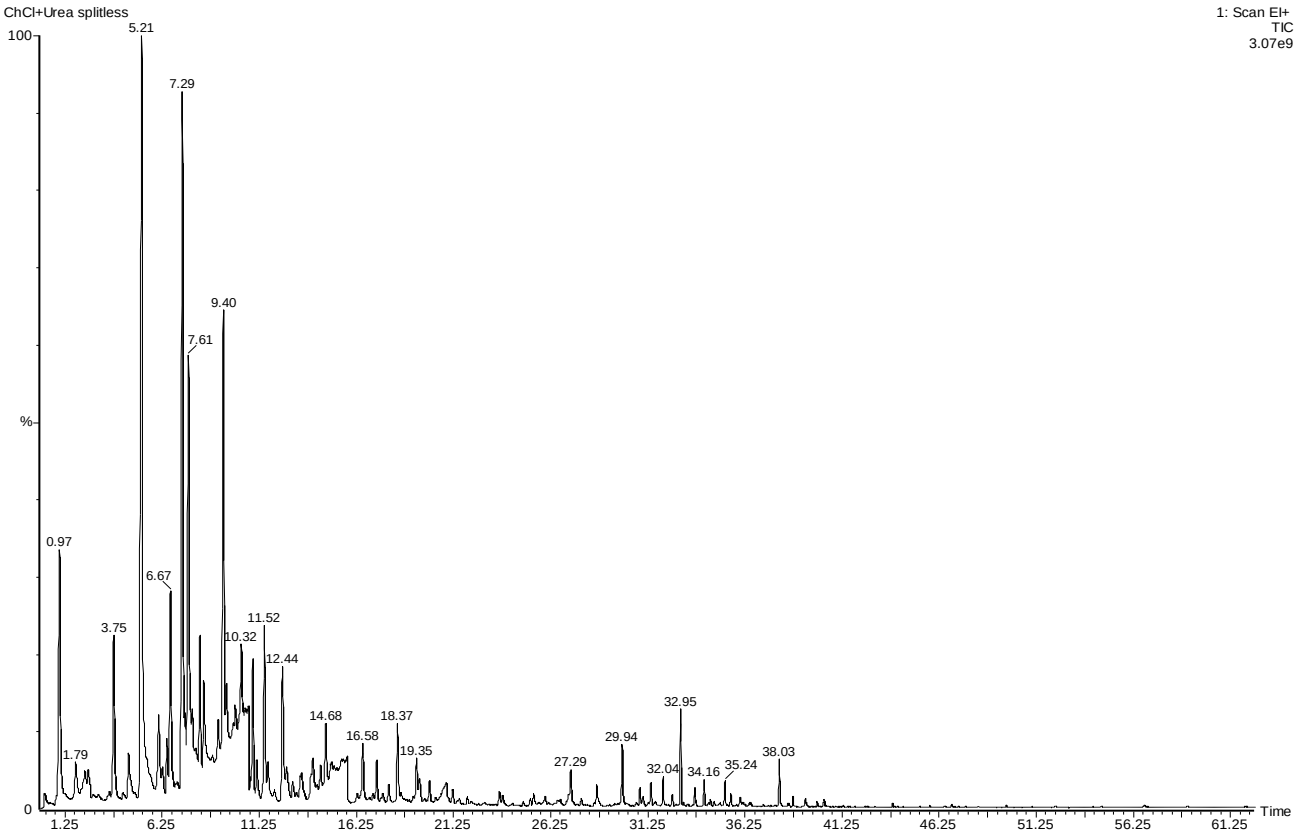

Appendix 5

Chromatograms (MS Full-scan) with integrated peaks (5 DESs)

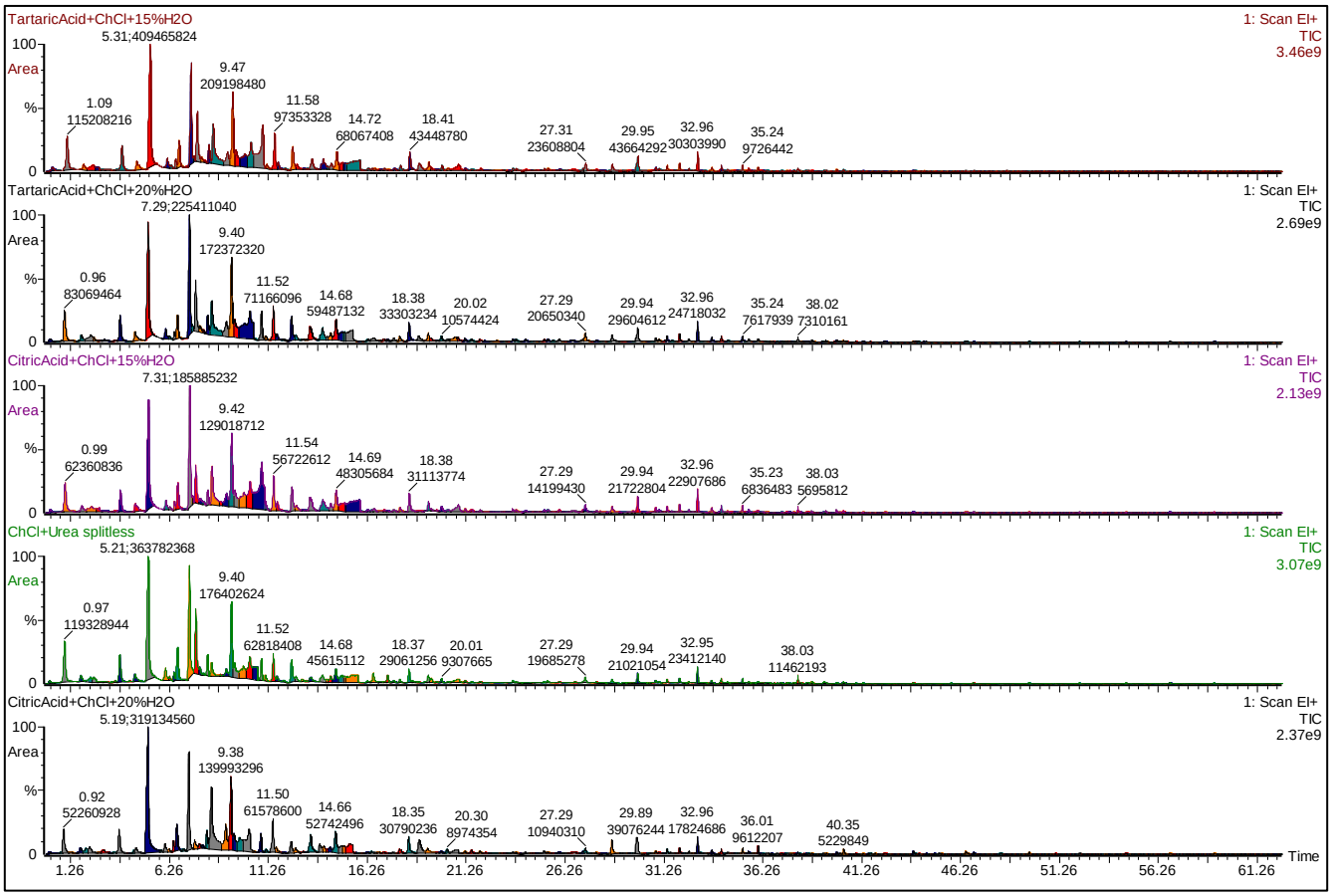

Appendix 6

Chromatograms (SIR) with integrated peaks (5 DESs) in different scales

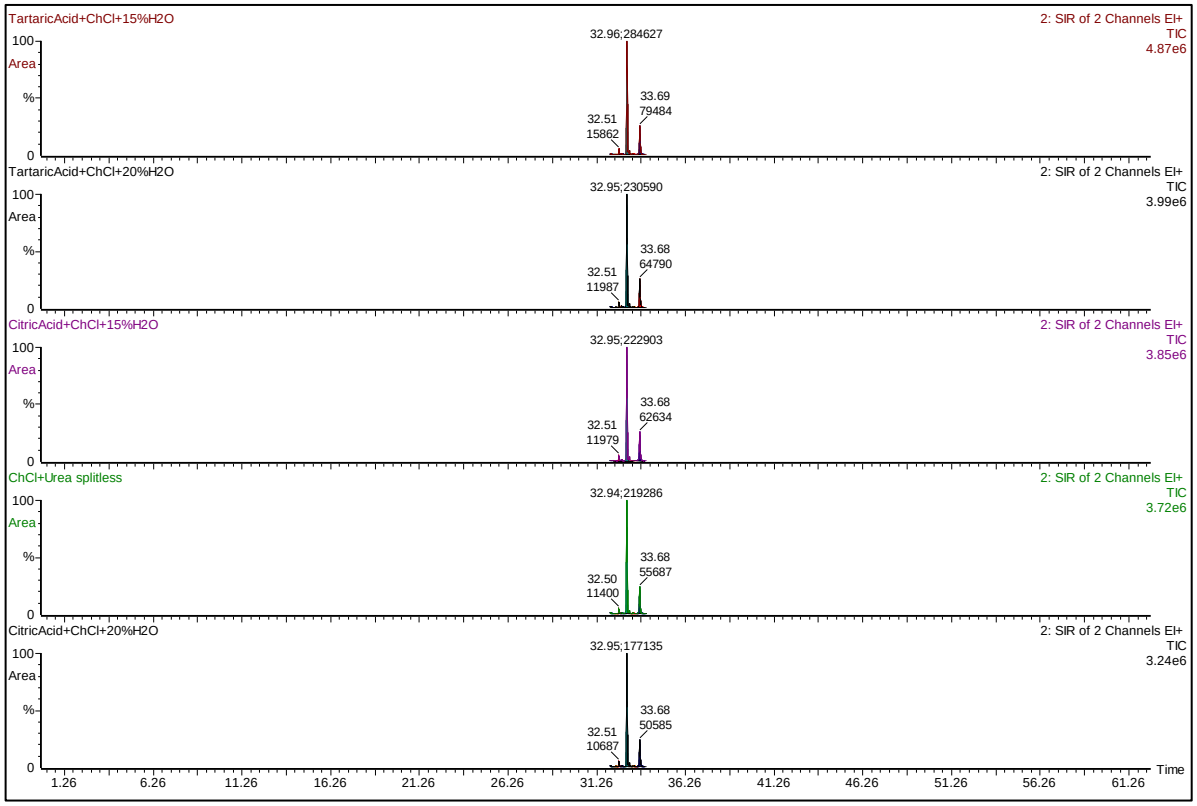

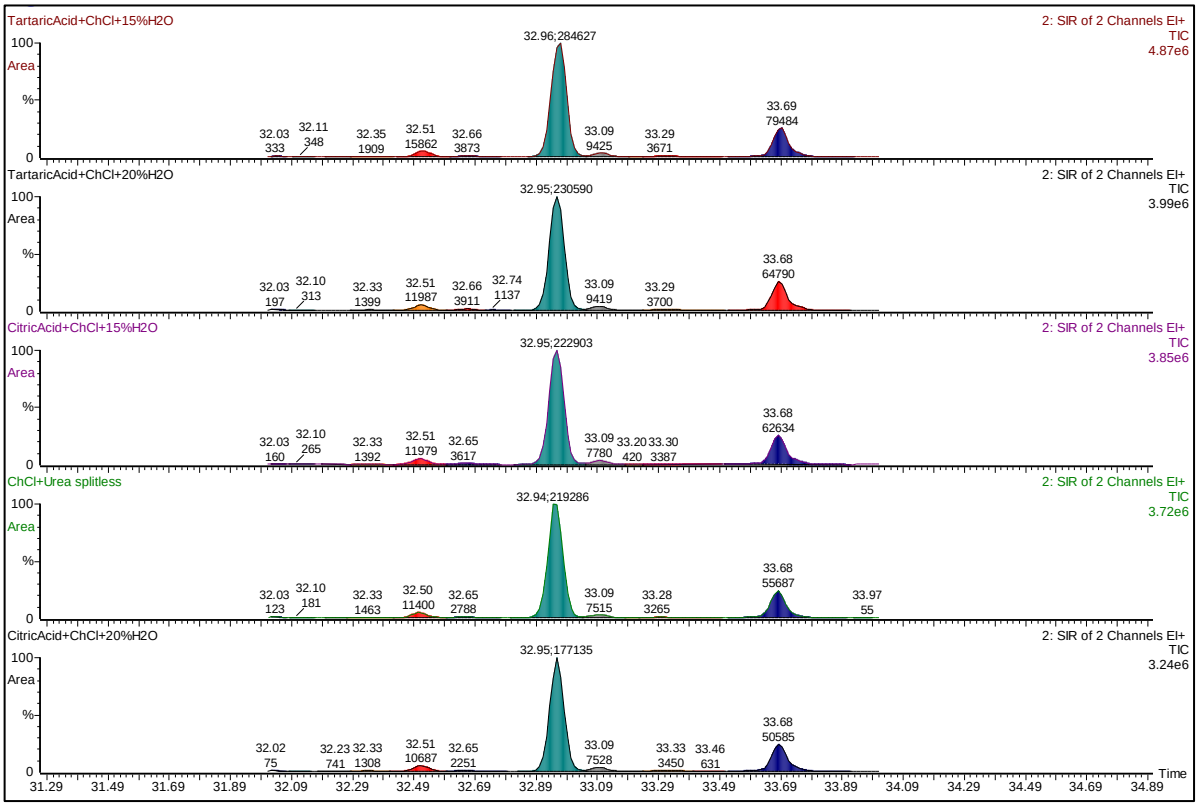

Appendix 7

Chromatograms (MS Full scan) with integrated peaks (sorption time)

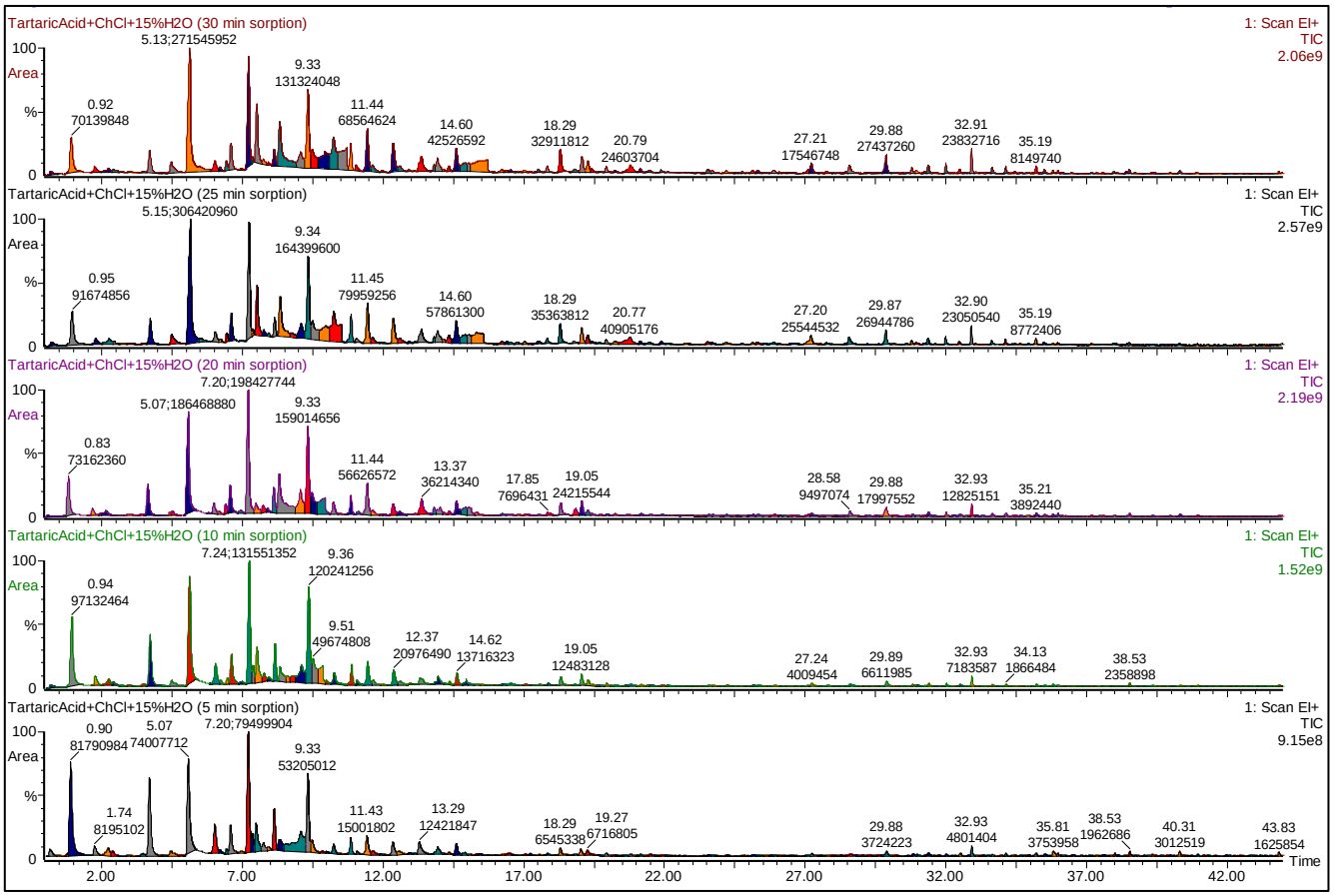

Appendix 8

Chromatograms (SIR) with integrated peaks (sorption time)

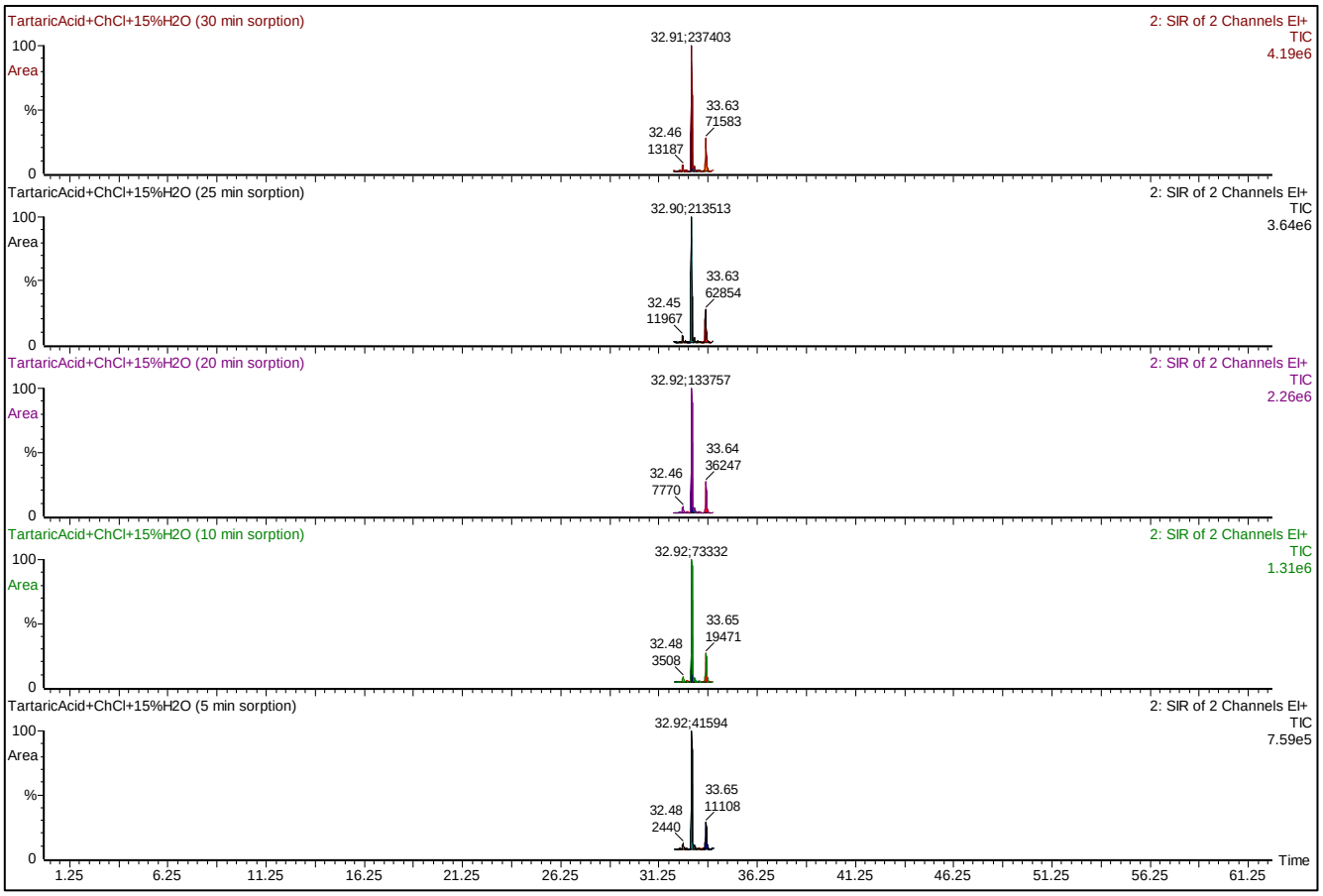

Appendix 9

Chromatograms (MS Full scan and SIR) with integrated peaks (equilibration time)

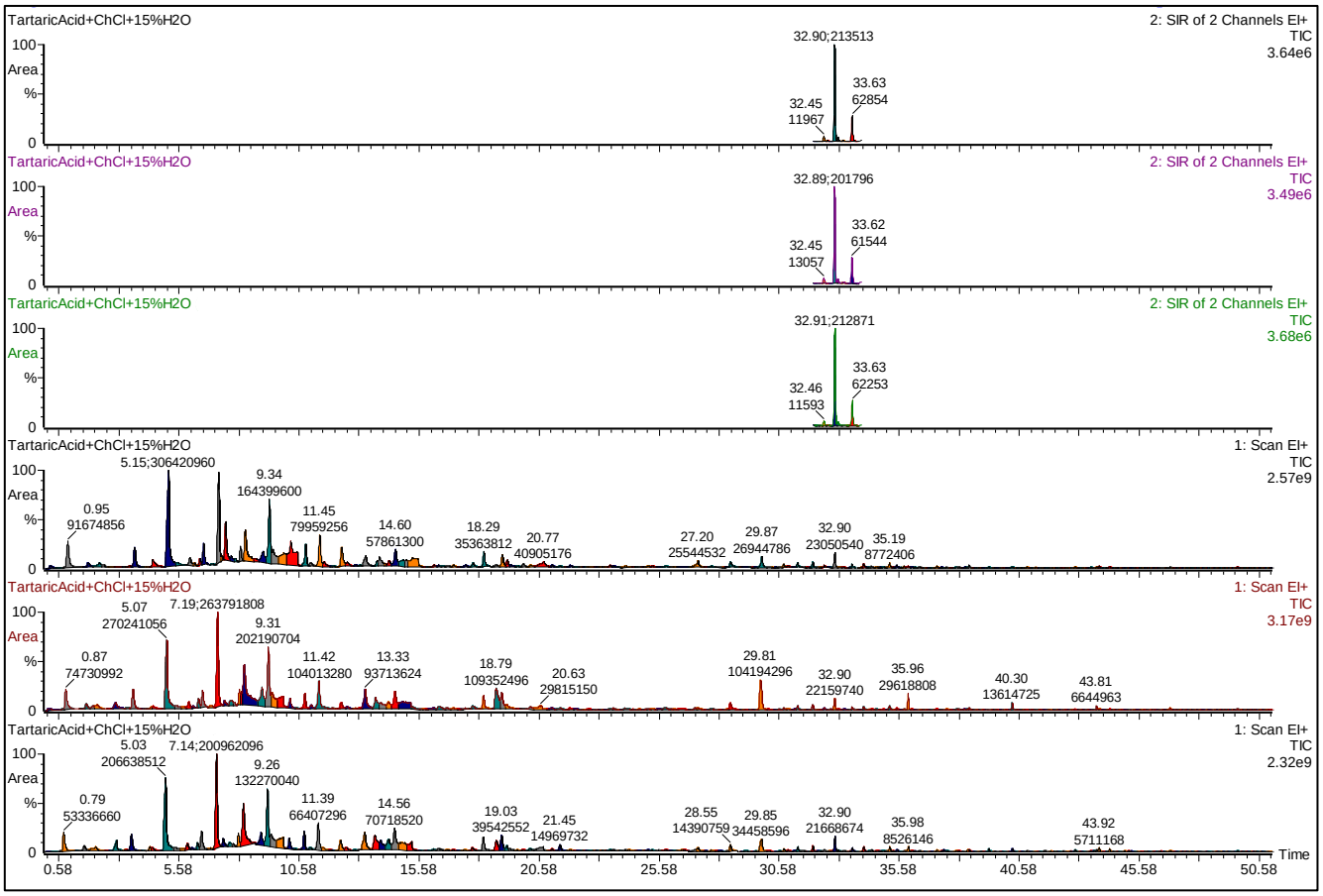

Appendix 10

Chromatograms in (MS Full scan and SIR) modes with integrated peaks (calibration curve)